CUEE Final-Year Project Report (2102499)

Energy Management System for Gewertz Square

Nattapong Kongkaew ID 6330164721

Pattararat Chaowarak ID 6330413021

Advisor: Assoc. Prof. Jitkomut Songsiri

Department of Electrical Engineering

Faculty of Engineering, Chulalongkorn University

Academic Year 2566

Advisor signature

.....

(.....)

Date .....

Abstract

To enhance campus sustainability, implementing an Energy Management System (EMS) is essential. This study investigates Gewertz Square sandbox within the Department of Electrical Engineering, Chulalongkorn University. The system includes load consumption, solar generation, and a battery. Three EMS aspects are proposed, including economic, operational, and RE 100 EMS, formulated as Mixed-Integer Linear Programming (MILP). These EMS aspects are analyzed for their impact on energy policies of the desired components in the system. The economic EMS has a specific purpose to minimize energy unit, energy cost, or maximize profit depending on users' selection when total load consumption is considered, which can be treated as uncontrollable load. Meanwhile, the operational EMS considers the controllable load from Air Conditioning systems (ACs) in two rooms treated as controllable load, focusing on ACs activation while minimizing electricity costs and encouraging islanding EMS. The RE 100 EMS aims to achieve self-reliance regardless of electricity expenses. Forecasting models consisting of load and solar forecasting models from NeuralProphet models are used to predict future data, serving as parameters in the actual EMS operation. An example of EMS operation in Economic EMS is simulated. In this work, two time-scale optimizations are formulated, Day-Ahead (DA) EMS: horizon 3 days with 15-minute resolution, and Hour-Ahead (HA) EMS: horizon 1 hour with 5-minute resolution. The HA EMS is designed to account for both errors from the DA EMS and optimal planning over an HA period. Hence, HA EMS utilizes DA solution as a guided planing by aligning HA solutions with DA solutions as the absolute of difference of power relating to the battery. Simulation results illustrate that the decision-making process of the battery varies for each proposed EMS. The study concludes that EMS implementation offers significant advantages over not utilizing one.

Keywords: Energy Management System (EMS), Mixed-Integer Linear Programming (MILP), NeuralProphet models.

The authors use Generative-AI (ChatGPT 3.5) to correct grammar.

Contents

List of Figures

List of Tables

1 Introduction

1.1 Motivation

The Department of Electrical Engineering, Chulalongkorn University, serving as a prominent hub for research and technological development in Thailand, is embarking on initiative to renovate its internal infrastructure, specifically known as Gewertz Square. Over the course of the next five years, the dedicated research team, in collaboration with the Center of Excellence in Electrical Power Technology (CEPT), is tasked with overseeing this crucial undertaking for primary objective which is to develop a prototype of net-zero energy building or further an islanding building that can autonomously operate without relying on the conventional electrical grid for its energy needs.

In line with the broader vision of promoting the sustainable development goal particularly in the aspect of sustainable cities and communities, the implementation of an Energy Management System (EMS) emerges as an indispensable element. [1] The EMS is endowed with the intelligence and flexibility required to execute energy policies that encompass various aspects including monitoring, planning, optimizing, scheduling, and demand-side management. These capabilities are essential to meet the multifaceted demands of energy consumption that correspond to a diverse set of technical objectives, economic objectives, and environmental objectives, all simultaneously as shown in Figure 1.

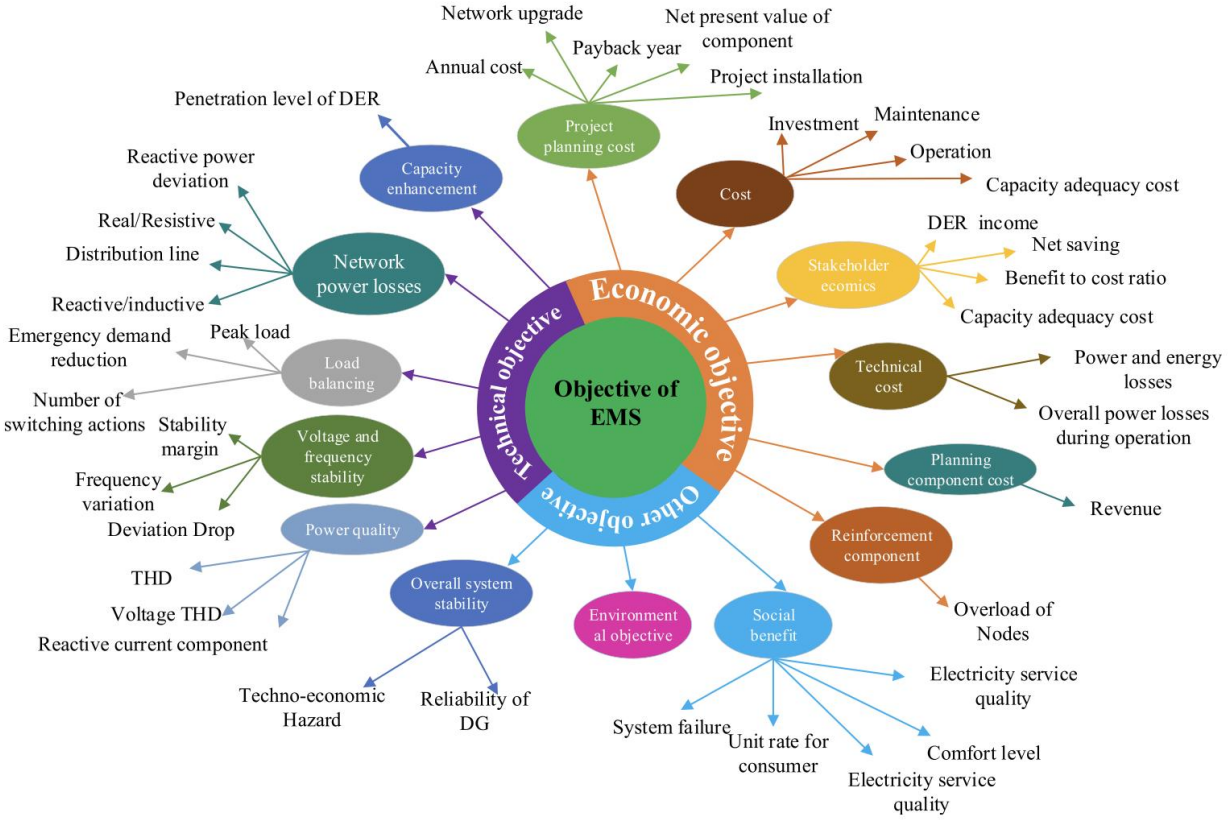

Figure 1: Overview of EMS objectives. Photo credit: Hussain et.al 2021, Multi-level EMS towards a smarter grid: a review.

In the scope of Gewertz Square, the primary focus is on the Building Energy Management System (BEMS). The typical objective of BEMS, especially when the system is connected to the utility network, is to maximize profit or minimize the cost of electricity, combining with other objectives such as the comfort level of users or peak load shaving. The investigation mainly focused on simulate the scheduling operation of the electrical components in the system. However, the scheduling operation must incorporate with the appliances, by considering value of lost load (VOLL) of the appliances as the indicator together with electricity tariff for different time interval for the objective function which is to minimize electricity cost [2]. The focus of demand response control in various residential sizes and

thermostat types centered on the characteristic of load consumption primarily from HVAC systems which also complies with ASHRAE standards illustrating the thermal comfort zone through a psychrometric chart was discussed in [3]. To enhance power utility efficiency, particularly in reducing peak load power consumption, decreasing power exchanges, and addressing power imbalances, energy storage systems were also introduced within Campus of University of Calabria [4]. By integration of solar generation together with energy storage system, the objective function relating to energy price and load elasticity were also investigated for several scenarios [5]. In the concept of grid-independent system, the islanding microgrid operation was examined for the complicated undertaking by considering the economic and environmental perspectives [6].

In exploring an EMS, a key factor lies in the development of mathematical formulations of the relationships among electrical components within a given system for different objective functions which can be then solved by optimization solvers. The mixed-integer linear programming (MILP) problem was modeled for an inverter-based air conditioning system together with the present of solar and battery integration for the objective of minimizing electricity cost [7]. The mixed-integer quadratic programming model predictive control (MIQP-MPC) problem was also formulated for the multiobjective function which is to minimize the total electricity cost simultaneously with maximizing the use of renewable energy for a smart home [8]. Additionally, MIQP was also proposed to compensate the leverage between the utility requirements and profits of selling electricity [9]. The integrated components of the proposed problem are photovoltaic cells with smart inverter, battery, electric vehicles, air conditioners, electric water heater, and grid electricity with the objective which is to minimize the cost of electricity while also smoothening buy and sell pattern using soft penalty, incorporating with reducing the trading electricity cost with the grid by penalize term power of home to grid and grid to home. The evaluation metric in this proposed problem is the ratio between peak load and mean load, another metric is the difference between the power at previous time index and the current time index, which both expected values should be small.

In actual EMS operation, two time scales of optimization were introduced, including day-ahead and intra-day schemes, to deal with intra-day uncertainty of forecasting data during the day. The concept is to use the solution from day-ahead optimization as parameters for intra-day optimization. There are many literatures that state this, but they differ in system model. [10] and [11] modeled their systems as Model Predictive Control (MPC) and focused mainly on robust optimization, while [12] used an ADMM-based procedure for optimization. The intra-day solution should align with the day-ahead solution, as suggested in [13], [14], and [15], by using the absolute difference between intra-day and day-ahead solutions.

This investigation reveals that Gewertz Square has the potential to serve as a pioneering example of a net-zero energy building, primarily due to an effective implementation of the EMS. Consequently, the primary objective of this project is to develop comprehensive mathematical formulations of the EMS that accommodate various objectives such as economic, operation, and environment proposed as three main different EMS.

- Economic EMS: economic objective depending on user-option selection for uncontrollable historical load consumption.
- Operational EMS: encourage ACs activation while minimize electricity cost and enabling islanding mode for controllable load at machine laboratory room and student room.
- RE 100 EMS: maximize the number of days without purchasing grid electricity.

The formulations will be achieved by modeling the problem as a Mixed-Integer Linear Programming (MILP). Subsequently, the project will simulate the solutions for various scenarios and proceed to implement these optimal solutions within an open-source platform, OpenEMS, thereby establishing effective energy scheduling policies as the device simulation. The actual operation is simulated by two time-scale optimizations, where the alignment of intra-day and day-ahead solutions used the absolute of difference of power relating to the battery.

1.2 Objectives

1. To study about how the EMS affects the energy policies of the desired electrical components in the system from the simulation result of each economic, operational, and environmental objective.
2. To implement the EMS on an open-source platform, OpenEMS.

1.3 Scope

1. Implementation of the algorithm is only within the scope of Gewertz building consisting of 2 buildings (machine laboratory room & student room) as shown in Figure 2.
2. The scope of this project is to construct the mathematical formulation in the concept of an offline EMS with different economic purpose by MATLAB and Python, then implement the algorithm in OpenEMS platform.
3. The electrical components used in EMS formulation at Gewertz building includes load consumption data, solar generation data, and a battery.

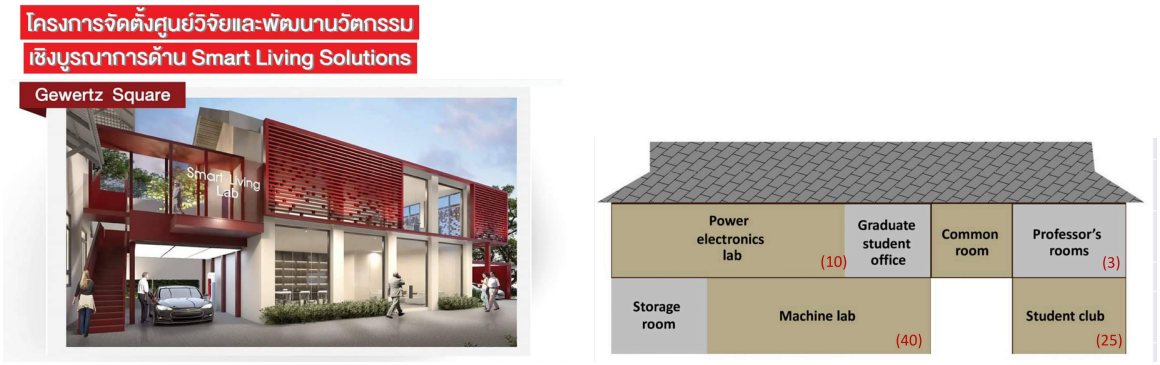

(a) Upcoming Gewertz Square. Photo credit: www.intaniamagazine.com

(b) Gewertz Square layout.

Figure 2: Gewertz Square overview.

1.4 Expected Results

1. Mathematical formulations and simulation results of EMS optimization problem based on different economic and operation objectives.
2. The simulation energy paradigm from optimization solution to the simulated device for each economic purpose exists in OpenEMS platform.

2 Background

This section explains the fundamental knowledge about Energy Management System (EMS) and mathematical formulation of models in the systems.

2.1 Energy Management System (EMS)

Energy Management System (EMS) is a computational and simulation-based system designed to efficiently investigate, manage, and optimize energy on a specific platform using computer technology under different purpose such as reduce the energy utility, electricity cost, and environmental effect. The EMS can be categorized into various aspects, including decision-making approaches, operational levels, operating time, and supervisory control, depending on the perspective. In this project, the primary focus

of the EMS is an offline operating time, and the Building Energy Management System (BEMS) at the operational level as shown in Figure 3.

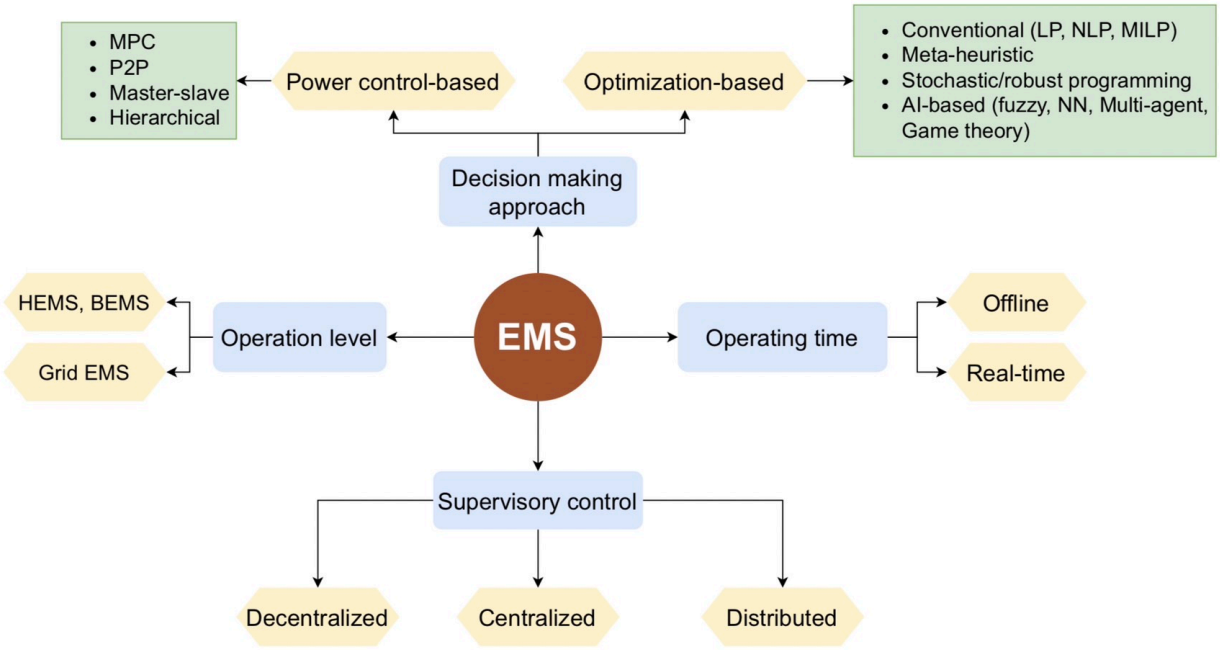

Figure 3: EMS problem under different perspective, Photo credit: www.cept.eng.chula.ac.th/th/news/2023/7681/, Communication Technologies for Grid Edge.

Concerning offline operating time, it implies the utilization of historical data. The distinctive feature is particularly suitable for planning, incorporating an acknowledgement of various factors such as forecasted load consumption, forecasted solar generation, and electricity tariffs to operate virtual real-time operational decision-making. Nevertheless, due to the inherent fluctuation of these variables, the initial planning may not be sufficiently precise, necessitating the transition to real-time operations to make decisions based on current conditions. The BEMS is specifically engineered to facilitate investigation, management, and enhancement of power consumption efficiency for building owners and operators. Its primary objective is the reduction of energy consumption, associated expense, and environmental impact, all while preserving the occupants' comfort or maintaining typical operational activities within the building. The BEMS encompasses both software and hardware components, prominently featuring sensors and controllers. These integrated components function collaboratively to collect, assess, and monitor load consumption quality and profile within the building. The acquired data is then utilized to facilitate real-time adjustments to the system for optimal performance and energy efficiency.

The BEMS functions as a decentralized EMS, gathering the information from both the supply and demand sides via advanced metering systems and ICT infrastructure. It conducts comprehensive analyses to identify unnecessary electricity consumption or instances of excessive usage. Subsequently, it provides recommendations for optimizing energy utilization, highlighting opportunities for more efficient energy usage by operating computation for planing and scheduling energy policies to the devices to function in alignment with these policies to achieve the desired objectives of the operating system.

In order to enable the function of the BEMS for the system by monitoring and formulation of energy policies, the BEMS is required to effectively manage the equity of energy and power across both supply side and demand side. For energy balance, it refers to the equity of total generation of the supply must equal to total consumption of the demand over the specific time interval: day, week, month, year to achieve sufficiency and sustainability. Likewise, for power balance, it also refers that total generating power must equal to total demand power for energy sub-minute interval for stability, security, and economics and environment, which can be reflected as primary, secondary, and tertiary response respectively.

In this project the supply side is mainly from both grid power generation and solar generation. It is the

necessity that this supply must satisfy the demands of systems' load consumption. The load consumption is mainly from historical based load and modeled AC systems. In order to achieve the equity of both the supply side and the demand side, the battery must be involved to manage this efficiently under the condition for economic and operational purpose such as minimizing cost of electricity. The specific feature of the EMS is the capability to monitor the energy and to control the devices in the system, leading to the mathematical formulation of the relation among the devices which is an optimization problem.

2.2 Mathematical formulation of models in the system

As outlined in the scope of work, the electrical components within Gewertz building includes the load consumption, the solar generation, and the battery. To initiate constructing the mathematical formulation, the distinctive characteristics of these electrical components must be elaborated.

2.2.1 Air conditioning system

The majority of the load consumption data is caused by air conditioning system (ACs). There were 4 rooms that were investigated its operational ACs at EE building which are EE 401, EE 404, EE 409, and EE 410. The investigation reveals that there is only 1 room that uses inverter-based ACs which is EE 401, others use non-inverter-based ACs. Based on the investigation findings, the inverter-based ACs demonstrates dynamic transient power consumption levels upon initial activation, stabilizing to its steady-state power consumption after an approximate duration of 20 minutes. However, in this project, the ACs model was constructed based on only the steady-state power consumption of the inverter-based ACs at the EE 401 room which can use power for four levels of its rated power $P_{\text{ac,rated}}$ at 50, 70, 80, and 100 percent.

Let $x_{\text{ac}}^{(j)}(t)$ be the state of using the AC where a 0 indicates the state of turning off and an 1 indicates the state of turning on. The superscript (j) indicates the level of power consumption from its rated power which has 4 levels as stated above. Hence, the constraint of AC power consumption is as the following.

$$P_{\text{ac}}(t) = \left(x_{\text{ac}}^{(1)}(t) + 0.5x_{\text{ac}}^{(2)}(t) + 0.7x_{\text{ac}}^{(3)}(t) + 0.8x_{\text{ac}}^{(4)}(t)\right) P_{\text{ac,rated}}. \tag{1}$$

In addition, the AC can either be turned off or set to one of the four specified levels as stated earlier. Therefore, the constraint of AC operation is as the following.

$$0 \leq \sum_{j=1}^{4} x_{\text{ac}}^{(j)}(t) \leq 1, \quad \text{where } x_{\text{ac}}^{(j)}(t) \in \{0,1\}, \quad \text{for } j = 1,2,3,4 \tag{2}$$

2.2.2 Solar generation

The solar generation in this project is simulated using historical data, as discussed in section 4.2. The power generated by the solar panel must be less than its MPPT (Maximum Power Point Tracking), of which the dynamic is a function of irradiance. But in this project, it is used based on historical solar generation data.

$$P_{\text{pv}}^{\text{max}}(t) = \text{COEFFICIENT} \cdot I(t) \leq \text{INSTALLED CAPACITY}, \quad P_{\text{pv}}(t) \leq P_{\text{pv}}^{\text{max}}(t) \tag{3}$$

2.2.3 Battery

In order to emphasize the demand for load consumption to be aligned with the solar generation, an Energy Storage System (ESS) becomes instrumental in facilitating ongoing operations with reduced reliance on grid electricity. Its primary function involves storing excess energy and subsequently releasing it when there is an insufficient supply, allowing for more efficient management of energy flow.

The battery behaves as the energy storage in this project. There are some definition of the variables that need to be explained. State of Charge (SoC) represents the current battery capacity as a percentage of maximum capacity. When the battery is being charged or discharged, it is charged or discharged as the power which $P_{\text{chg}}(t)$ indicates the charging power into the battery and $P_{\text{chg}}(t)$ indicates the discharging power out from the battery with charging efficiency η_c and discharging efficiency η_d. The battery is modeled to behave relatively similar to its physical counterpart using dynamic equations for the energy stored in the current time index and the percentage of charge or discharge. Hence, the dynamic equation constraint is described by its state of charge, governed by a first-order state equation as shown below.

$$\text{SoC}(t+1) = \text{SoC}(t) + \frac{100}{\text{BattCapacity}} \left(\eta_c P_{\text{chg}}(t) \Delta t - \frac{P_{\text{dchg}}(t) \Delta t}{\eta_d} \right) \tag{4}$$

where BattCapacity is total battery capacity and Δt is time resolution.

In addition, the charge and discharge rate must less than its maximum charging rate and maximum discharging rate respectively. Let $x_{\text{chg}}(t)$ and $x_{\text{dchg}}(t)$ be variables indicating the status of charging and discharging the battery respectively, where 0 indicates the status that is not operating and an 1 indicates the status that is operating. Hence, the constraints limitation of charging and discharging the battery can be shown as below.

$$P_{\text{chg}}(t) \leq x_{\text{chg}}(t) \cdot \text{MAX CHARGE RATE}, \tag{5}$$
$$P_{\text{dchg}}(t) \leq x_{\text{dchg}}(t) \cdot \text{MAX DISCHARGE RATE}. \tag{6}$$

Moreover, the battery cannot be charged and discharged simultaneously. Therefore, for any time index, only one of $x_{\text{chg}}(t)$ and $x_{\text{dchg}}(t)$ is 1. The non-simultaneous charge and discharge constraint is shown below,

$$0 \leq x_{\text{chg}}(t) + x_{\text{dchg}}(t) \leq 1 \quad \text{where } x_{\text{chg}}(t) \in \{0, 1\} \text{ and } x_{\text{dchg}}(t) \in \{0, 1\}. \tag{7}$$

Due to the fact that the physical battery may degrade when it is fully charged or runs out of energy, so the constraint limitation of maximum charge and minimum charge is added to enforce that the energy stored should be within this interval,

$$\text{SoC}_{\text{min}} \leq \text{SoC}(t) \leq \text{SoC}_{\text{max}}, \tag{8}$$

where SoC_{min} and SoC_{max} are minimum and maximum state of charge of the battery respectively.

3 Methodology

The components of the Gewertz building consist of (i) controllable load, (ii) uncontrollable load, (iii) a solar panel, (iv) a battery, and (v) the grid. The load consumption of Gewertz building can be separated into uncontrollable load and controllable load. The uncontrollable load represented loads that cannot be shifted or interrupted in their schedule, such as lights or refrigerators, while the controllable load included the air conditioner systems in the machine laboratory room and student room, as discussed in section 2.2.1. The solar panel is the main power source during daytime, the constraint of solar panel was considered when it was treated as a variable as discussed in section 2.2.2. The battery power can be on either the generation or consumption side depending on the mode, which can be either charging or discharging. The battery model was further explained in section 2.2.3. The last important component is the grid, which is used to buy electricity when the generated power is not adequate and sell electricity when there is excess power generation. The power flow of each component can be shown in Figure 4.

In the proper workflow, the methodology consists of two main sections which are optimization simulation and testing in OpenEMS platform as shown in Figure 6 and Figure 7 respectively. The

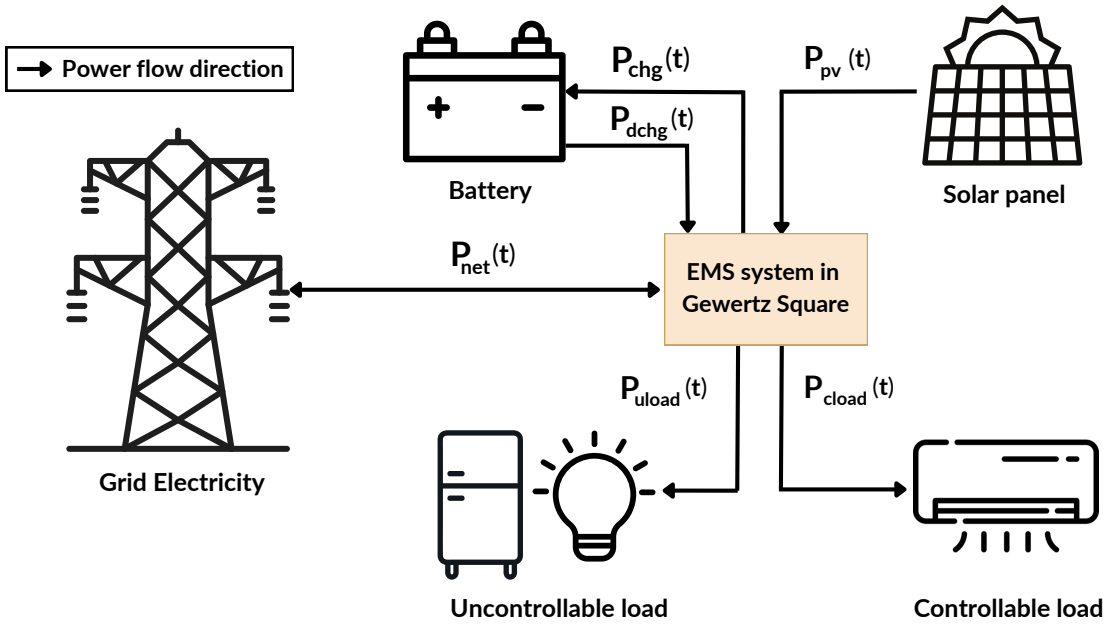

Figure 4: Overall system of EMS.

optimization procedure aims to identify the optimal operation of the EMS and then test in real-time operation on the OpenEMS platform as device simulation.

However, this project focuses on the optimization simulation. The procedure commences with obtaining historical load consumption and solar generation data from Prof. Surapong's meters. Subsequent preprocessing and archival steps are followed by user inputs, including battery specifications, and electricity tariffs, which are added for an EMS simulation. Next, the schedule for each device is obtained by solving optimization problem. The simulation results are then interpreted, assessing the chosen EMS formulation's feasibility, culminating in a conclusive analysis of its mathematical completeness and effectiveness in covering usage scenarios. In the real-time operation, the EMS operates as discussed in section 3.4.3. The contribution of this work lies in the optimization formulations of various EMS objectives and data analytics, as depicted in Figure 5. The EMS has been formulated as optimization problems targeting different objectives. The data analytics contribution pertains to forecasting models, specifically load and solar forecasting used in the actual EMS operation.

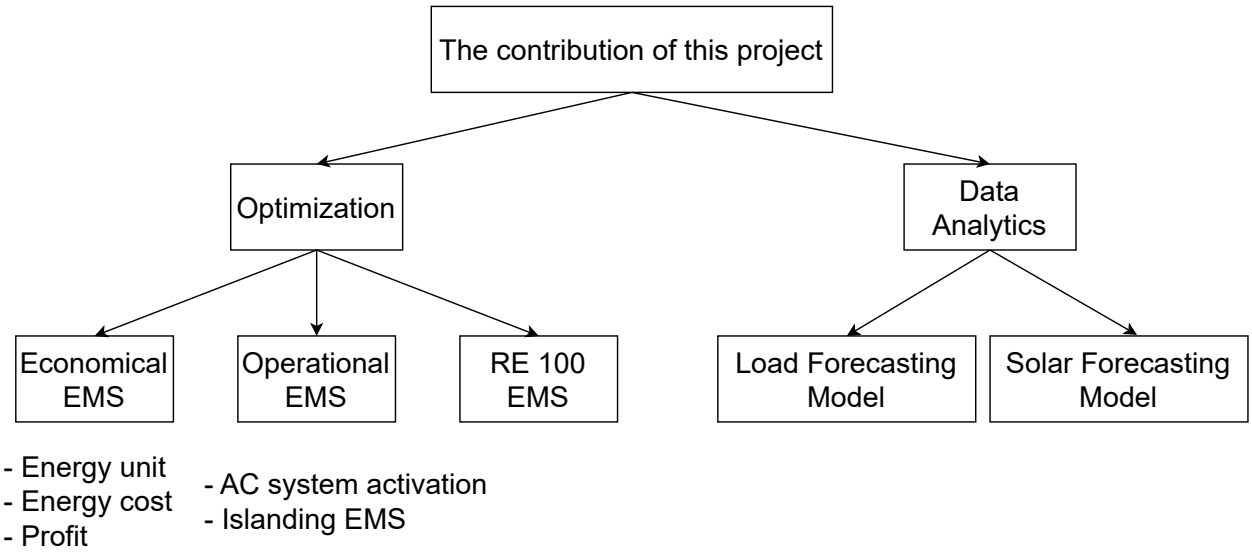

Figure 5: The contribution of this project.

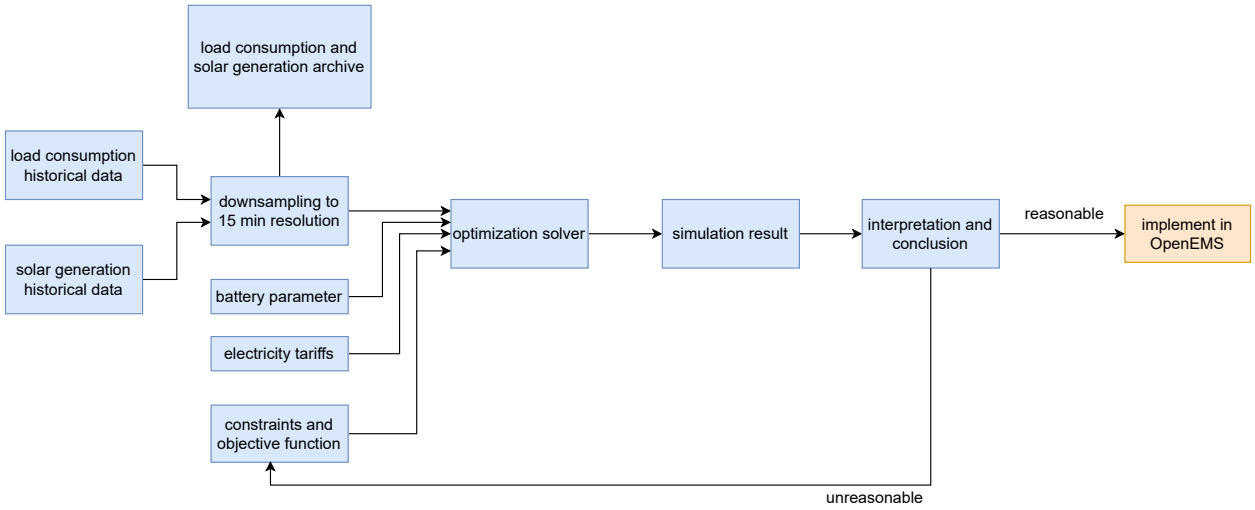

Figure 6: The optimization simulation procedure.

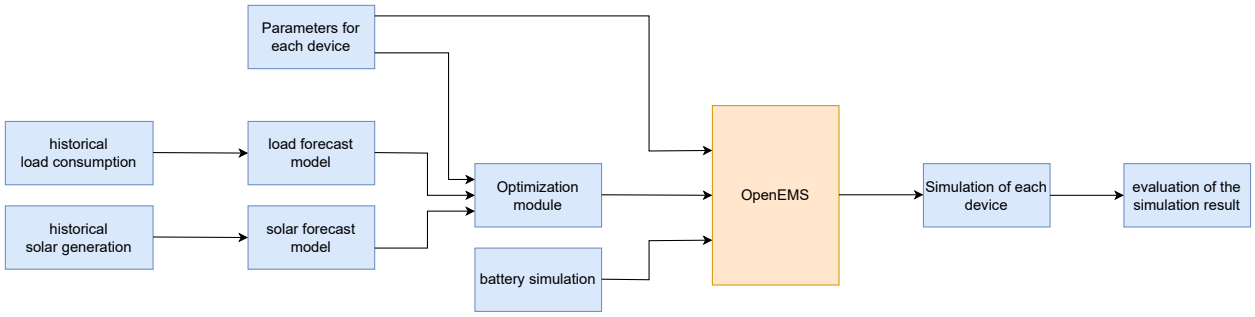

Figure 7: The OpenEMS simulation procedure.

The list of variables and parameters used are shown in Table 1 and Table 2. Also, the values of the parameters used are shown in Table 3.

Table 1: Variables in the system.

Variable	Description	unit
D	Number of day	no unit
t	Time index	no unit
T	Maximum time index	no unit
Δt	Time resolution	hour
$P_{\text{net}}(t)$	Generation power - Consumption power	kW
$P^{-}_{\text{net,d}}$	Upper bound of $P^{-}_{\text{net}}(t)$ in each day d	kW
$P_{\text{pv,hist}}(t)$	Historical solar generation power	kW
$P_{\text{pv}}(t)$	Solar generation power	kW
$P^{(i)}_{\text{chg}}(t)$	Power charged to i^{th} battery	kW
$P^{(i)}_{\text{dchg}}(t)$	Power discharged from the i^{th} battery	kW
$P_{\text{uload}}(t)$	Power of uncontrollable load	kW
$P_{\text{cload}}(t)$	Power of controllable load	kW
$P_{\text{ac,m}}(t)$	Power of AC in machine laboratory room	kW
$P_{\text{ac,s}}(t)$	Power of AC in student room	kW
$\text{SoC}_i(t)$	State of charge of i^{th} battery	%
$x^{(i)}_{\text{chg}}(t)$	Charging status of i^{th} battery	no unit
$x^{(i)}_{\text{dchg}}(t)$	Discharging status of i^{th} battery	no unit
$x^{(j)}_{\text{ac,m}}(t)$	AC status at level j of machine laboratory room	no unit
$x^{(j)}_{\text{ac,s}}(t)$	AC status at level j of student room	no unit
$P_{\text{net,DA}}(t)$	Generation power - Consumption power from DA solution	kW
$P_{\text{net,HA}}(t)$	Generation power - Consumption power from HA solution	kW
$P^{(i)}_{\text{chg,DA}}(t)$	Power charged to i^{th} battery from DA solution	kW
$P^{(i)}_{\text{chg,HA}}(t)$	Power charged to i^{th} battery from HA solution	kW
$P^{(i)}_{\text{dchg,DA}}(t)$	Power discharged from i^{th} battery from DA solution	kW
$P^{(i)}_{\text{dchg,HA}}(t)$	Power discharged from i^{th} battery from HA solution	kW
$\text{SoC}_{i,\text{DA}(t)}(t)$	State of charge of i^{th} battery from DA solution	%
$\text{SoC}_{i,\text{HA}(t)}(t)$	State of charge of i^{th} battery from HA solution	%

Table 2: Parameters in the system.

Parameter	Description	unit
$P_{\text{ac,m,rated}}$	Rated power of AC in machine laboratory room	kW
$P_{\text{ac,s,rated}}$	Rated power of AC in student room	kW
SoC_{min}	Minimum state of charge of battery	%
SoC_{max}	Maximum state of charge of battery	%
η_c	Battery charging efficiency	no unit
η_d	Battery discharging efficiency	no unit
$b(t)$	Electricity buy rate	THB/kWh
$s(t)$	Electricity sell rate	THB/kWh
$w_{\text{ac,m}}$	Weight of AC status of machine laboratory room	no unit
$w_{\text{ac,s}}$	Weight of AC status of student room	no unit
w_{m}	Weight of managing multiple batteries	THB/%
w_{c}	Weight of encouragement charging battery	THB/%
w_{s}	Weight of encouragement smooth charging battery	THB
w_{net}	Weight corresponding to difference between $P_{\text{net}}(t)$ from DA and HA solution	THB/kW
w_{chg}	Weight corresponding to difference between $P^{(i)}_{\text{chg}}(t)$ from DA and HA solution	THB/kW
w_{dchg}	Weight corresponding to difference between $P^{(i)}_{\text{dchg}}(t)$ from DA and HA solution	THB/kW

Table 3: Parameter values in each EMS simulation.

Parameter	Economic EMS			Operational EMS		RE 100 EMS	unit
	Energy unit	Energy cost	Profit	ACs activation	Islanding EMS		
BattCapacity	-	150	150	150	150	125	kWh
SoC_{min}	-	40	40	40	40	20	%
SoC(1)	-	50	50	50	50	50	%
SoC_{max}	-	70	70	70	70	80	%
MAX CHARGE RATE	-	45	45	45	45	30	kW
MAX DISCHARGE RATE	-	75	75	75	75	30	kW
PV install capacity	-	48	48	16	16	50	kW
P_{uload}	-	-	-	< 0.3	< 0.3	-	kW
$P_{\text{ac,m,rated}}$	-	-	-	11.13	11.13	-	kW
$P_{\text{ac,s,rated}}$	-	-	-	6.62	6.62	-	kW
$w_{\text{ac,m}}$	-	-	-	2	2	-	THB
$w_{\text{ac,s}}$	-	-	-	1	1	-	THB
w_{m}	-	0	0	0	0	1	THB/%
w_{c}	-	0	0	0.1	0.1	0	THB/%
w_{s}	-	0	0	0	0	0	THB

3.1 Mathematical formulation of EMS

In this project, the objective of the EMS can be divided into three main objectives which are economic EMS, operational EMS, and RE 100 EMS. Each formulation associated with the electrical components within the system over discrete time index in the horizon t = 1, 2, $\cdots$, T with time resolution 15 minutes. The formulations used the historical data which implies an offline operating system that suitable for planning and scheduling. The historical data included load consumption data, solar generation data, and the other parameters such as battery parameters and the power rated of the load consumption due to air conditioning system.

In the actual operation, the power of all electrical devices must satisfy the power balance which means that the total generation power must equal to the total consumption power. Because of this, the variable $P_{\text{net}}(t)$ was defined in order to calculate how much the electricity needs from the grid, calculating from

$$P_{\text{net}}(t) = \text{total generation power} - \text{total consumption power}. \tag{9}$$

The total generation power includes solar generation power and power discharged from the battery and the total consumption power includes the power used to charge the battery and load consumption which can be further categorized into controllable and uncontrollable loads. Consider the sign of $P_{\text{net}}(t)$, if

- $P_{\text{net}}(t) \geq 0$, there is excess generation, no require power from the grid, and if
- $P_{\text{net}}(t) \leq 0$, there is insufficient power to satisfy the demand side, meaning that the power from the grid is required.

Hence, the power balance can be shown as below

$$P_{\text{net}}(t) = P_{\text{pv}}(t) + P_{\text{dchg}}(t) - P_{\text{uload}}(t) - P_{\text{cload}}(t) - P_{\text{chg}}(t). \tag{10}$$

The battery is crucial in this project, every constraints are considered in options. The battery's explicit constraints are as follows

1. Dynamic equation of the state of charge of the battery (4),
2. Limitation of charging and discharging (5) and (6),
3. Non-simultaneous charge and discharge (7), and
4. Limitation of maximum charge and minimum charge (8).

However, some functionalities may not be satisfied throughout the operation, so the battery-related objective is included in the objective function rather than being in the constraint. Hence, the objective function of the EMS is in the form of,

$$\text{Objective Function} = J_{\text{cost}} + J_{\text{battery}}, \tag{11}$$

where J_{cost} is the main objective term relating to the desired operation of the system of which one of the three options must be chosen by users from economic, operational, and environmental objective which will be discussed later in section 3.1.1, section 3.1.3, and section 3.1.4 respectively, and J_{battery} is the objective relating to the desired battery functionality which will be discussed later in section 3.1.2.

An example of an EMS that aims to minimize electricity costs while maintaining identical SoC patterns across multiple batteries and promoting battery charging can be formulated as an optimizaton problem shown as following,
Let z be the optimization variable for $t = 1, \ldots, T$.

$$
\begin{aligned}
\underset{z}{\text{minimize}} \quad & \text{Energy cost} + (\text{Identical SoC pattern for multibattery Obj.} + \text{Encourage charging battery Obj.}) \\
\text{subject to} \quad & \text{Power balance constraint,} \quad \text{for } t = 1, \ldots, T \\
& \text{Battery dynamic equation constraint,} \quad \text{for } t = 1, \ldots, T \\
& \text{Limitation of maximum and minimum charge constraint,} \quad \text{for } t = 1, \ldots, T \\
& \text{Limitation of charging and discharging constraint,} \quad \text{for } t = 1, \ldots, T \\
& \text{Non-simultaneous charge and discharge constraint,} \quad \text{for } t = 1, \ldots, T
\end{aligned}
\tag{12}
$$

3.1.1 Economic EMS

In terms of economic objective, three aspects of the main objectives were considered including energy unit, energy cost, and profit. The term J_{cost} in the equation (11) depends on the option chosen by the user. The assumption and the goal corresponding to the option is different. The overall system can be shown in Figure 8.

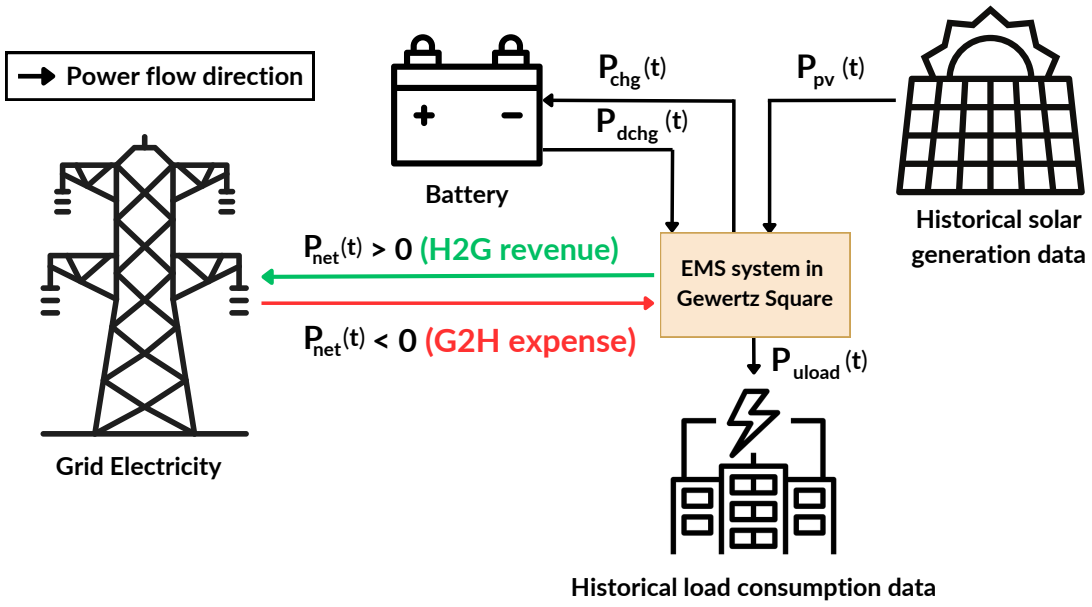

Figure 8: Overall system of **Economic EMS**.

Assumption. The Gewertz building was connected to the MEA grid and could purchase electricity when needed. Because of this, the supply side of the system was from both the grid and solar generation, while the demand side was only from the total load consumption of the Gewertz building. The historical total load consumption and solar generation data were used in this EMS, meaning that they were treated as problem parameters. The battery, serving as the energy storage, was also installed.

Goal. This mathematical formulation was designed to simulate the decision-making process of the EMS regarding electricity purchase and battery scheduling under the objective function, which depends on the user's selection: to minimize the electricity unit, to minimize the electricity cost, or to maximize the electricity profit.

To investigate the decision-making process of the EMS, the decision variables include the net power required from the grid $P_{\text{net}}(t)$, the charging and discharging power of the battery with their respective statuses $P_{\text{chg}}(t)$, $P_{\text{dchg}}(t)$, $x_{\text{chg}}(t)$, $x_{\text{dchg}}(t)$, and its state of charge $\text{SoC}(t)$.

J_{cost} = **Energy unit**. The max function was introduced to obtain the amount of power unit required from the grid when the generation is not adequate for consumption, i.e., when P_{net} is negative, the energy drawn from the grid in the positive value is

$$\text{Energy unit} = \sum_{t=1}^{T} \max(0, -P_{\text{net}}(t))\Delta t. \tag{13}$$

where Δt is time resolution (hour).

J_{cost} = **Energy cost**. To minimize the cost of buying electricity, the expense can be calculated from

$$\text{expense} = \text{buy rate (THB/kWh)} \cdot \text{electricity unit (kWh)}. \tag{14}$$

Then the electricity price in the positive value is

$$\text{Energy cost} = \sum_{t=1}^{T} b(t) \max(0, -P_{\text{net}}(t))\Delta t, \tag{15}$$

where $b(t)$ is a predetermined electricity buy rate (THB/kWh).

J_{cost} = **Profit**. Assuming that the system can sell electricity to the grid (referred to as home-to-grid). The objective function is to maximize the electricity profit which is

$$\text{profit} = \text{revenue - expense} \tag{16}$$

where each term is calculated from

$$\begin{aligned}
\text{revenue} &= \text{sell rate (THB/kWh)} \cdot \text{electricity unit (kWh)} = s(t) \max(0, P_{\text{net}}(t))\Delta t \\
\text{expense} &= \text{buy rate (THB/kWh)} \cdot \text{electricity unit (kWh)} = b(t) \max(0, -P_{\text{net}}(t))\Delta t
\end{aligned}$$

where $s(t)$ is predetermined electricity sell rate (THB/kWh).
So, the profit can be written as

$$\sum_{t=1}^{T} \left[s(t) \max\left(0, P_{\text{net}}(t)\right) - b(t) \max\left(0, -P_{\text{net}}(t)\right) \right] \Delta t$$

To maximize the profit we can minimize the negative profit, which is

$$\text{Profit} = \sum_{t=1}^{T} \left[b(t) \max(0, -P_{\text{net}}(t)) - s(t) \max(0, P_{\text{net}}(t)) \right] \Delta t. \tag{17}$$

The mathematical formulation of **Economic EMS** is shown as below.
Let $z = \left(P_{\text{net}}(t), P^{(i)}_{\text{chg}}(t), P^{(i)}_{\text{dchg}}(t), x^{(i)}_{\text{chg}}(t), x^{(i)}_{\text{dchg}}(t), \text{SoC}_i(t) \right)$ be the optimization variable where $i = 1, 2$ for $t = 1, \ldots, T$.
The optimization problem is,

$$\begin{aligned}
\underset{z}{\text{minimize}} \quad & J_{\text{cost}} + J_{\text{battery}} \\
\text{subject to} \quad & \text{Power balance constraint (10)}, \quad \text{for } t = 1, \ldots, T \\
& \text{Battery explicit constraints (4)} - \text{(8)}, \quad \text{for } t = 1, \ldots, T
\end{aligned} \tag{18}$$

where J_{cost} is the option selected by users from Enegy unit, Energy cost, or Profit, and,
J_{battery} is the desired battery functionality selected by users from Multiple batteries, Charging battery, and Smooth charging battery.

3.1.2 Battery objectives

As stated earlier, some battery functionalities should be added into the objective function. The term J_{battery} can be chosen by users. These include managing multiple batteries, charging them efficiently, and ensuring smooth charging processes. In general J_{battery} is in the form of,

$$J_{\text{battery}} = w_{\text{m}} J_{\text{multibatt}} + w_{\text{c}} J_{\text{chargebatt}} + w_{\text{s}} J_{\text{smoothcharge}}, \tag{19}$$

where w_{m} is a positive weight for identical SoC patterns of multiple battery system,
w_{c} is a positive weight for encouragement charging battery, and
w_{s} is a positive weight for smooth charging battery.

Typically, a system that has n components should operate as if there are $n-1$ devices. In order to preserve the system reliability, the multiple battery system is introduced. Moreover, an important requirement is that each battery should supply the load demand equally to preserve its capacity and performance. However, this requirement may not be satisfied throughout the operation. Therefore, the SoC deviation term, as shown in (20), is added to the cost function instead of being in the constraint,

$$J_{\text{multibatt}} = \sum_{t=1}^{T} \sum_{i=1}^{n-1} \sum_{j=i+1}^{n} |\text{SoC}_i(t) - \text{SoC}_j(t)|, \quad (\%) \tag{20}$$

where n is the number of the battery, and the subscript numbers are the i^{th} and j^{th} battery.
Notably, a system with n components will have $\binom{n}{2}$ summation terms. However, if $n \geq 3$, we can introduce a central variable $\text{SoC}(t)$ and the SoC deviation of each battery can be calculated relative to this central term, so the number of summation terms will be reduced to n terms.

$$J_{\text{multibatt}} = \sum_{t=1}^{T} \sum_{i=1}^{n} |\text{SoC}_i(t) - \text{SoC}_{\text{c}}(t)|, \quad (\%) \tag{21}$$

where $\text{SoC}_{\text{c}}(t)$ is the central variable. In this project, two batteries in the systems are considered, the SoC deviation term in (20) is reduced to

$$J_{\text{multibatt}} = \sum_{t=1}^{T} |\text{SoC}_1(t) - \text{SoC}_2(t)|. \quad (\%) \tag{22}$$

The result of managing multiple battery objective is elaborately explained in section 5.5.

During the daytime, solar generation is the primary source of the system. Excess generation can be curtailed if it is adequate to meet load consumption. Without the encouragement to charge the battery term, the result in the operational EMS shows that the ACs in student rooms are turned off even when there is generation. Hence, including this term may affect the battery to be charged and later uses, resulting in the activation of the AC system. The encouragement to charge the battery term can be pursued by minimizing the difference between the upper bound of the SoC and the actual SoC during operation, as shown below,

$$J_{\text{chargebatt}} = \sum_{t=1}^{T} \left(\text{SoC}_{\text{max}} - \text{SoC}(t)\right) / \left(\text{SoC}_{\text{max}} - \text{SoC}_{\text{min}}\right). \quad \text{(no unit)} \tag{23}$$

Adding encouragement charging battery objective affects the system operation, as shown in Figure 9. Without charging, excess generation is curtailed, resulting in minor priority loads being turned off. But with the charging objective, the battery is charged instead of curtailing the excess generation, allowing the student room's AC system to be turned on for the entire schedule.

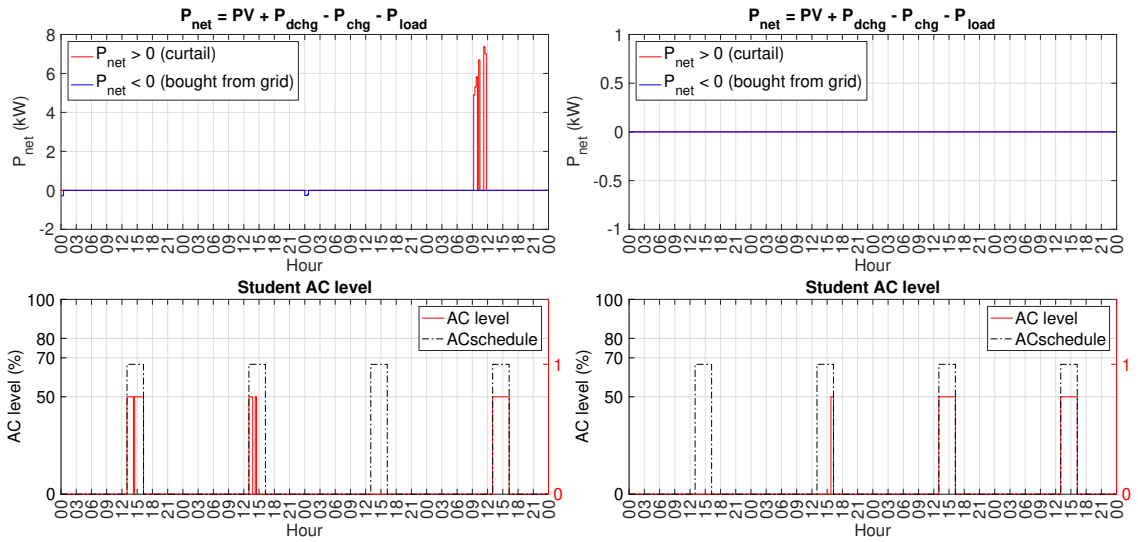

Figure 9: Without and with encouragement charging battery.

Another important aspect is the smooth operation of charging and discharging, which is crucial because fluctuations in rapid charging and discharging during actual operation may impact the battery controller and the energy flow during each state. The encouragement of smooth charging and discharging can be expressed as a penalty on the charging and discharging power at consecutive time indices of the battery, as shown below,

$$J_{\text{smoothcharge}} = \sum_{t=1}^{T-1} \sum_{i=1}^{n} \left| P_{\text{chg}}^{(i)}(t+1) - P_{\text{chg}}^{(i)}(t) \right| + \left| P_{\text{dchg}}^{(i)}(t+1) - P_{\text{dchg}}^{(i)}(t) \right|, \quad \text{(kW)} \tag{24}$$

where the superscript is the i^{th} battery, and n is the number of battery which is 2 in this project. Figure 10 indicates that expenses steadily decrease as the total power difference increases. Observing the weight within the range of 0.0 - 1.0, we found that similar expenses are in this range but total power differences vary. We attempted to adjust the weight, and the results are shown in Figure 11. As the weight to this penalty increases, the charging and discharging profile become smoother.

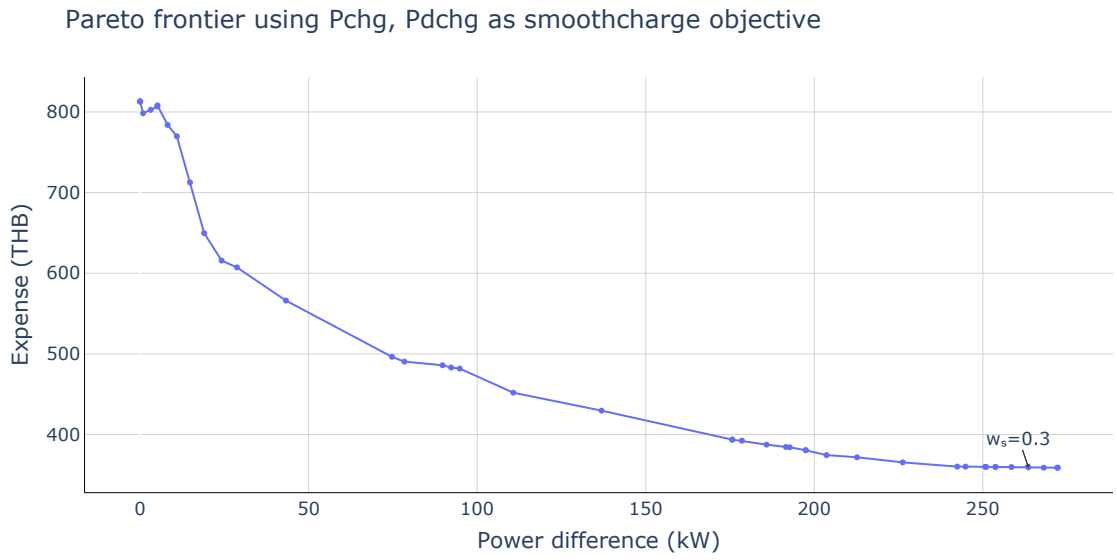

Figure 10: Electricity cost vs. Total power difference.

Note that: In order to tune weight, each term in (24) should be divided by MAX CHARGE RATE and MAX DISCHARGE RATE, respectively.

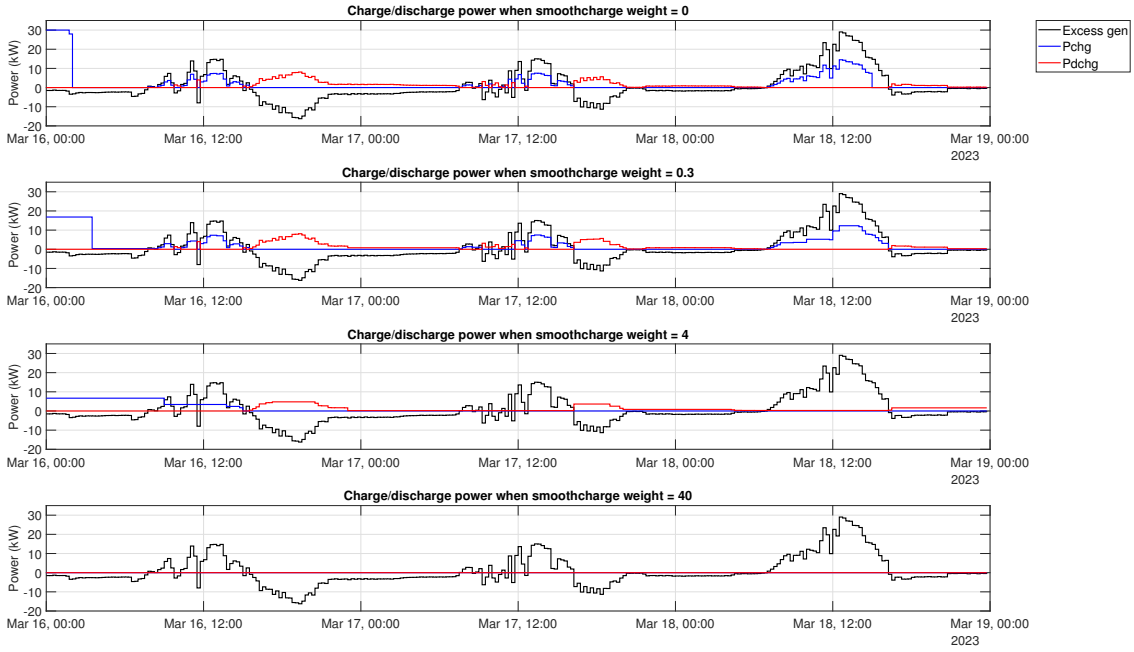

Figure 11: Smooth charging battery under different weights.

Alternatively, the encouragement of smooth charging and discharging can also be expressed as a penalty on the difference in the states of charge and discharge at consecutive time indices of the battery, as shown below,

$$J_{\text{smoothcharge}} = \sum_{t=1}^{T-1} \sum_{i=1}^{n} \left| x_{\text{chg}}^{(i)}(t+1) - x_{\text{chg}}^{(i)}(t) \right| + \left| x_{\text{dchg}}^{(i)}(t+1) - x_{\text{dchg}}^{(i)}(t) \right|, \quad \text{(no unit)} \tag{25}$$

where the superscript is the i^{th} battery, and n is the number of battery which is 2 in this project.

3.1.3 Operational EMS

In terms of operational EMS, it refers to the operation of the demand side, which means that the load can be interruptible. In this EMS, the load consumption is now separated into uncontrollable and controllable loads. The overall system of the operational EMS is shown in Figure 12.

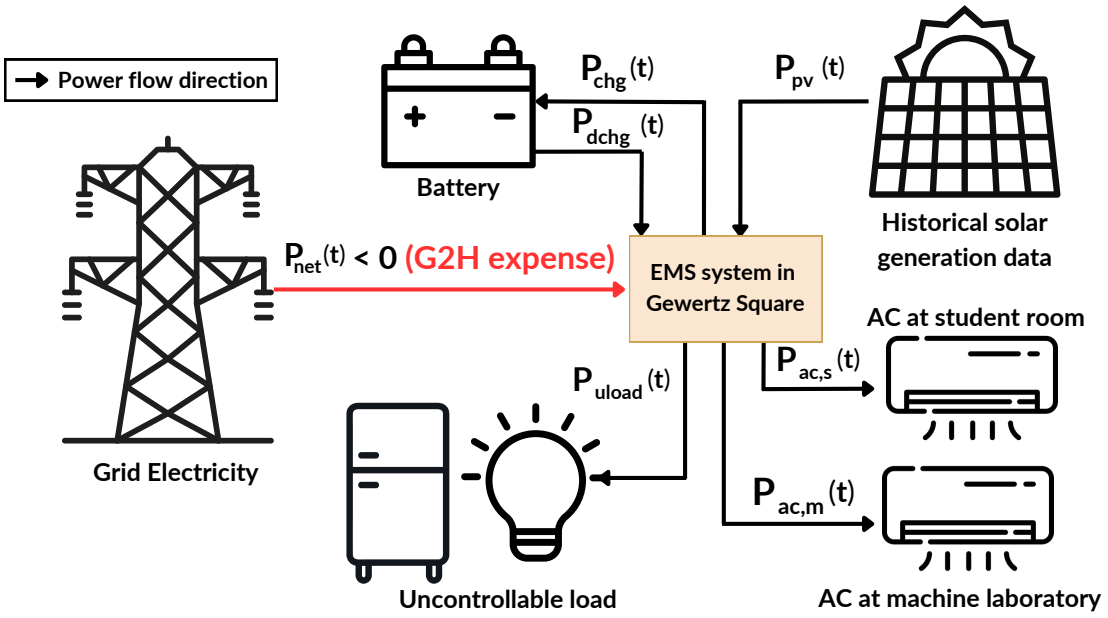

Figure 12: Overall system of **Operational EMS**.

Assumption. We assume that the load consumption is mainly caused by the base load obtained from historical load consumption, treated as uncontrollable load, and the AC systems in two rooms: the machine laboratory room and the student room, treated as controllable load, which have characteristics as specified in section 2.2.1. With this assumption, the net power, $P_{\text{net}}(t)$, is now defined as follows,

$$P_{\text{net}}(t) = P_{\text{pv}}(t) + P_{\text{dchg}}(t) - P_{\text{uload}}(t) - P_{\text{chg}}(t) - P_{\text{ac,m}}(t) - P_{\text{ac,s}}(t).$$

Goal. Similar to the Economic EMS as stated in section 3.1.1, the term J_{cost} can be chosen from Energy unit, Energy unit, and Profit. But in this EMS, the controllable loads are now variables in the optimization problem, the term encouraging AC systems activation in a permissive schedule is added in the objective function as follows,

$$\text{Objective Function} = J_{\text{cost}} + J_{\text{battery}} - \sum_{t \in O} [w_{\text{ac,m}} \sum_{j=1}^{4} x_{\text{ac,m}}^{(j)}(t) + w_{\text{ac,s}} \sum_{j=1}^{4} x_{\text{ac,s}}^{(j)}(t)], \tag{26}$$

where O is an index set containing the time indices for which AC is encouraged,
$w_{\text{ac,m}}$ is a positive weight to encourage air conditioner utilization in machine laboratory room, and
$w_{\text{ac,s}}$ is a positive weight to encourage air conditioner utilization student room.
Notably, the AC system in the machine laboratory has higher priority than the one in the student room, so $w_{\text{ac,m}}$ is chosen to be larger than $w_{\text{ac,s}}$ which both AC systems have the permissible schedule during 1.00 - 4.00 p.m.

The mathematical formulation of **Operational EMS** is shown as below.
Let $z = \left(P_{\text{net}}(t), P_{\text{chg}}^{(i)}(t), P_{\text{dchg}}^{(i)}(t), x_{\text{chg}}^{(i)}(t), x_{\text{dchg}}^{(i)}(t), \text{SoC}_i(t), P_{\text{ac,m}}(t), P_{\text{ac,s}}(t), x_{\text{ac,m}}^{(j)}(t), x_{\text{ac,s}}^{(j)}(t)\right)$ be the optimization variable where $i = 1, 2$ for $t = 1, \ldots, T$.

The optimization problem is,

$$\begin{aligned} \underset{z}{\text{minimize}} \quad & J_{\text{cost}} + J_{\text{battery}} - \sum_{t\in O}[w_{\text{ac,m}} \sum_{j=1}^{4} x_{\text{ac,m}}^{(j)}(t) + w_{\text{ac,s}} \sum_{j=1}^{4} x_{\text{ac,s}}^{(j)}(t)] \\ \text{subject to} \quad & \text{Power balance constraint (10)}, \quad \text{for } t = 1,\ldots,T \\ & \text{AC systems power consumption constraints for both rooms (1)}, \quad \text{for } t = 1,\ldots,T \\ & \text{AC systems operation constraints for both rooms (2)}, \quad \text{for } t = 1,\ldots,T \\ & \text{Battery explicit constraints (4) – (8)}, \quad \text{for } t = 1,\ldots,T \end{aligned} \tag{27}$$

Consider the system operating in the islanding mode, it refers to the elimination of requirement grid electricity. The main challenge occurs when generation exceeds load demand, potentially damaging components in the system. To prevent reverse power flow, solar generation can be curtailed by controlling its inverter, ensuring the total power remains at zero by the specific change within the variable $P_{\text{net}}(t)$. Because of this, more assumption is added in the grid connection system and the solar generation power. The overall system is shown in Figure 13.

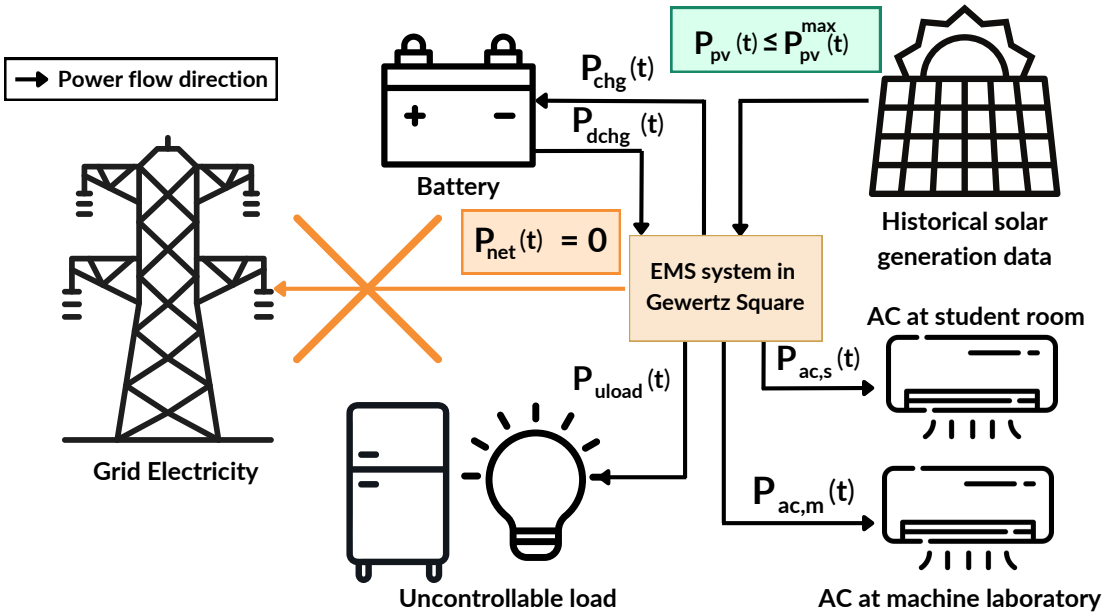

Figure 13: Overall system of **Islanding EMS**.

Assumption. We assume that the system has no connection to the grid and solar generation, $P_{\text{pv}}(t)$, is now treated as a decision variable in the optimization problem. The value of solar generation is adjustable during periods of excess solar generation by reducing the power generation from its MPPT (maximum power point tracking),

$$P_{\text{pv}}(t) \le P_{\text{pv}}^{\text{max}}(t), \tag{28}$$

where $P_{\text{pv}}^{\text{max}}(t)$ is the historical solar generation power,
and the variable $P_{\text{net}}(t)$ was enforced to be zero,

$$P_{\text{net}}(t) = P_{\text{pv}}(t) + P_{\text{dchg}}(t) - P_{\text{uload}}(t) - P_{\text{chg}}(t) - P_{\text{ac,m}}(t) - P_{\text{ac,s}}(t) = 0 \tag{29}$$

Goal. As the system operates in islanding mode, grid electricity becomes unnecessary. Consequently, the objective function within this EMS aims to promote AC operation. The objective function is shown

as follows,

$$\text{Objective Function} = J_{\text{battery}} - \sum_{t \in O} [w_{\text{ac,m}} \sum_{j=1}^{4} x_{\text{ac,m}}^{(j)}(t) + w_{\text{ac,s}} \sum_{j=1}^{4} x_{\text{ac,s}}^{(j)}(t)]. \tag{30}$$

The mathematical formulation of **Islanding EMS** is shown as below.
Let $z = \left(P_{\text{net}}(t), P_{\text{chg}}^{(i)}(t), P_{\text{dchg}}^{(i)}(t), x_{\text{chg}}^{(i)}(t), x_{\text{dchg}}^{(i)}(t), \text{SoC}_i(t), P_{\text{ac,m}}(t), P_{\text{ac,s}}(t), x_{\text{ac,m}}^{(j)}(t), x_{\text{ac,s}}^{(j)}(t)\right)$ be the optimization variable where $i = 1, 2$ for $t = 1, \ldots, T$.
The optimization problem is,

$$\begin{aligned}
\underset{z}{\text{minimize}} \quad & J_{\text{battery}} - \sum_{t \in O} [w_{\text{ac,m}} \sum_{j=1}^{4} x_{\text{ac,m}}^{(j)}(t) + w_{\text{ac,s}} \sum_{j=1}^{4} x_{\text{ac,s}}^{(j)}(t)] \\
\text{subject to} \quad & \text{Solar generation power constraint (28)}, \quad \text{for } t = 1, \ldots, T \\
& \text{Net-zero export power constraint (29)}, \quad \text{for } t = 1, \ldots, T \\
& \text{AC systems power consumption constraints for both rooms (1)}, \quad \text{for } t = 1, \ldots, T \\
& \text{AC systems operation constraints for both rooms (2)}, \quad \text{for } t = 1, \ldots, T \\
& \text{Battery explicit constraints (4) – (8)}, \quad \text{for } t = 1, \ldots, T
\end{aligned} \tag{31}$$

3.1.4 RE 100 EMS

"One hundred percent renewable energy" (RE 100) means that the electricity consumed in the building comes exclusively from renewable energy sources, which are solar generation power and discharging power from the battery. In this project, the achievement of RE is measured within a one-day range. A day qualifies as an RE achievement if there is no power bought from the grid at any time index within that day. The overall system of this EMS is the same as the economic EMS shown in Figure 8.

Assumption. The system of this EMS is similar to the economic EMS, where the primary power source is solar generation, which can be considered renewable energy. In this EMS, the power drawn from the grid is considered regardless of electricity expense, and the desired characteristic of power is either drawing from the grid for the entire day or not drawing at all.

Goal. The aim of this EMS is to achieve RE 100 as many days as possible while satisfying the system's demand. To minimize the power drawn from the grid, which is a negative component of $P_{\text{net}}(t)$ defined as $P_{\text{net}}^{-}(t)$ for the entire day, it makes sense to minimize its upper bound. $P_{\text{net}}^{-}(t)$ is partitioned into $P_{\text{net},d}^{-}$ as the power drawn from the grid in each day d. Consequently, the objective function is to minimize $\|P_{\text{net},d}^{-}\|_{\infty}$. The infinity norm is applied to the loss function to concentrate the optimal solution $P_{\text{net}}(t)$ at $P_{\text{net},d}^{-}$ for each day, and later using the epigraph form technique, the function can be cast a linear programming problem.

The proposed mathematical formulation of RE 100 EMS is shown below.
Let $z = \left(P_{\text{net}}(t), P_{\text{chg}}^{(i)}(t), P_{\text{dchg}}^{(i)}(t), x_{\text{chg}}^{(i)}(t), x_{\text{dchg}}^{(i)}(t), \text{SoC}_i(t)\right)$ be optimization variable where $i = 1, 2$ for $t = 1, 2, 3, \ldots, T$

$$\begin{aligned}
\underset{z}{\text{minimize}} \quad & \sum_{d=1}^{D} \|P_{\text{net},d}^{-}\|_{\infty} + J_{\text{battery}} \\
\text{subject to} \quad & \text{Power balance constraint (10)}, \quad \text{for } t = 1, \ldots, T \\
& \text{Battery explicit constraints (4) – (8)}, \quad \text{for } t = 1, \ldots, T
\end{aligned} \tag{32}$$

where $\max(0, -P_{\text{net}}(t)) = P_{\text{net}}^{-}(t) = \left(P_{\text{net},1}^{-}, P_{\text{net},2}^{-}, \ldots, P_{\text{net,D}}^{-}\right)$, and $d = 1, 2, 3, \ldots, D$.

3.2 Load and Solar forecasting model

The forecasting models in this project are used to forecast future load consumption and solar generation. These forecasts are then utilized by the optimization module to plan the operation of the electrical components. There are two prediction models which are the hour-ahead and the day-ahead forecasting model.

For the load forecasting model, the input features for these models include: (i) past load consumption, (ii) ambient temperature, (iii) machine lab hours, and (iv) machine lab days. To forecast the load profile, the past load consumption and ambient temperature are used as lagged regressors, while lab machine day and hour are used as future regressors for training the NeuralProphet model.

Similarly, the irradiance forecasting model has input features: (i) irradiance of clear sky model as a future regressor and (ii) cloud index as a lagged regressor to predict the solar irradiance by the Neural Prophet model. The irradiance features from National Centers Environmental Prediction (NCEP) and Visual crossing were investigated as the future regressors. After that, convert the predicted irradiance value into predicted solar generation power by multiplying it by a coefficient obtained from linear regression between actual irradiance and actual solar generation power.

3.2.1 NeuralProphet model

NeuralProphet is based on Prophet model and mixed with other techniques such as AR-net for its autoregressive term which can produce more understandable predictive elements [16]. A mathematical model of NeuralProphet is simplified as

$$\hat{y}(t) = T(t) + S(t) + E(t) + F(t) + A(t) + L(t) \tag{33}$$

where:

- $\hat{y}(t)$ is the predicted feature,
- $T(t)$ represents the trend term,
- $S(t)$ denotes the seasonal term,
- $E(t)$ represents the term associated with events,
- $F(t)$ accounts for the effect from future-known exogenous inputs,
- $A(t)$ represents the auto-regression term,
- $L(t)$ accounts for the effect from lagged exogenous inputs.

This model is preferred for its capability to decompose forecasting values into multiple components, based on either the target or the datetime index. It explicitly displays trend, seasonal, and event terms in its output. Additionally, it can be trained using its own lagged target as well as other lagged or future regressors.

3.2.2 Day-Ahead model

The Day-Ahead model forecasts data for the next three days using 15-minute resolution features from the previous day. In this project, $d_p = \frac{\text{minutes in previous day}}{\text{time resolution}} = \frac{1440(\text{minutes})}{15(\text{minutes})} = 96$ and $d_f = \frac{\text{time horizon}}{\text{time resolution}} = \frac{3\times1440(\text{minutes})}{15(\text{minutes})} = 288$.

Load forecasting model

Input features:

(i) Total load consumption in the previous day, $P_{\text{load}}(t), P_{\text{load}}(t-1), \ldots, P_{\text{load}}(t-(d_p-1))$,
(ii) Ambient temperature in the next 3 days, $\hat{T}_{\text{ncep}}(t+1), \hat{T}_{\text{ncep}}(t+2), \ldots, \hat{T}_{\text{ncep}}(t+d_f)$,
(iii) Machine lab hour in the next 3 days, $L_{\text{h}}(t+1), L_{\text{h}}(t+2), \ldots, L_{\text{h}}(t+d_f)$,
(iv) Machine lab day in the next 3 days, $L_{\text{d}}(t+1), L_{\text{d}}(t+2), \ldots, L_{\text{d}}(t+d_f)$,
(v) Solar irradiance in the next 3 days, $\hat{I}_{\text{ncep}}(t+1), \hat{I}_{\text{ncep}}(t+2), \ldots, \hat{I}_{\text{ncep}}(t+d_f)$.

Output features:

Predicted load consumption in the next 3 days $\hat{P}_{\text{load}}(t+1), \hat{P}_{\text{load}}(t+2), \ldots, \hat{P}_{\text{load}}(t+d_f)$.

The load forecasting model under the day-ahead scheme was trained on NeuralProphet model using feature (i) as a lag regressor and (ii) - (v) as future regressors.

Solar forecasting model

Input features:

(i) Solar irradiance in the previous day, $I(t), I(t-1), \ldots, I(t-(d_p-1))$,
(ii) Cloud index in the previous day, $\text{CI}(t), \text{CI}(t-1), \ldots, \text{CI}(t-(d_p-1))$,
(iii) Solar irradiance from clear sky model in the next 3 days, $I_{\text{clr}}(t+1), I_{\text{clr}}(t+2), \ldots, I_{\text{clr}}(t+d_f)$,
(iv) Solar irradiance from NCEP in the 3 days, $I_{\text{ncep}}(t+1), I_{\text{ncep}}(t+2), \ldots, I_{\text{ncep}}(t+d_f)$.

Output features:

Predicted solar irradiance in the next 3 days $\hat{I}(t+1), \hat{I}(t+2), \ldots, \hat{I}(t+d_f)$.

The irradiance forecasting model under the hour-ahead scheme was trained on NeuralProphet model using feature (i) and (ii) as lag regressors and (iii) and (iv) as future regressors.

3.2.3 Hour-Ahead model

The Hour-Ahead forecasts data for the next 60 minutes using 5-minute resolution features with 60 minutes data. In this project, $h_p = \frac{\text{minutes in past time range}}{\text{time resolution}} = \frac{60(\text{minutes})}{5(\text{minutes})} = 12$ and $h_f = \frac{\text{time horizon}}{\text{time resolution}} = \frac{60(\text{minutes})}{5(\text{minutes})} = 12$.

Load forecasting model

Input features:

(i) Total load consumption in the past 60 minutes, $P_{\text{load}}(t), P_{\text{load}}(t-1), \ldots, P_{\text{load}}(t-(h_p-1))$,
(ii) Ambient temperature in the next 60 minutes $\hat{T}_{\text{ncep}}(t+1), \hat{T}_{\text{ncep}}(t+2), \ldots, \hat{T}_{\text{ncep}}(t+h_f)$,
(iii) Machine lab hour in the next 60 minutes $L_{\text{h}}(t+1), L_{\text{h}}(t+2), \ldots, L_{\text{h}}(t+h_f)$,
(iv) Machine lab day in the next 60 minutes $L_{\text{d}}(t+1), L_{\text{d}}(t+2), \ldots, L_{\text{d}}(t+h_f)$,
(v) Solar irradiance in the next 60 minutes $\hat{I}_{\text{ncep}}(t+1), \hat{I}_{\text{ncep}}(t+2), \ldots, \hat{I}_{\text{ncep}}(t+h_f)$.

Output features:

Predicted load consumption in the next 60 minutes $\hat{P}_{\text{load}}(t+1), \hat{P}_{\text{load}}(t+2), \ldots, \hat{P}_{\text{load}}(t+h_f)$.

The load forecasting model under the hour-ahead scheme was trained on NeuralProphet model using feature (i) as a lag regressor and (ii) - (v) as future regressors.

Solar forecasting model

Input features:

(i) Solar irradiance in the past 60 minutes, $I(t), I(t-1), \ldots, I(t-(h_p-1))$,
(ii) Cloud index in the past 60 minutes, $\text{CI}(t), \text{CI}(t-1), \ldots, \text{CI}(t-(h_p-1))$,
(iii) Solar irradiance from clear sky model in the next 60 minutes, $I_{\text{clr}}(t+1), I_{\text{clr}}(t+2), \ldots, I_{\text{clr}}(t+h_f)$,
(iv) Solar irradiance from NCEP in the next 60 minutes, $I_{\text{ncep}}(t+1), I_{\text{ncep}}(t+2), \ldots, I_{\text{ncep}}(t+h_f)$.

Output features:

Predicted solar irradiance in the next 60 minutes $\hat{I}(t+1), \hat{I}(t+2), \ldots, \hat{I}(t+h_f)$.

The irradiance forecasting model under the Hour-Ahead scheme was trained on NeuralProphet model using feature (i) and (ii) as lag regressors and (iii) and (iv) as future regressors.

3.2.4 Model evaluation metric

There are many commonly evaluation metrics which are used to indicate performance of time series prediction. In this project, 6 metrics are computed to evaluate the predicted total load consumption and irradiance including (i) Mean Absolute Error (MAE), (ii) Root Mean Squared Error (RMSE), (iii) Mean Absolute Percentage Error (MAPE), (iv) Normalized Mean Absolute Error (NMAE), and (v) Mean Bias Error (MBE). The mathematical formula of (i) - (v) are defined below.

$\text{MAE} = \frac{1}{N}\sum_{i=1}^{N}\left|y_i - \hat{y}_i\right|$, $\text{RMSE} = \sqrt{\frac{1}{N}\sum_{i=1}^{N}(y_i - \hat{y}_i)^2}$, $\text{MAPE} = \frac{100}{N}\sum_{i=1}^{N}\left|\frac{y_i - \hat{y}_i}{y_i}\right|$,

$\text{NMAE} = \frac{\text{MAE}}{\max_{1\le i\le N}\{y_i\} - \min_{1\le i\le N}\{y_i\}}$, for load forecasting model,

$\text{NMAE} = \frac{\text{MAE}}{\frac{1}{N}\sum_{i=1}^{N} y_i}$, for irradiance forecasting model,

$\text{MBE} = \frac{1}{N}\sum_{i=1}^{N} y_i - \hat{y}_i$

where y_i is ground truth, $\hat{y}_i$ is predicted value, and N is the number of samples. The values of (i) - (iv) are non-negative, with lower values indicating that the predicted values are closer to the actual values. However, MBE can be negative, which means the predicted values tend to be less than the ground truth. A positive MBE indicates that the predicted values are usually higher than the actual values.

3.3 Optimization techniques

Optimization is one of the mathematic problems of which the purpose is to determine an optimal solution of an objective function or a cost function. There are 3 elements of the optimization problem which are optimization variable, an objective function or a cost function, and constraints.

In this context, the optimization is essential for the EMS. Its primary aim is to address the inquiry of how electric devices in the system should function in order to achieve predetermined objectives while satisfying specific constraints imposed by the principles of power equality, the inherent physics governing each device, and operational limitations.

3.3.1 Mixed-Integer Linear Programming (MILP)

To initiate solving the optimization problem, it is essential to determine the type of mathematical formulation. In this project, the formulations were constructed as a Mixed-Integer Linear Programming (MILP) problem.

The MILP is an optimization problem which both objective function and constraints are linear, but restrictions on the optimization variable that has some components which are integer values. In the following, the linear objective function can be written as $c^T x$ and the optimization variable x has the component at $j+1$ to n be the integer values.

Therefore, the MILP is defined by

$$\begin{array}{ll} \text{minimize} & c^T x \\ \text{subject to} & Ax \preceq b \\ & Gx = h \end{array} \tag{34}$$

- $x = (x_1, x_2, \ldots, x_n) \in \mathbf{R}^n$ is the optimization variable where $(x_1, x_2, \ldots, x_j) \in \mathbf{R}^j$ and $(x_{j+1}, x_{j+2}, \ldots, x_n) \in \mathbf{Z}^{n-j}$
- $A \in \mathbf{R}^{m\times n}$ and $b \in \mathbf{R}^m$
- $G \in \mathbf{R}^{p\times n}$ and $h \in \mathbf{R}^p$

3.3.2 MILP solvers

In this section, three optimization solvers were investigated which are (i) MATLAB intlinprog, (ii) Python Scipy, and (iii) Python MIP. The performance of each solver is evaluated by comparing the solving time and optimal value, p^*, for minimizing the feasible LP which guaranteed the feasibility of MILP. There are 50 randomly generated test cases with 100 inequality constraints, 100 bounded real variables, x, and 100 bounded integer variables, z. The standard form of the test cases can be shown below.

$$\begin{array}{ll} \text{minimize} & c^T\tilde{x} \\ \text{subject to} & A\tilde{x} \preceq b \\ & l \preceq \tilde{x} \preceq u \end{array} \tag{35}$$

- $\tilde{x} = (x, z)$ is the optimization variable where $x \in \mathbf{R}^{100}$ and $z \in \mathbf{Z}^{100}$
- $c \in \mathbf{R}^{200}$, $A \in \mathbf{R}^{100\times200}$ is sparse with density 0.1, and $b \in \mathbf{R}^{100}$
- $l, u \in \mathbf{R}^{200}$

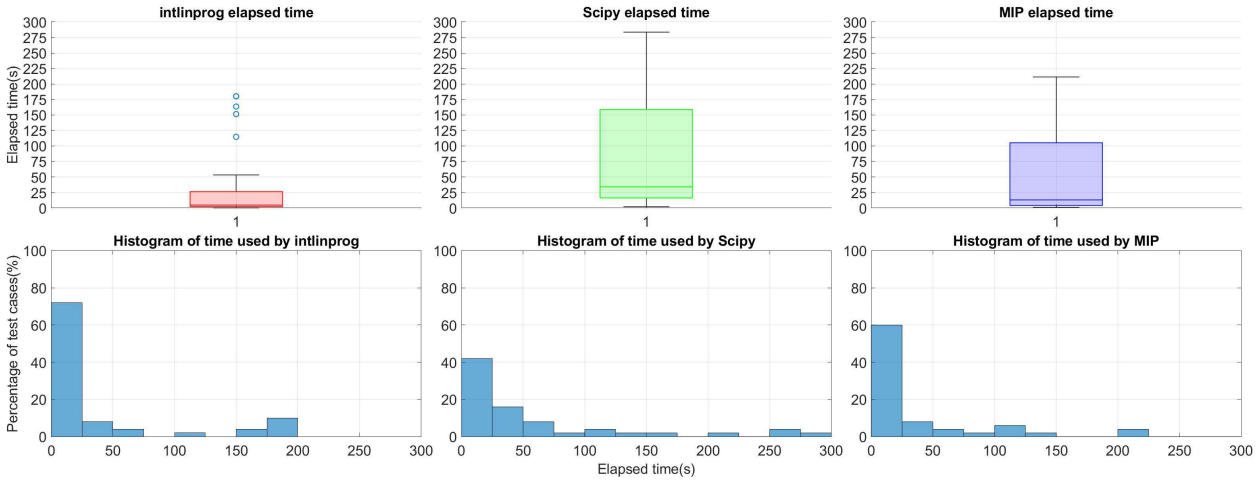

Figure 14: Performance comparation of optimization solvers.

Figure 14 displays the elapsed times of each solver when solving the test cases. It was observed that, while all solvers tended to take less than 50 seconds, intlinprog usually required significantly less time than the others. When looking at the histogram, intlinprog and MIP achieved solutions in under 50 seconds for at least 60% of the test cases. In contrast, Scipy not only had the highest median solving time but also showed a wide range of solving times. Additionally, all solvers returned the same optimal value for all test cases. However, the optimal solutions differed in some batches, as the problem may have had non-unique solutions.

3.3.3 Common objective function pattern

In this work, we often encounter an objective function that relates to electricity expense and revenue. This quantity is typically a function of total net power which can be negative or positive (9). So, the max function is introduced to obtain the power required from the grid, which is only the negative part,

$$c \cdot \max(0, a^T x + b), \quad \text{where } a, x \in \mathbf{R}^n \text{ and } b, c \in \mathbf{R}.$$

of which we can see that this is a nonlinear function. In general, suppose that we have an affine function which can be positive or negative depending on x, we can apply the epigraph form technique by introduce

a new optimization variable t. Then, we can solve the equivalent linear programming instead, yields

$$\underset{x}{\text{minimize}} \quad c \cdot \max(0, a^T x + b) \iff \underset{x,t}{\text{minimize}} \quad t$$
$$\text{subject to } c \cdot (a^T x + b) \leq t \quad \text{and} \quad 0 \leq t,$$

which can be cast a linear objective function with linear constraints, and hence this is linear programming.

The important constraint for the EMS is the power balance constraint (10) which is linear in variables $P_{\text{net}}(t)$, $P_{\text{chg}}(t)$, $P_{\text{dchg}}(t)$, and $P_{\text{cload}}(t)$.
Additionally, the constraints of the system are the constraints related to the electric components which are air conditioning system, solar generation, and battery.
The constraints of airconditioning system are

- The constraint of AC power consumption (1) which is linear in variables $P_{\text{ac}}(t)$, $x_{\text{ac}}^{(1)}(t)$, $x_{\text{ac}}^{(2)}(t)$, $x_{\text{ac}}^{(3)}(t)$, and $x_{\text{ac}}^{(4)}(t)$.
- The constraint of AC operation (2) which is linear in variables $x_{\text{ac}}^{(1)}(t)$, $x_{\text{ac}}^{(2)}(t)$, $x_{\text{ac}}^{(3)}(t)$, and $x_{\text{ac}}^{(4)}(t)$.

The constraint of solar generation is

- The constraint of solar generation (3) which is linear in variable $P_{\text{pv}}(t)$.

The constraints of battery are

- The dynamic equation constraint of battery (4) which is linear in variables $\text{SoC}(t+1)$, $\text{SoC}(t)$, $P_{\text{chg}}(t)$, and $P_{\text{dchg}}(t)$.
- The limitation of charge and discharge constraints (5) and (6), which are linear in variables $P_{\text{chg}}(t)$, $P_{\text{dchg}}(t)$, $x_{\text{chg}}(t)$, and $x_{\text{dchg}}(t)$.
- The non-simultaneous charge and discharge constraint (7), which is linear in variables $x_{\text{chg}}(t)$ and $x_{\text{dchg}}(t)$.
- The limitation of maximum state of charge and minimum state of charge constraint which is linear in variable $\text{SoC}(t)$.

Since, all the constraints above are linear constraints with the binary value variables, $x_{\text{chg}}(t)$, $x_{\text{dchg}}(t)$, and $x_{\text{ac}}(t)$, which are integer. Hence, the formulated mathematical optimization in this project is MILP problem.

The 'intlinprog' is a MATLAB function that we used to find the MILP solution in this project. According to the MATLAB documentation, the 'intlinprog' algorithm has six stages. First, the size of the problem is reduced by removing redundant constraints and variables. Next, the relaxation version of the original problem is solved as a linear programming problem. The constraints of the problem are then tightened or removed. In the following step, cut generation is applied by adding linear inequality constraints to narrow the feasible region of the LP relaxation problem. Various heuristic techniques are used to obtain the upper bound of the objective function. Finally, the Branch and Bound algorithm is used to find the optimal solution.

3.4 EMS operation

One can use the proposed EMS formulations to provide energy planning with a given horizon and resolution. We optimize EMS for two time scales: (i) Day-Ahead (DA) EMS (horizon of 3 days with 15-minute resolution), and (ii) Hour-Ahead (HA) EMS (horizon of 1 hour with 5-minute resolution).

3.4.1 DA EMS

For the DA EMS, we use the 3-day forecast solar generation and load consumption data, shown in Figure 15, from the day-ahead model as parameters to optimize for 3-days ahead.

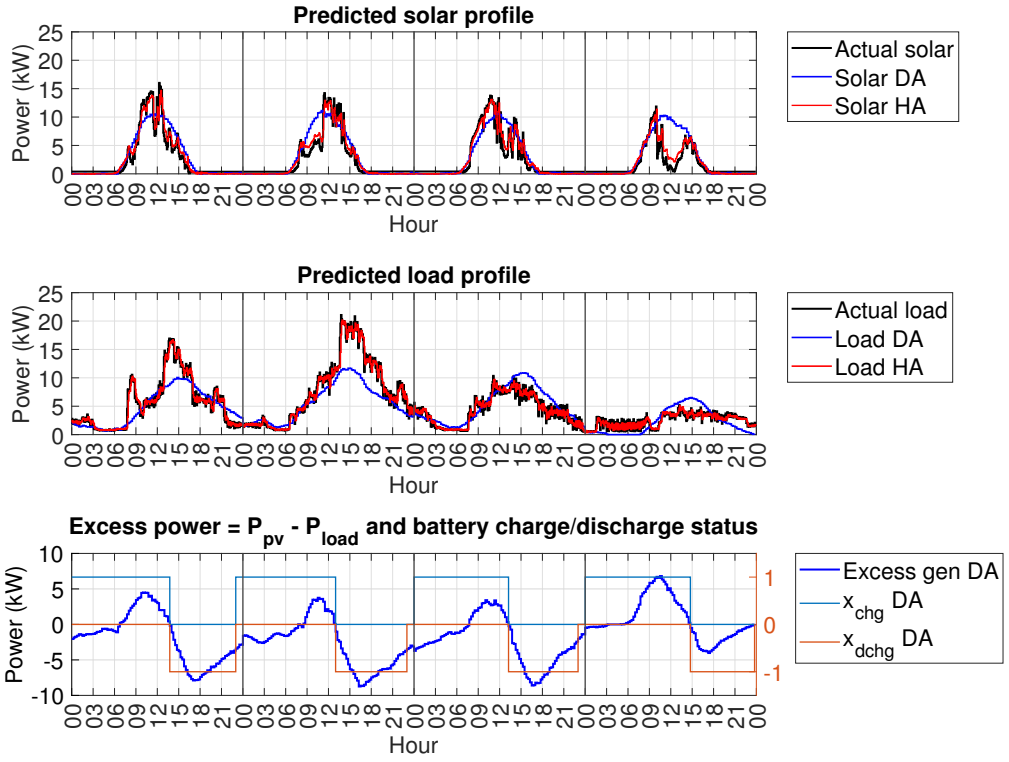

Figure 15: Forecasted load and solar profile with battery status during November $1^{\text{st}} - 4^{\text{th}}$, 2023.

The optimization solution is the optimal system operation of the objectives in the 3-day ahead period, which represents a trade-off between energy cost and battery functionality.

Optimization problem for DA EMS.

Let $z = \left(P_{\text{net,DA}}(t), P^{(i)}_{\text{chg,DA}}(t), P^{(i)}_{\text{dchg,DA}}(t), x^{(i)}_{\text{chg,DA}}(t), x^{(i)}_{\text{dchg,DA}}(t), \text{SoC}_{i,\text{DA}(t)}(t)\right)$ be the optimization variables for $t = 1, \ldots, T$ and $i = 1, 2$.

The DA optimization problem is,

$$\begin{aligned} \underset{z}{\text{minimize}} \quad & J_{\text{cost}} + J_{\text{battery}} \\ \text{subject to} \quad & \text{Power balance constraint (10)}, \quad \text{for } t = 1, \ldots, T \\ & \text{Battery explicit constraints (4)} - \text{(8)}, \quad \text{for } t = 1, \ldots, T \end{aligned} \tag{36}$$

where $T = \frac{\text{DA horizon}}{\text{DA resolution}} = \frac{3\times24\times60}{15} = 288$.

Figure 15 displays the forecasted load and solar profile along with battery status in the DA plan during November $1^{\text{st}} - 4^{\text{th}}$, 2023. It was found that the DA forecasted load and solar profile were inaccurate, especially during 12:00 to 15:00 of each day. When looking at the battery status in the DA plan, the batteries were mostly charged when there was excess generation and discharged when generation was inadequate. The batteries were charged during 00:00 to 06:00 which was quite unreasonable. Since, the generation was deficit but the solution appears to charge the batteries. That was the reason due to the objective of J_{battery}, which promotes the battery to keep charging. Also, the day-ahead forecasting

data is not accurate due to their long prediction horizon. Therefore, we use forecasting data from the hour-ahead model, which has more granularity resulting in higher accuracy, and then optimize for the hour ahead.

3.4.2 HA EMS

Since DA EMS yields the most appropriate decision-making process for the battery in long horizon, while the uncertainty in the short-term should be taken care of. For this reason, the HA EMS should be designed to account for both errors from the DA EMS and optimal planning over the period.

To align the HA solution with the DA solution, we utilize parameters $P_{\text{net,DA}}(t)$, $P^{(i)}_{\text{chg,DA}}(t)$, and $P^{(i)}_{\text{dchg,DA}}(t)$ obtained from the DA EMS. The DA solutions are accounted for HA EMS for a 1-hour window. The HA solutions are encouraged to align with the neighboring DA solution at the closest time (labeled as green arrows) as shown in Figure 16. Notably, the last index of the HA solution aligns with the first DA solution retrieved from DA EMS in the next-hour period.

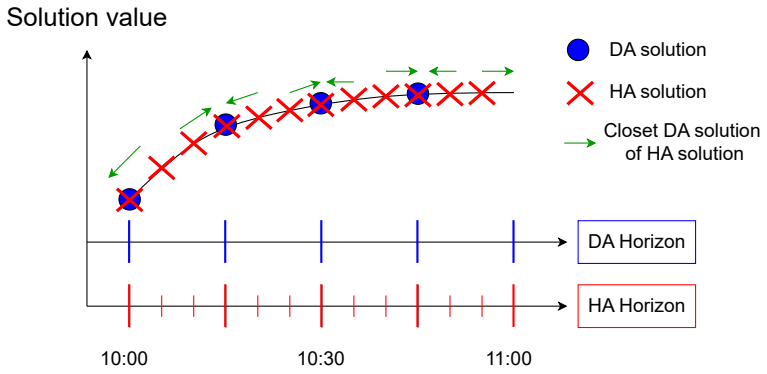

Figure 16: DA solutions accounted for HA solutions for 1 hour.

Since, the number of solutions in 1-hour window of DA and HA optimization are not equal, we introduce $P_{*,\text{ref}}(t)$ as the reference power from DA solution that HA solution must align with, where $*$ is the variable name, e.g. net, chg, and dchg. Hence,

$$P_{*,\text{ref}}(t) = P_{*,\text{DA}}(\tau), \tag{37}$$

where τ is the index of DA solution that is closest to index t of HA solution. For example,

$$P_{*,\text{ref}}(10:00) = P_{*,\text{DA}}(10:00), \quad P_{*,\text{ref}}(10:10) = P_{*,\text{DA}}(10:15), \text{and} \quad P_{*,\text{ref}}(10:20) = P_{*,\text{DA}}(10:15).$$

Therefore, we define the cost of the difference between the DA and HA solutions as

$$\begin{aligned} J_{\text{trackDA}} = \sum_{t=1}^{T} \Bigg\{ & w_{\text{net}} \left| P_{\text{net,HA}}(t) - P_{\text{net,ref}}(t) \right| + w_{\text{chg}} \sum_{i=1}^{2} \left| P^{(i)}_{\text{chg,HA}}(t) - P^{(i)}_{\text{chg,ref}}(t) \right| \\ & + w_{\text{dchg}} \sum_{i=1}^{2} \left| P^{(i)}_{\text{dchg,HA}}(t) - P^{(i)}_{\text{dchg,ref}}(t) \right| \Bigg\}. \end{aligned} \tag{38}$$

The power difference terms are used as HA solution should be close the DA solution. For instance, if we were at 23:25 and solving for HA EMS, $P_{\text{net,DA}}(t)$, $P_{\text{chg,DA}}(t)$, and $P_{\text{dchg,DA}}(t)$ during 23:30 and 00:30 will be used as parameters for HA EMS as shown in Figure 17. By using $P_{\text{net,DA}}(t)$, $P_{\text{chg,DA}}(t)$, and $P_{\text{dchg,DA}}(t)$ as parameters in the objective function, we allow the HA solution to differ from the DA solution if necessary.

Optimization problem for HA EMS.

Let $z = \left(P_{\text{net,HA}}(t), P^{(i)}_{\text{chg,HA}}(t), P^{(i)}_{\text{dchg,HA}}(t), x^{(i)}_{\text{chg,HA}}(t), x^{(i)}_{\text{dchg,HA}}(t), \text{SoC}_{i,\text{HA}}(t)\right)$ be the optimization variables for $t = 1, \ldots, T$ and $i = 1, 2$.
The HA optimization problem is,

$$\begin{aligned} \underset{z}{\text{minimize}} \quad & J_{\text{cost}} + J_{\text{battery}} + J_{\text{trackDA}} \\ \text{subject to} \quad & \text{Power balance constraint (10)}, \quad \text{for } t = 1, \ldots, T \\ & \text{Battery explicit constraints (4)} - \text{(8)}, \quad \text{for } t = 1, \ldots, T \end{aligned} \tag{39}$$

where $T = \frac{\text{HA horizon}}{\text{HA resolution}} = \frac{60}{5} = 12$.

3.4.3 Rolling optimization procedure.

EMS implementation requires both DA and HA planning. The two EMS optimization will be solved in the rolling procedures. Figure 17 illustrates the procedure for the rolling EMS. Assume that we initiate the procedure at the end of day d, i.e., at 23:55 of day d.
Note that:
DA solution for 3-day ahead yields solution 288 steps, denoted as DA(1), DA(2), ..., DA(288).
HA solution for 1-hour ahead yields solution 12 steps, denoted as HA(1), HA(2), ..., HA(12).
The DA and HA planning process is shown as follow.
DA EMS procedure: The following steps repeat daily for day d.

Step 1: Forecast 3 day-ahead load and solar profile using the past 1 day load and solar profile as discussed in section 3.2.2.

Step 2: For $d = 0$, set $\text{SoC}_{\text{DA}}(1)$ equal to SoC(1) as shown in Table 4. Otherwise, set SoC(1) equal to $\text{SoC}_{\text{DA}}(97)$ which corresponding to 00:00 of DA solution from previous DA EMS update.

Step 3: Assign system parameters, as shown in Table 4, to DA EMS.

Step 4: Solve optimization for DA EMS shown in equation (36).

Step 5: Log the first day of DA solution as DA plan.

Step 6: Repeat step 1 - 5 at 23:55 of each day.

HA EMS procedure: The following steps repeat every 5 minutes.

Step 1: Forecast next hour load and solar profile using past hour and solar profile as discussed in section 3.2.3.

Step 2: Construct $P_{*,\text{ref}}(t)$ using DA solution as discussed in (37) and assign as parameters for HA EMS.

Step 3: For 00:00 of day d, set $\text{SoC}_{\text{HA}}(1)$ equal to SoC(1) as shown in Table 4. Otherwise, set each SoC(1) equal to $\text{SoC}_{\text{HA}}(2)$ from previous HA EMS update.

Step 4: Assign system parameters, as shown in Table 4, to HA EMS.

Step 5: Solve optimization for HA EMS shown in equation (39).

Step 6: Log the first 5 minute of HA solution as HA plan.

Step 7: Repeat step 1 - 6 every 5 minute.

The parameters used for both EMS time-scale are shown in Table 4.

Table 4: Parameter values for DA and HA EMS.

Parameter	DA	HA	unit
Resolution	15	5	minute
Horizon	$3 \times 24 \times 60$	1×60	minute
T	$\frac{3 \times 24 \times 60}{15} = 288$	$\frac{1 \times 60}{5} = 12$	no unit
w_{m}	1	1	THB/%
w_{c}	1	0.07	THB
w_{s}	0.3	0.06	THB
w_{net}	0	0.1	THB/kW
w_{chg}	0	0.3	THB/kW
w_{dchg}	0	0.2	THB/kW
BattCapacity	150	150	THB/%
$\mathsf{SoC}_{\mathsf{min}}$	20	20	%
SoC(1)	50	50	%
$\mathsf{SoC}_{\mathsf{max}}$	80	80	%
MAX CHARGE RATE	30	30	kW
MAX DISCHARGE RATE	30	30	kW

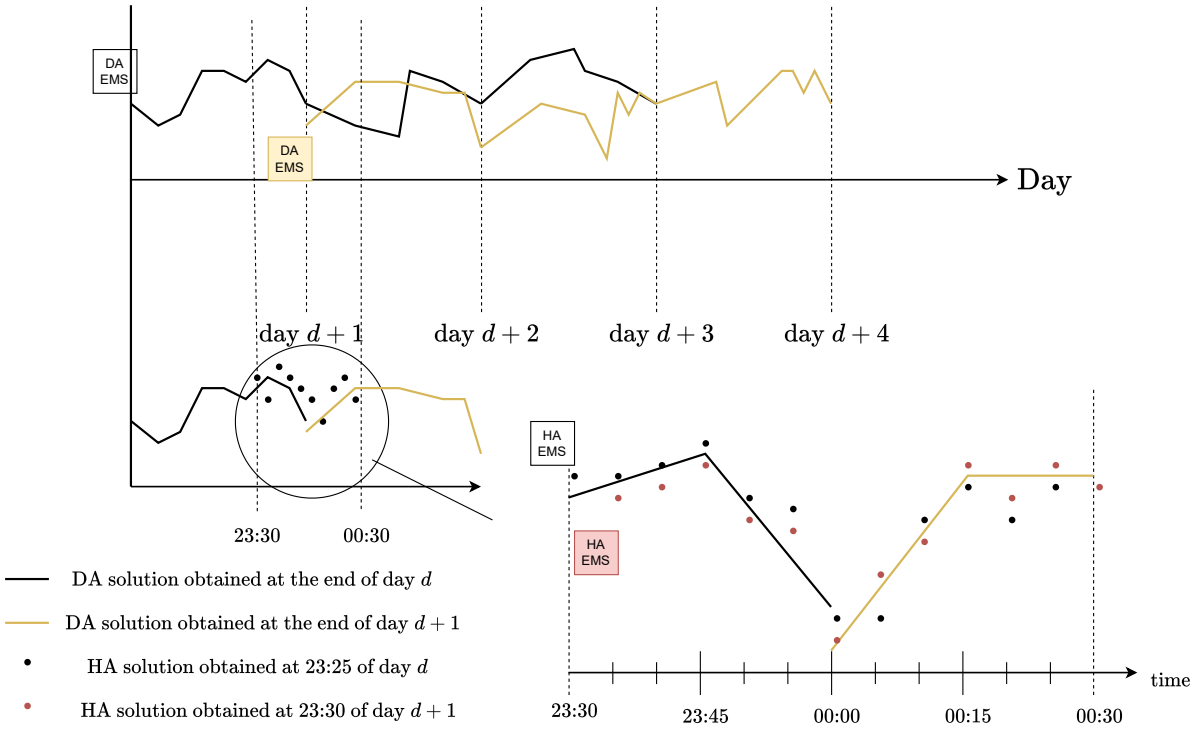

Figure 17: EMS operation procedure.

4 Data Description

This section explains the data which relate to the components and formulations of this project.

4.1 List of data and sources

In the scope of Gewertz building, the electrical components include load consumption, solar generation, and battery. The data used in this project consist of load consumption data, solar generation data, electricity tariffs as the input of forecasting and optimization modules. Also, the solar irradiance and ambient temperature, clear sky model, and cloud index are the input features of load and solar forecasting models.

4.1.1 Load consumption and solar generation data

The load consumption data were received directly from Prof. Surapong's meters at Gewertz building with a time resolution of approximately 670 ms, from March 2023 to February 2024. The maximum peak load of consumption is around 35 kW, occurring in April 2023.

Similarly, the solar generation data were also received directly from Prof. Surapong's meters, but it is the data of solar generation at the EE building, with a maximum installation capacity of 8 kWp. Then, the solar generation data were emulated for use in the entire Gewertz building.

4.1.2 Solar irradiance and ambient temperature

Solar irradiance and ambient temperature data can be obtained from three different sources: (i) EE station, (ii) Visual Crossing, and (iii) NCEP, spanning from January 2023 to December 2023. The resolution from each source is 1 minute, 1 hour, and 15 minutes, respectively. The actual values are obtained from the EE station, while Visual Crossing provides measured data from many stations, shown in Figure 18, which are interpolated weighting closer stations more than farther stations. The closet station is in Bangkok metropolis which is located 4 kilometers away from the EE station. NCEP provides predicted values. Notably, future irradiance can also be predicted using the clear sky model. In this project, solar irradiance and temperature obtained from the EE station are used as ground truth and compared to the others.

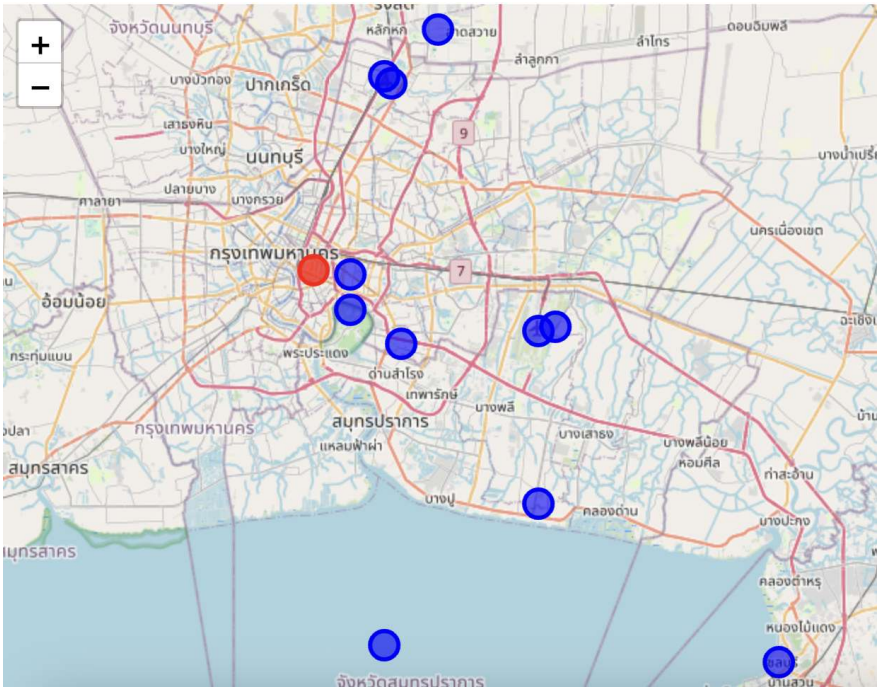

Figure 18: Visual Crossing weather stations, EE building (red) and other stations (blue).

4.1.3 Clear sky model

The clear sky model is a forecasting model that predicts the maximum future irradiance in the absence of clouds, and the value depends on the location. In this case, data from the Gewertz building is selected, with a 5-minute resolution for the HA model and a 15-minute resolution for the DA model, covering the period from January 2023 to December 2023.

4.1.4 Cloud Index

Cloud index is measured data from the Himawari satellite received at the EE station. The image data were transformed into numerical data, with each time index represented in a 9x9 table. However, only the number in the middle pixel was used as the feature of the irradiance model. The data resolution is 10 minutes ranging from January 2023 to December 2023.

4.1.5 Electricity tariffs

Electricity tariffs refer to the purchasing rate for electricity that vary with time of use. In this project, the calculation method utilized is known as Time of Use (TOU) for the university building, due to its installed voltage within the range of 22-33 kV. Under this TOU scheme, there are 2 schemes used in this project which are TOU 0 and TOU 1.

The **TOU 0 scheme** uses the energy charge for this residential category is 5.8 THB/kWh during On-Peak (9.00 a.m. - 00.00 a.m.) and 2.6 THB/kWh during Off-Peak (00.00 a.m. - 9.00 a.m.). In selling scenario, the sell rate is fixed at 2 THB/kWh.

The **TOU 1 scheme** uses the step energy charge 2 THB/kWh (11.00 p.m. - 10.00 a.m.), 3 THB/kWh (10.00 a.m. - 3.00 p.m.), 5 THB/kWh (3.00 p.m. - 6.00 p.m.), and 7 THB/kWh (6.00 p.m. - 11.00 p.m.). In selling scenario, the sell rate is fixed at 2 THB/kWh during 11.00 p.m. - 6.00 a.m. and 2.5 THB/kWh during 6.00 a.m. - 11.00 p.m.

Examples of TOU 0 and TOU 1 are illustrated in Figure 19.

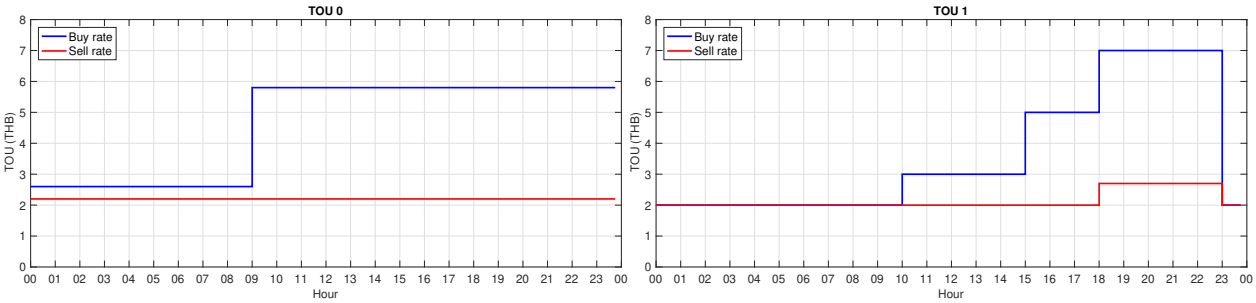

Figure 19: Buy rate and sell rate under TOU 0 and TOU 1 scheme.

4.2 Data pre-processing analysis

After receiving the historical data from the meters, the load consumption and solar generation data were preprocessed by downsampling to 5 minutes and 15 minutes. However, before preprocessing the solar generation data, the solar panel installation capacity in each EMS must be scaled up as follows: Economic and RE 100 EMS have 48 kW, while Operational EMS has 16 kW. Then, each load and solar within the same day was matched for 4 consecutive days, archived as (.mat & .csv) files, and categorized into 6 types: high-load & high-solar, high-load & low-solar, medium-load & high-solar, medium-load & low-solar, low-load & high-solar, and low-load & low-solar. The data spanned from March 2023 to February 2024, resulting in 259 batches of archived historical data. These batches served as parameters for simulating solar generation and uncontrollable load within the context of this project. An example of load consumption and solar generation data is illustrated in Figure 20.

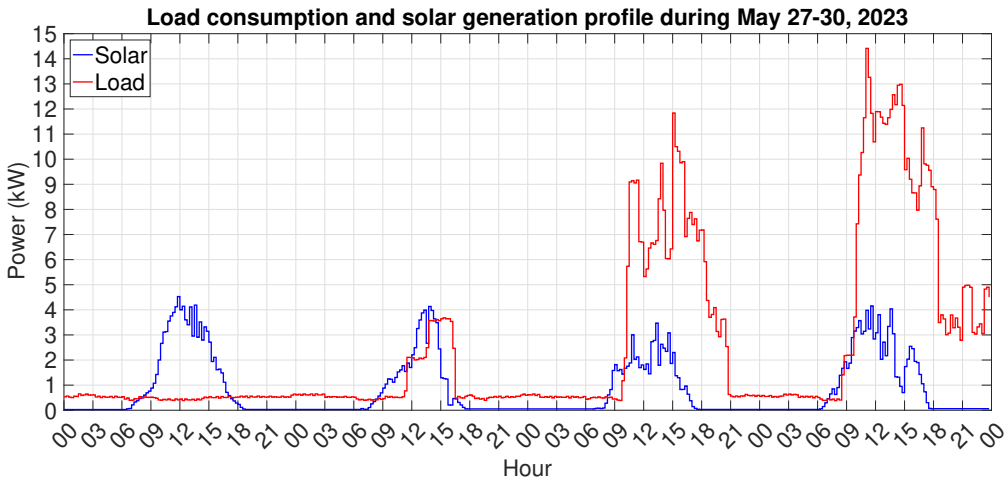

Figure 20: Load consumption and solar generation data during May 27-30, 2023.

4.2.1 Comparison analysis of solar irradiance

To predict solar generation, we must first predict solar irradiance. The accuracy of predicted solar irradiance from different sources was analyzed, as shown in Figure 21. The R-squared of the data is 0.21 and 0.42 for Visual Crossing and NCEP, respectively. In Thailand, sunlight was mostly present in the 7 AM - 6 PM period; therefore, we only measured the error of irradiance values during this period using irradiance from the EE station as the actual value. As depicted in Figure 22, the MAE of irradiance from Visual Crossing was significantly higher than the MAE of irradiance from NCEP in the 7:00 - 10:00 period. However, they were opposite at 17:00. The MAE of irradiance from both sources increased during 7:00 to 12:00 and declined after 13:00. This means that the irradiance from NCEP was closer to the irradiance from the EE station. Since the measured data from Visual Crossing are quite far from the EE station, as stated in section 4.1.2. Therefore, we choose irradiance from NCEP as feature for load and solar forecasting model.

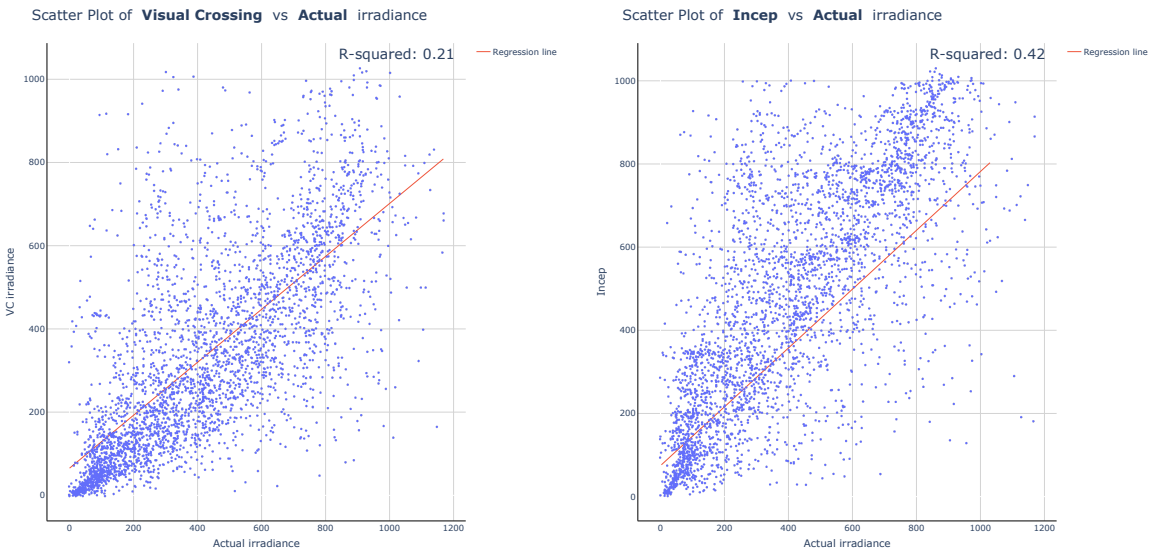

(a) I_{vsc} vs. I_{actual}.

(b) I_{ncep} vs. I_{actual}.

Figure 21: Irradiance from different sources.

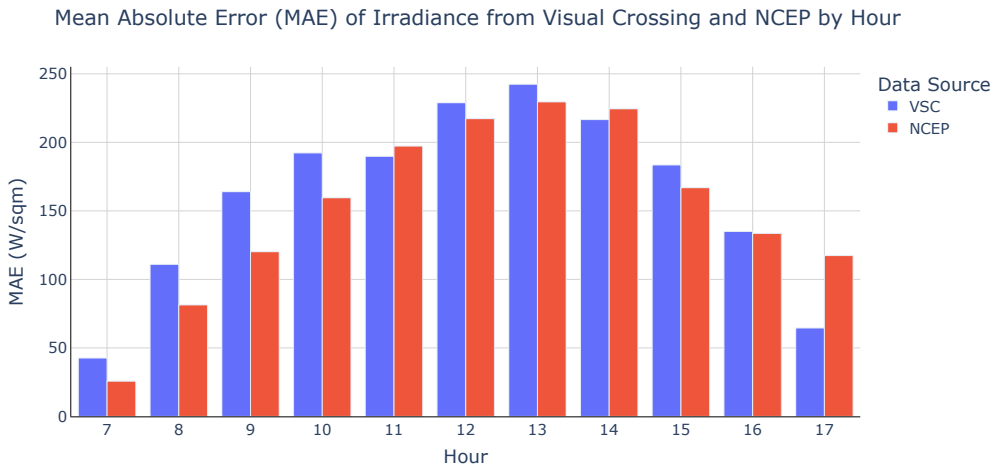

Figure 22: Mean Absolute Error (MAE) of irradiance from different sources.

4.2.2 Comparison analysis of ambient temperature

Figure 23 shows the hourly mean absolute error (MAE) of temperature from Visual Crossing and NCEP. NCEP's MAE consistently exceeded that of Visual Crossing's at every hour. Overall, NCEP's MAE fluctuated around 1.4 degrees Celsius, whereas Visual Crossing's MAE was lower, at less than 1 degree Celsius. This indicates that Visual Crossing's temperature was closer to the EE station's. Despite this, we chose NCEP's temperature as a model feature due to its higher accuracy in solar irradiance.

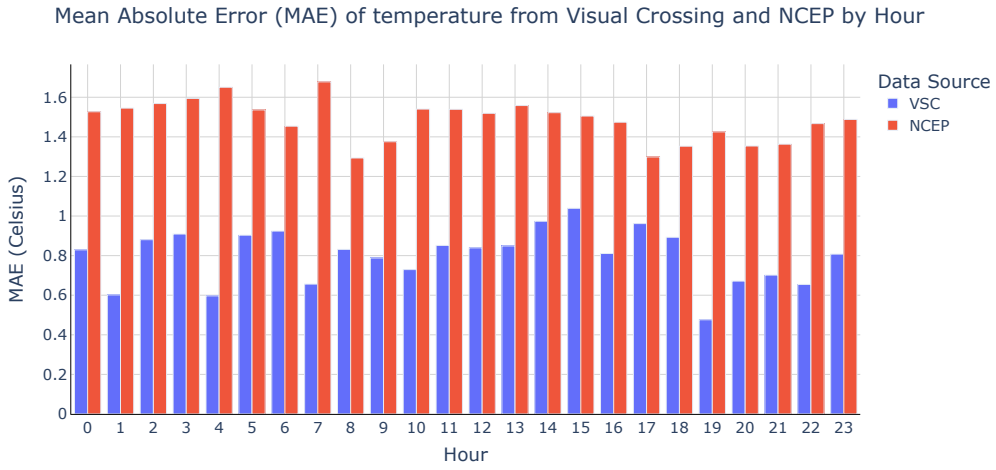

Figure 23: Mean Absolute Error (MAE) of ambient temperature from different sources.

The hourly MAE of irradiance and ambient temperature from different sources is shown in Table 5.

Table 5: Hourly MAE of irradiance and ambient temperature from different sources.

Hourly MAE	Irradiance (W/sqm)		Ambient temperature ($^{\circ}C$)	
	VSC	NCEP	VSC	NCEP
0	-	-	0.83	1.53
1	-	-	0.60	1.55
2	-	-	0.88	1.57
3	-	-	0.91	1.59
4	-	-	0.60	1.65
5	-	-	0.90	1.54
6	-	-	0.92	1.45
7	42.61	25.68	0.66	1.68
8	110.94	81.37	0.83	1.29
9	163.99	120.19	0.79	1.38
10	192.29	159.57	0.73	1.54
11	189.76	197.27	0.85	1.54
12	228.91	217.29	0.84	1.52
13	242.36	229.53	0.85	1.56
14	216.60	224.47	0.97	1.52
15	183.50	166.91	1.04	1.51
16	134.93	133.52	0.81	1.47
17	64.53	117.38	0.96	1.30
18	-	-	0.89	1.35
19	-	-	0.48	1.43
20	-	-	0.67	1.35
21	-	-	0.70	1.36
22	-	-	0.65	1.47
23	-	-	0.81	1.49

4.3 Preparing data for the experiment

4.3.1 Load forecasting model

Before training models, since the load consumption and ambient temperature had some missing data, they were imputed using linear interpolation. Next, the machine lab hour, $L_h(t)$, and machine lab day, $L_d(t)$, were added to the data. The machine lab day was a binary variable where 1 means that there was a lab on that day. The machine lab hour was an integer variable representing the hour of the lab. For example, if it is 4:15 PM, then the value of machine lab hour would be 16. The machine lab hour and day functions were defined as follows.

$$L_d(t) = \begin{cases} 1, & \text{if t is lab day} \\ 0, & \text{otherwise.} \end{cases}$$

$$L_h(t) = \begin{cases} 13, & 13 \leq t \leq 14 \text{ and } L_d(t) = 1 \\ 14, & 14 \leq t \leq 15 \text{ and } L_d(t) = 1 \\ 15, & 15 \leq t \leq 16 \text{ and } L_d(t) = 1 \\ 16, & 16 \leq t \leq 17 \text{ and } L_d(t) = 1 \\ 17, & 17 \leq t \leq 18 \text{ and } L_d(t) = 1 \\ 0, & \text{otherwise.} \end{cases}$$

They were then split into training and validation set with 80:20 ratio. In the following step, The models were trained using training set and evaluated on validation set.

4.3.2 Irradiance forecasting model

In this experiment, there are two irradiance forecasting models: (i) an hour-ahead irradiance forecasting model, and (ii) a day-ahead irradiance forecasting model. The training data of irradiance forecasting model are splitted into training set and test set, one ranges from Jan 1, 2023 to November 30, 2023, another one ranges from December 1, 2023 to December 31, 2023. The time resolution of each model depends on the forecasting scheme discussed earlier in section 3.2.

5 Simulation results

The simulation results consist of seven sections. The first three explains the purpose of the formulations under different economic, operational, and environmental objectives, the advantages of the EMS from an evaluation metric based on the simulation results, the best scenario where the EMS efficiently impacts the energy management policies and the battery functionality. The forth section illustrates the comparison between a single and a double battery system. Then, the renewable energy achievement is discussed in the fifth section for different EMS. Finally, the last two sections depict the load forecasting model and solar forecasting model performances respectively.

5.1 Economic EMS

The primary objective of the mathematical formulation of Economic EMS is to simulate the decision-making process of the EMS regarding electricity purchase and battery scheduling under objective functions that vary based on the user-option selected for the term J_{cost}, as stated in section 3.1.1.

5.1.1 Energy cost: electricity cost saved by EMS

The assumption is that the system can purchase the electricity from the grid when necessary and the goal is to minimize the electricity expense from purchasing grid electricity. The evaluation metric of is to compare electricity expenses of a dataset which is in high load & high solar scenario under TOU 0 and TOU 1. The setting parameters are shown in Table 3.

Figure 24(b) and Figure 24(c) elaborately illustrated that without EMS the expense is around 3,500 THB for TOU 0 and 3,200 THB for TOU 1. The histograms in Figure 24(a) indicate that when both solar generation and load consumption are high, with EMS can generally save expenses from without EMS amounting to 850 THB and 950 THB under TOU 0 and TOU 1 respectively, concluding that because the charaterisitic of TOU 1 that has higher price in the evening results to the charge of battery during daytime to discharge in the nighttime instead of utilizing grid electricity in order to reduce the expense. Another same dataset illustrated in Figure 25 and Figure 26 indicate that the EMS can reduce the electricity expense up to 950 THB under TOU 0 and up to 1,150 THB under TOU 1. Additionally, the EMS is beneficial to the purpose of reduction the electricity cost in every scenario for both TOU 0 and TOU 1 as shown in section 9.2.

Also, the EMS effectively manages battery operations. Shown in Figure 25, when solar generation exceeds consumption, the battery charges; conversely, when consumption surpasses solar generation, the battery discharges within the state of charge range, avoiding simultaneous charging and discharging. Since the daytime buy rate is flat, the battery's charge and discharge depend solely on excess power generation. However, when the TOU changes to a ladder system as depicted in Figure 26, the battery is significantly charged during the low-price period by both excess power generation and grid power, to supply the load during the high-price period. On the last day, despite reaching maximum state of charge, there is high expense due to insufficient battery generation and discharge to meet the huge demands, resulting in the need to purchase grid electricity. The histogram of negative energy, which represents the energy drawn from the grid as shown in Figure 27, indicates that both TOU schemes require the same amount of energy. However, as discussed earlier, the pattern of TOU significantly affects the electricity. cost.

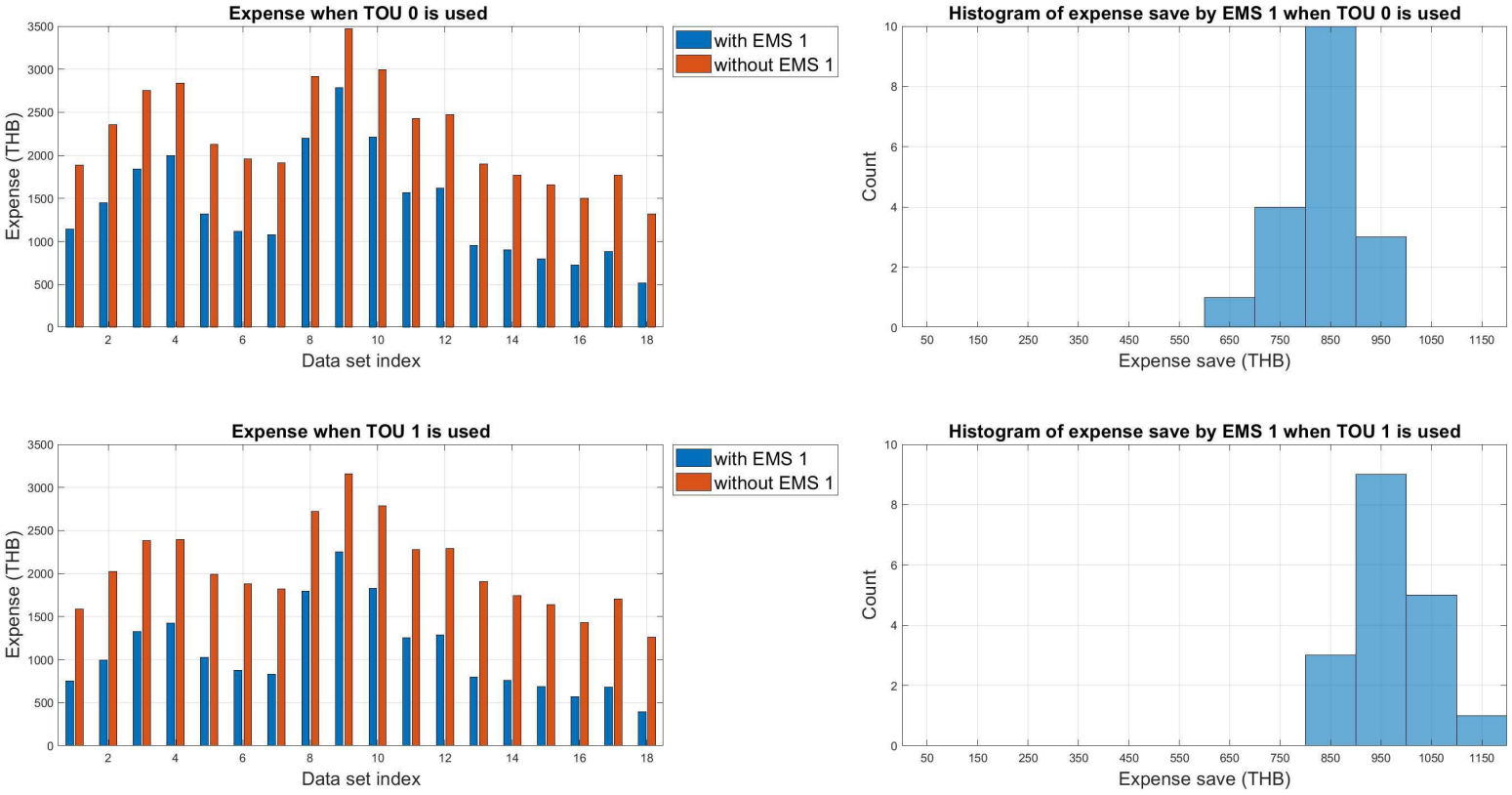

(a) Histogram of expenses saved under TOU 0 and TOU 1.

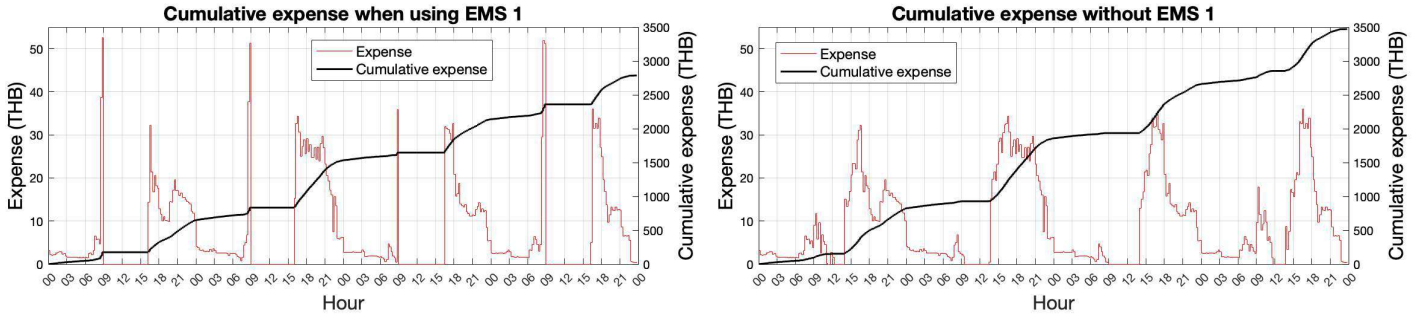

(b) under TOU 0.

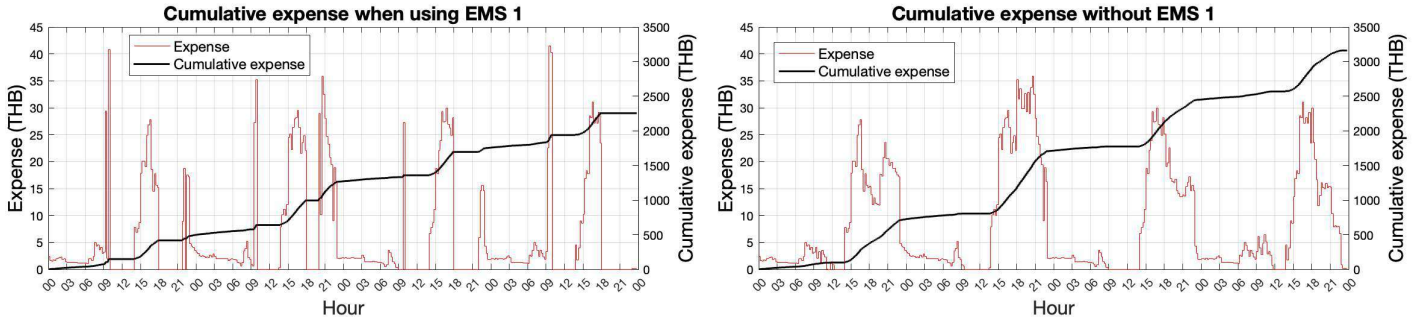

(c) under TOU 1.

Figure 24: Electricity expenses saved by Energy cost option in high load & high solar scenario.

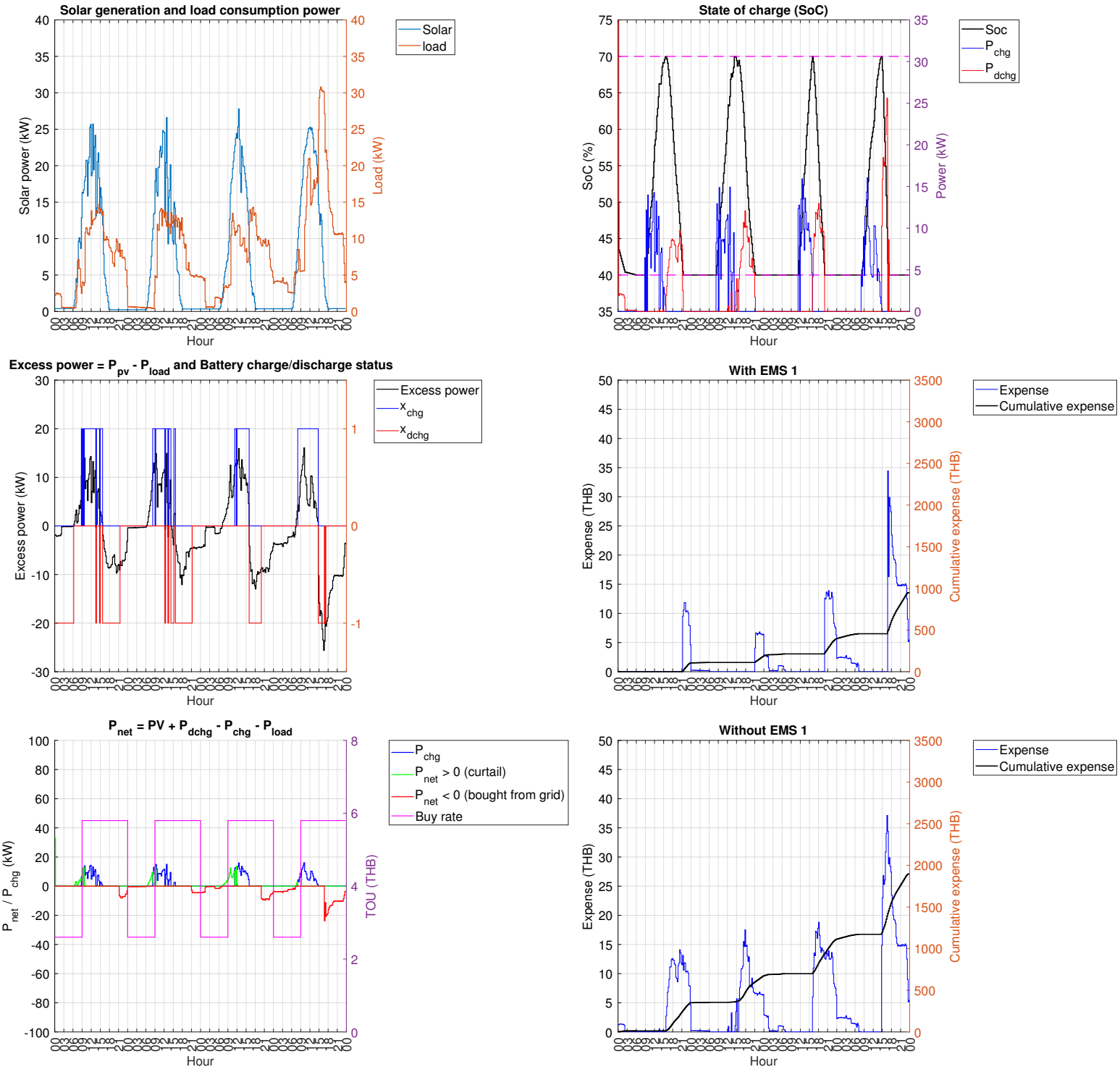

Figure 25: Overall operation of Energy cost option under **TOU 0** in high solar & high load scenario.

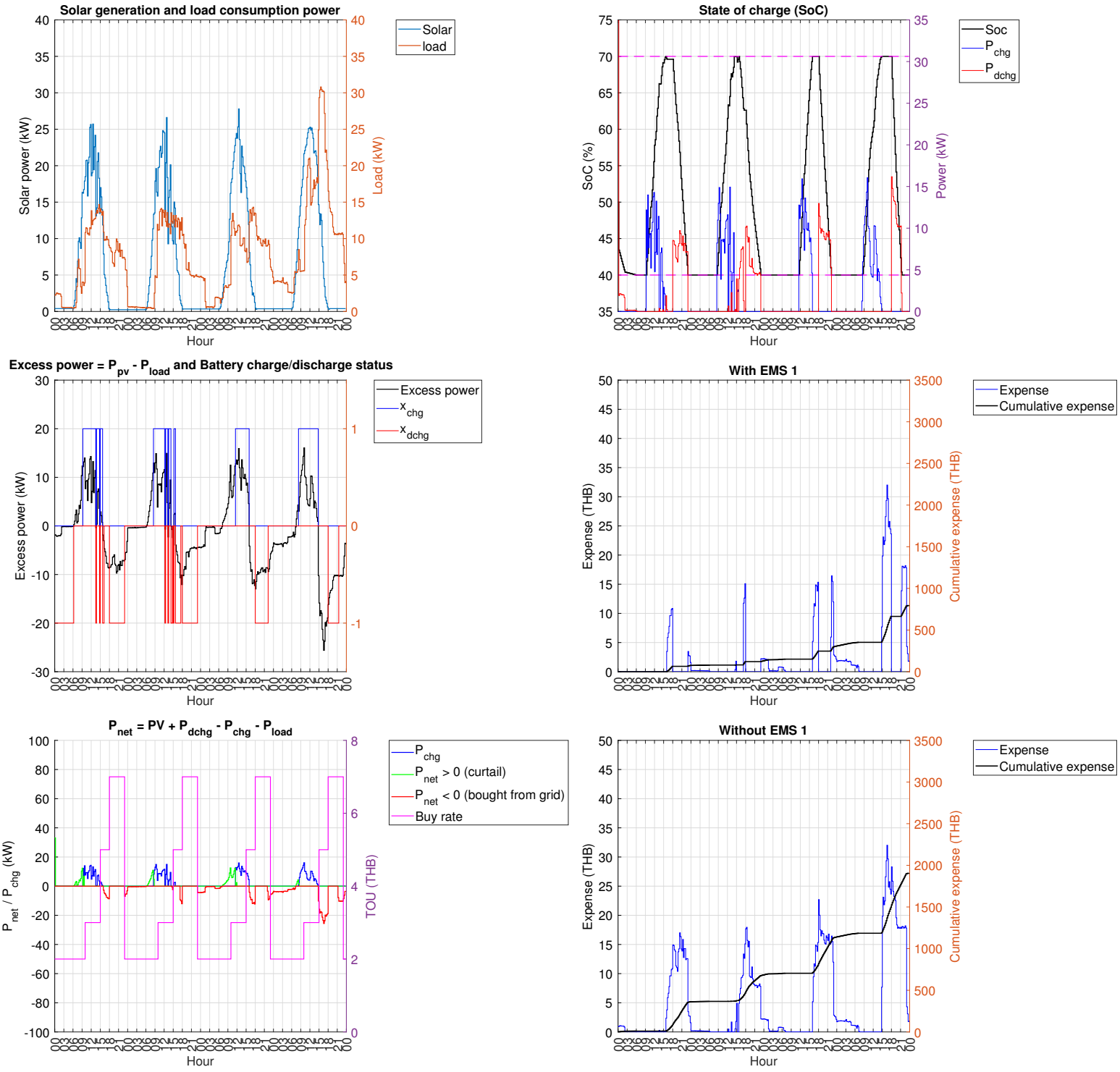

Figure 26: Overall operation of Energy cost option under **TOU 1** in high solar & high load scenario.

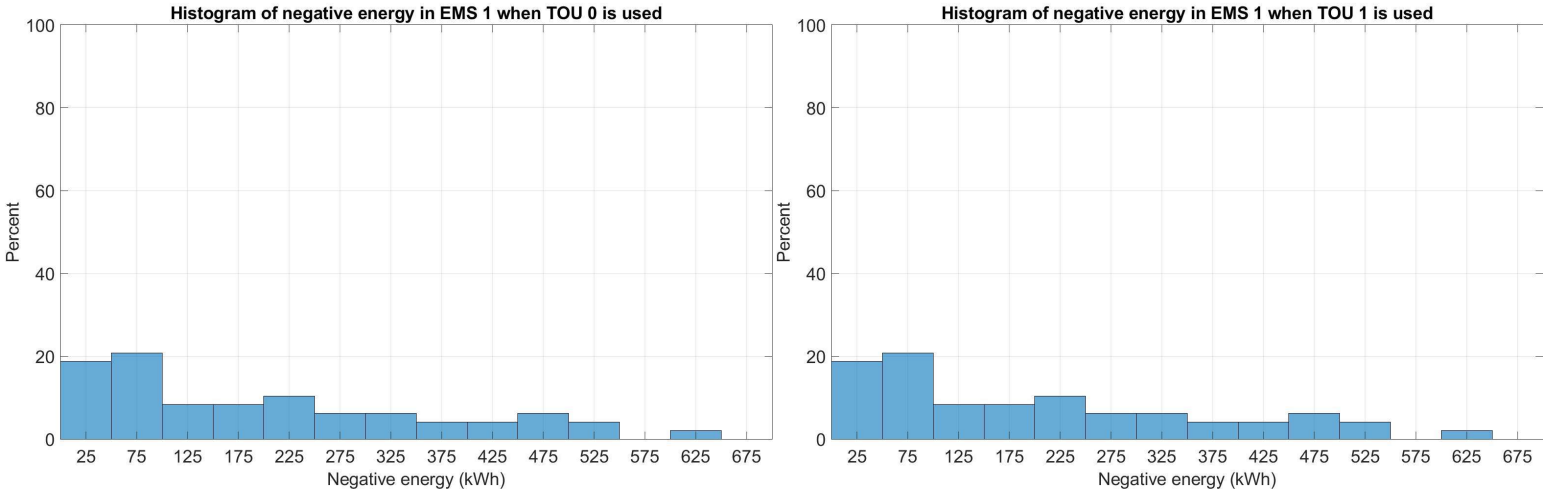

Figure 27: Histograms of negative energy in Energy cost option under TOU 0 and TOU 1.

5.1.2 Profit: electricity profit increased by EMS

The assumption is similar when users select 'Energy cost' as the option, but differs in system's capability to sell electricity to the grid. The evaluation metric of this EMS is to compare electricity profit of a dataset which is in high load & high solar scenario under TOU 0 and TOU 1. The setting parameter is shown in Table 3.

Without EMS, the net expense for the 4-day period is around 3,300 THB for TOU 0 and 3,000 THB for TOU 1. The details corresponding to those days under TOU 0 and TOU 1 were plotted as in Figure 28(b) and Figure 28(c) respectively. The cumulative profit shows that using EMS lowers electricity costs compared to without EMS, reducing them by about 550 THB for TOU 0 and 750 THB for TOU 1. The histograms shown in Figure 28(a) indicate that when both solar generation and load consumption are high, the EMS can generally save expenses amounting to 575 THB and 725 THB under TOU 0 and TOU 1, respectively. This conclusion stems from the characteristic of TOU 1, which has higher prices in the evening, resulting in the battery charging during the daytime to supply demands during the nighttime instead of purchasing grid electricity. Another same dataset which is in high solar & low load scenario was illustrated in Figure 29 and Figure 30, which gained the profit up to 300 THB under TOU 0 and 250 THB under TOU 1. The expenses saved by EMS for the other scenarios shown in section 9.3.

The EMS effectively manages battery operations. But in this EMS that is capable of selling the electricity to the grid, Figure 29 shows that under TOU 0 on day 2, the battery is charged during excess generation period but there is some period that the power is sell to the grid instead of charging the battery in order to obtain the revenue. Besides, the battery always discharges when there is insufficient excess generation especially when the electricity price is high. But in the case under TOU 1 as shown in Figure 30, the battery managed to sell the electricity from discharging during high selling price period in order to obtain the revenue as mush as possible while maintain the less expense for the entire period to satisfy the objective function which is to maximize electricity profit. The histogram of energy drawn from the grid, as shown in Figure 31, indicates that TOU 1 has a distribution that requires more energy than that of TOU 0. This is likely because of the need to draw energy during low-price periods to sell or use it during higher-price periods.

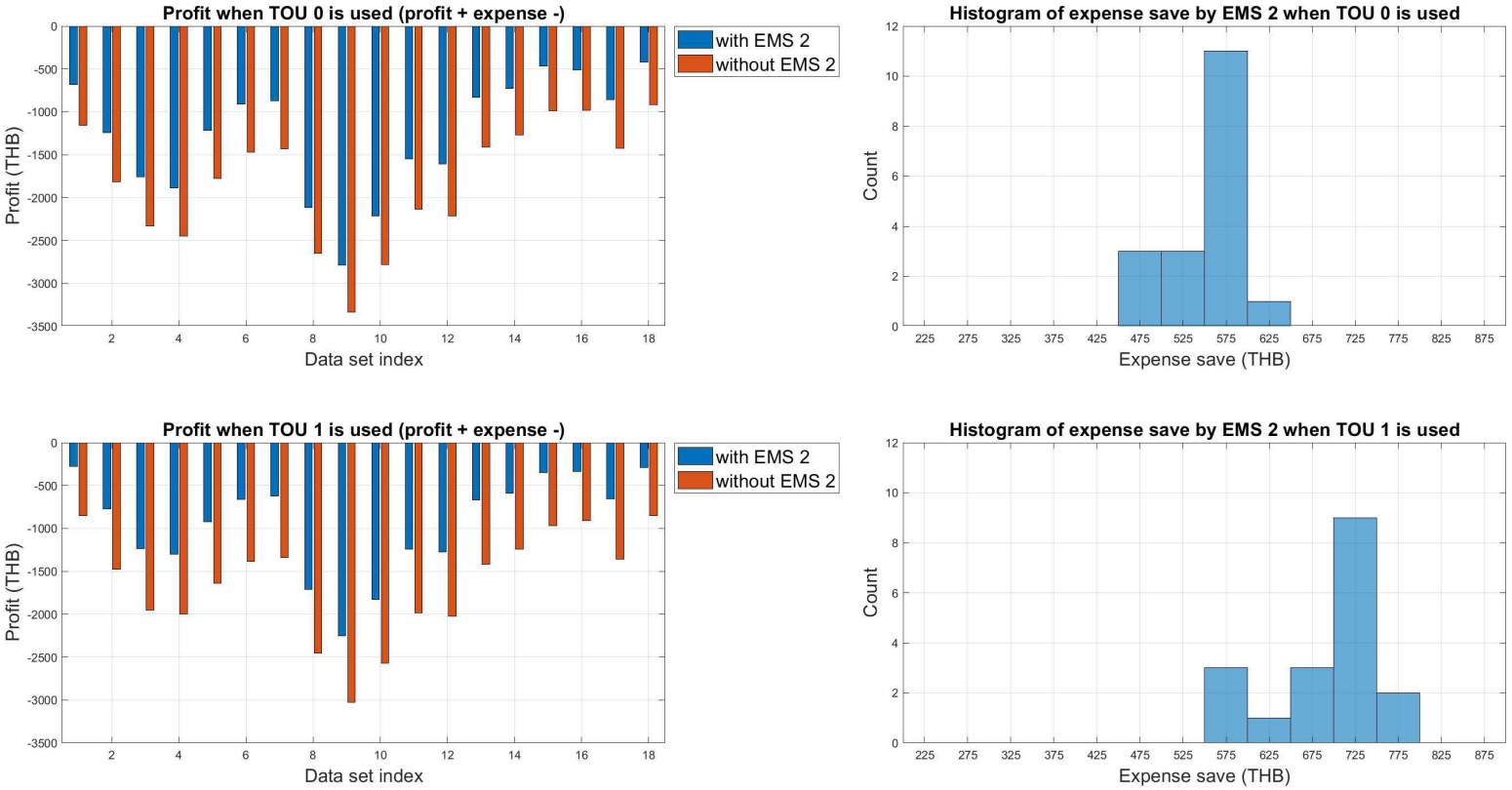

(a) Histogram of expenses saved under TOU 0 and TOU 1.

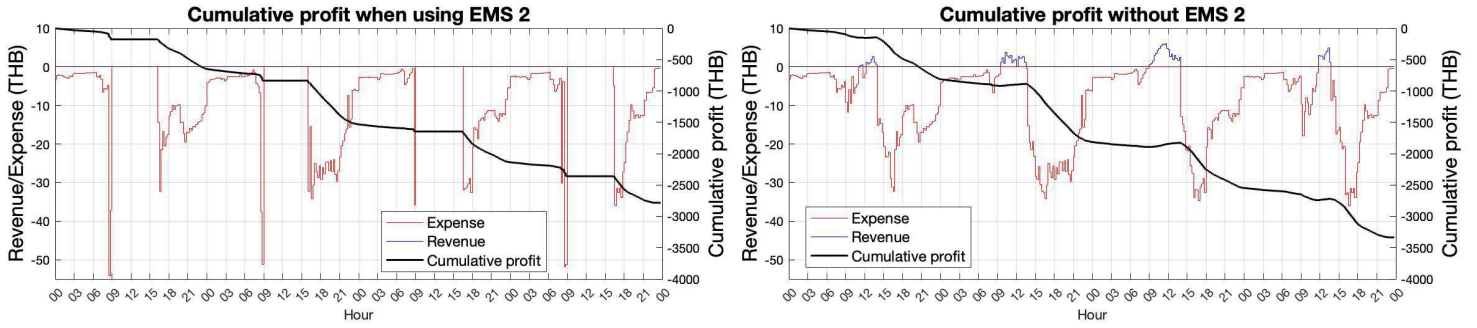

(b) under TOU 0.

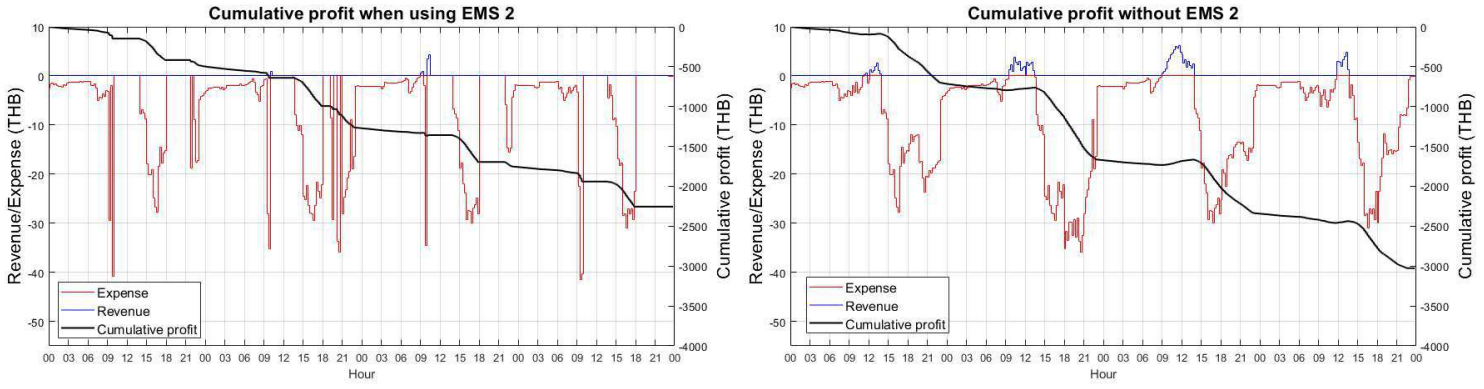

(c) under TOU 1.

Figure 28: Electricity expenses saved by Profit option in high load & high solar scenario.

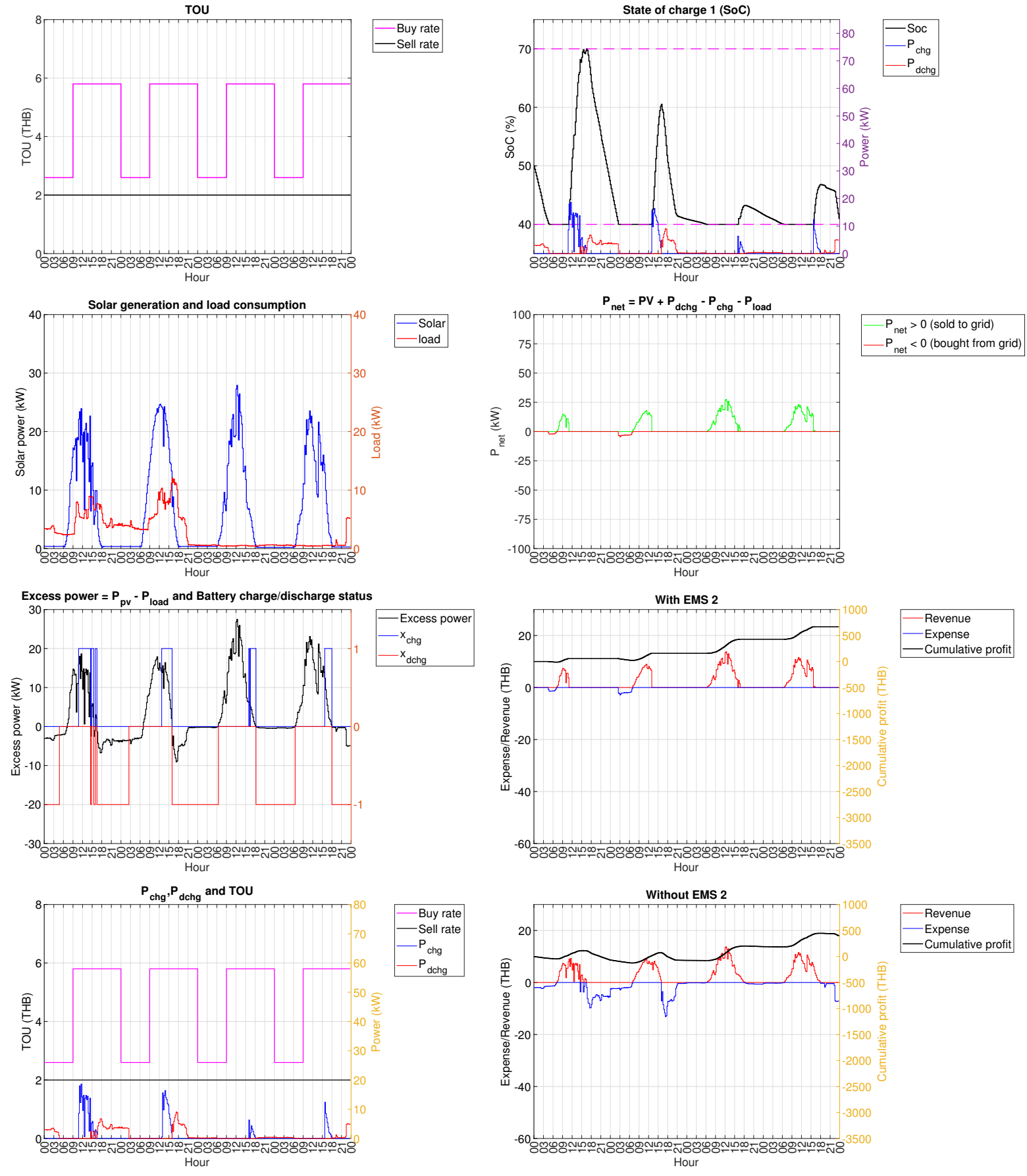

Figure 29: Overall operation of Profit option under **TOU 0** in high solar & low load scenario.

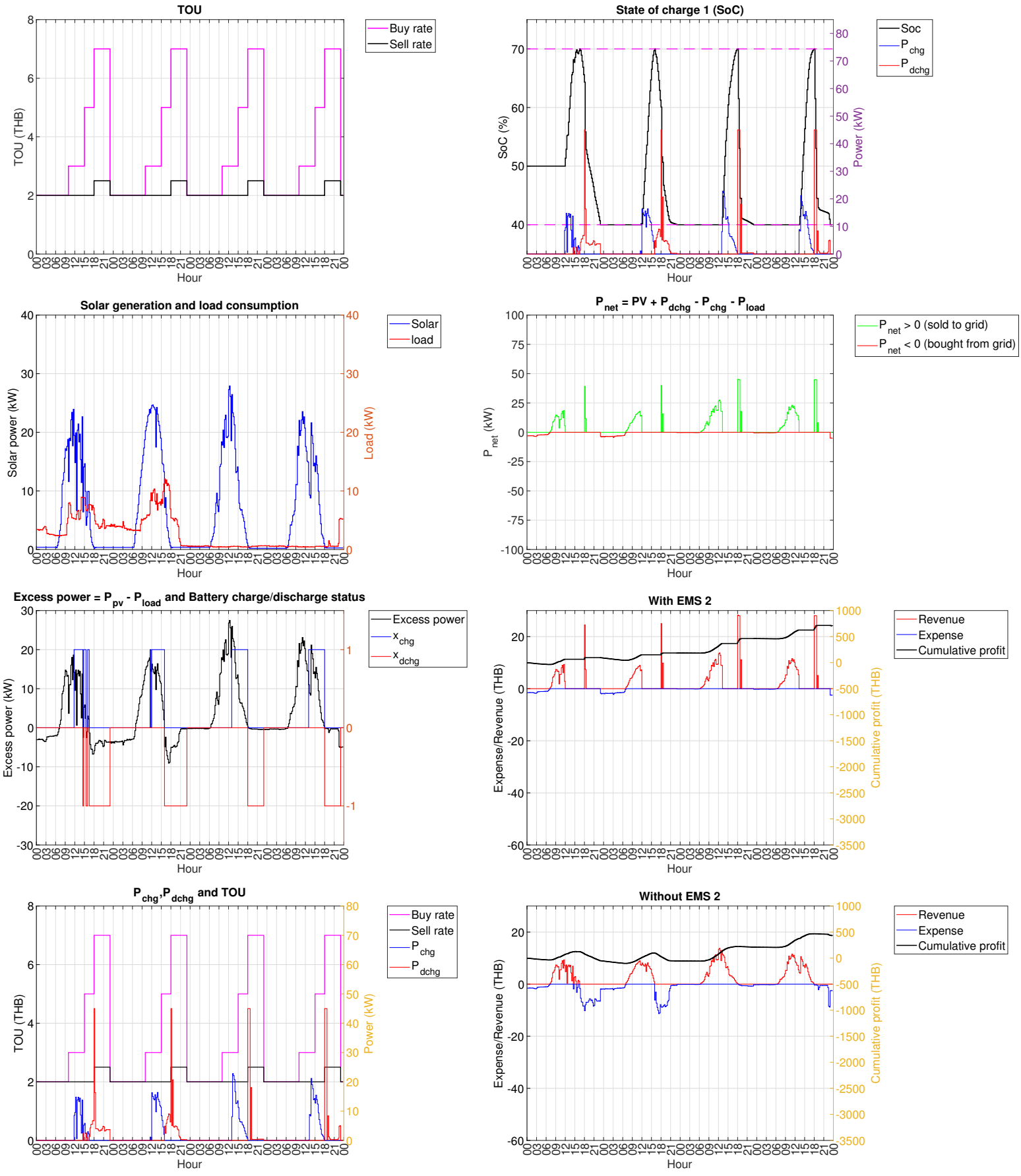

Figure 30: Overall operation of Profit option under **TOU 1** in high solar & low load scenario.

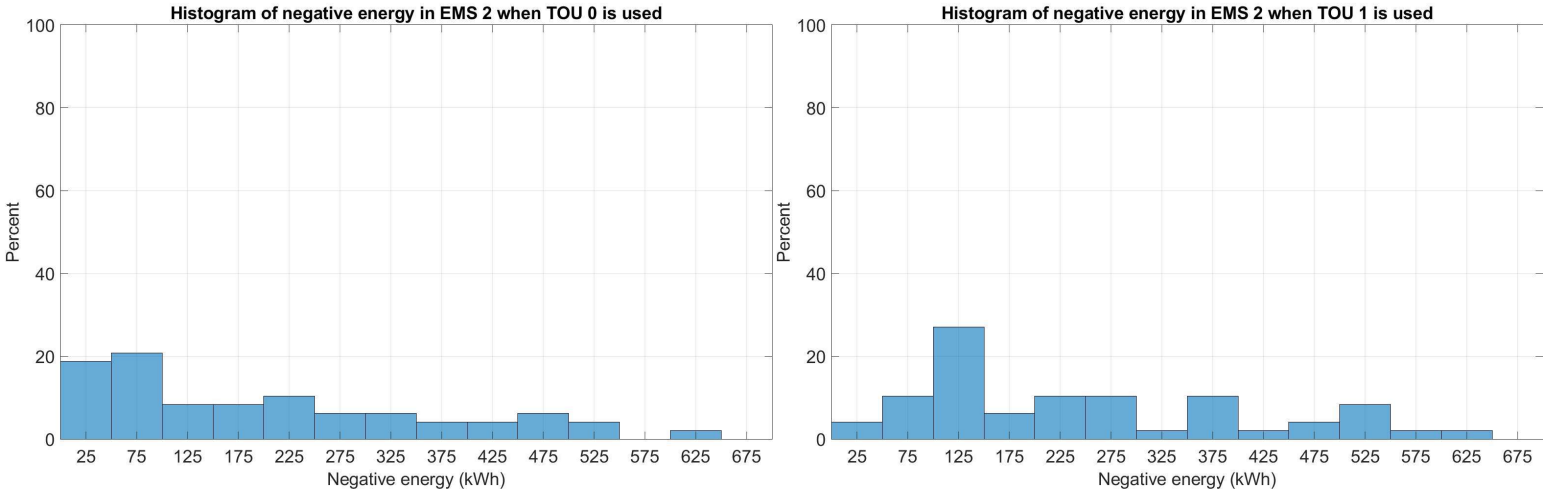

Figure 31: Histograms of negative energy in Profit option under TOU 0 and TOU 1.

5.2 Operational EMS: encourage ACs activation while minimizing electricity expense by EMS

In this EMS, the controllable load originating mainly from the machine laboratory room and student room was studied with the goal of activation within the permissible schedule from 1:00 p.m. to 4:00 p.m. The setting parameter is shown in Table 3.

Since the load consumption is controllable, the evaluation metric is to compare the electricity expense required to turn on the ACs in both rooms under two scenarios which are high solar generation and low solar generation as shown in Figure 32. The EMS can enhance the islanding system, because in both scenarios, with EMS, expenses for most datasets are zero, while without EMS, there are always expenses. The EMS can significantly save the electricity expense as the histogram of expense saved shown.

The EMS significantly enhances the ACs activation. Figure 33 shows the most beneficial result is that the ACs in both rooms can be turned on without incurring high expenses in the high solar scenario. Conversely, the ACs were turned off in a low solar scenario, as evident in Figure 34. Also, the case that requires the grid electricity is shown in Figure 35 which will be discussed later in section 5.3.

Figure 36 shows the percentage of ACs activation in both rooms under high solar and low solar scenarios, respectively. In this figure, 100% ACs activation means the ACs can be turned on at the lowest level of power consumption, which is 50% of rated power of AC, during the schedule for four days, while 0% ACs activation means the ACs can not be turned on at all. In the high solar generation scenario, the ACs can be turned on for four days in most cases. However, when the solar generation is low, the student's ACs is activated for four days in only half of the low solar generation cases. When comparing TOU 0 with TOU 1, ACs activation in both rooms is nearly identical, as most of the cases have zero expenses.

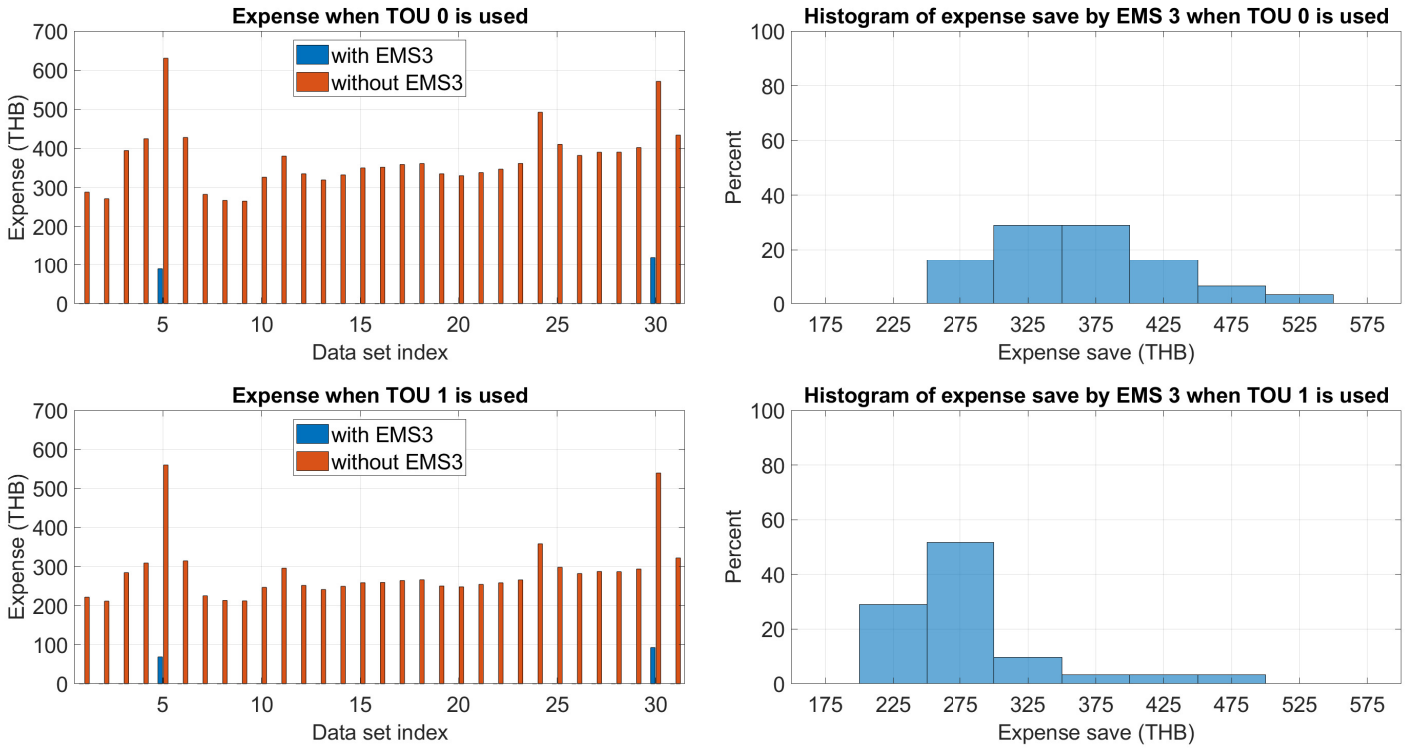

(a) High solar generation scenario.

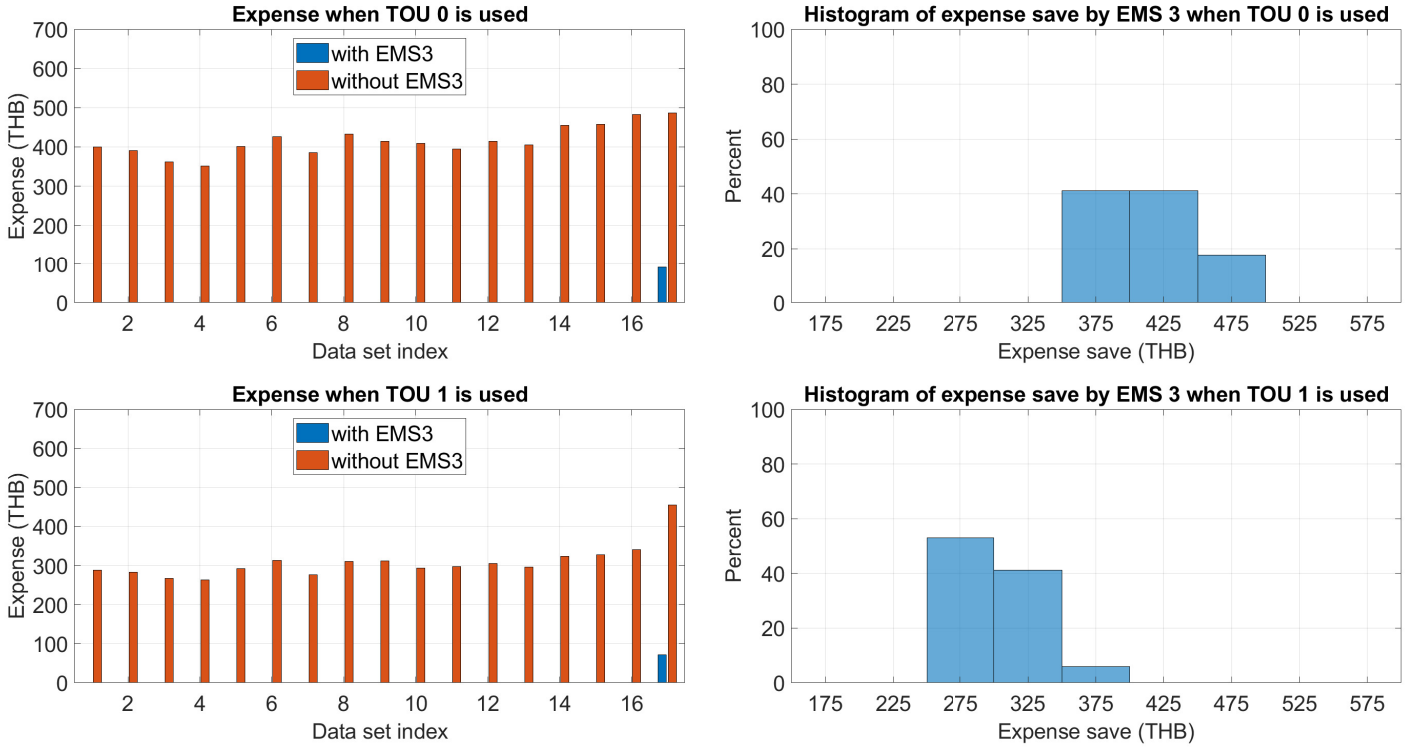

(b) Low solar generation scenario.

Figure 32: Histogram of expenses saved by Operational EMS under TOU 0 and TOU 1.

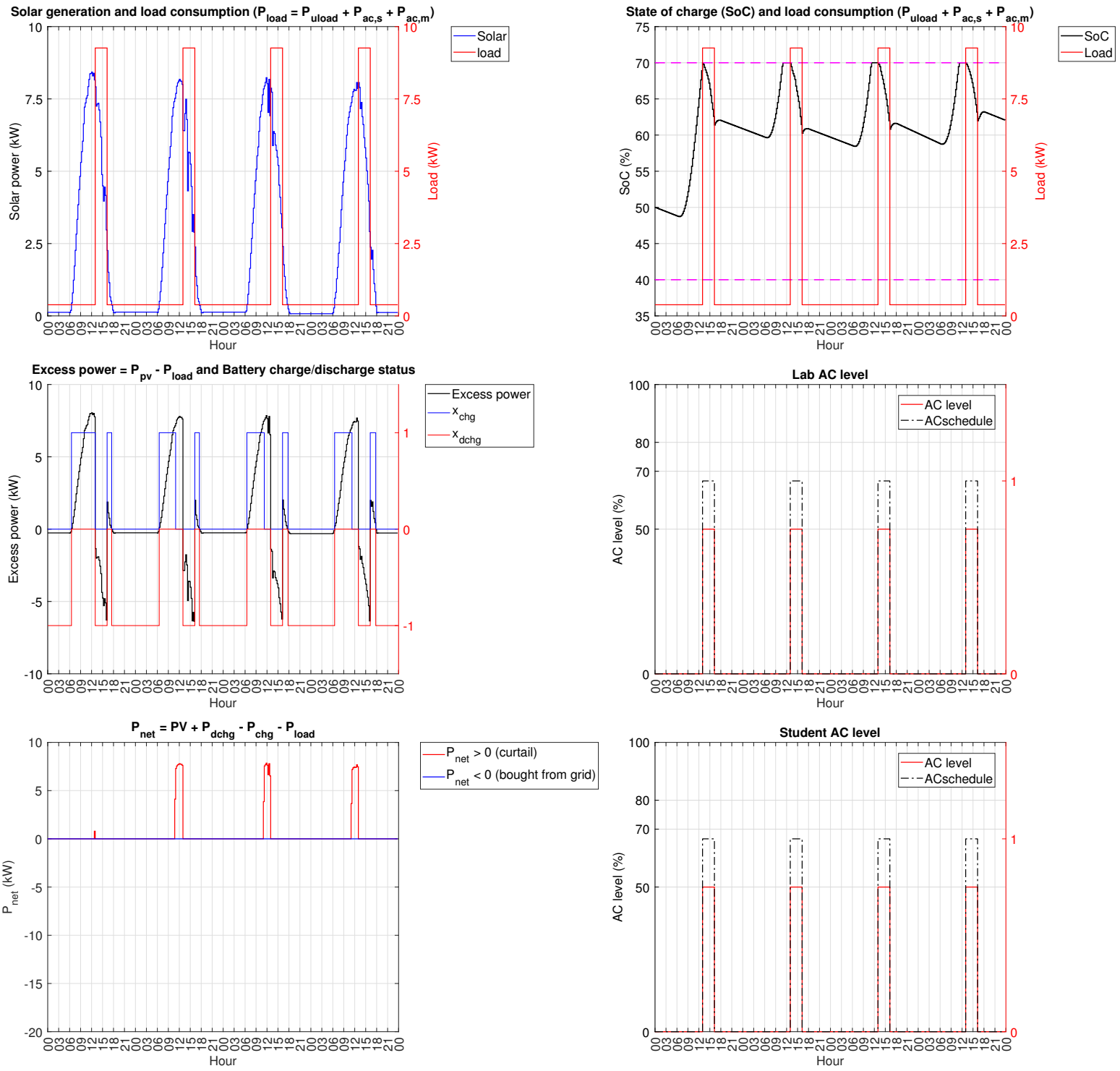

Figure 33: Encouraging the use of ACs in both the machine laboratory room and the student room under **high solar generation scenario**.

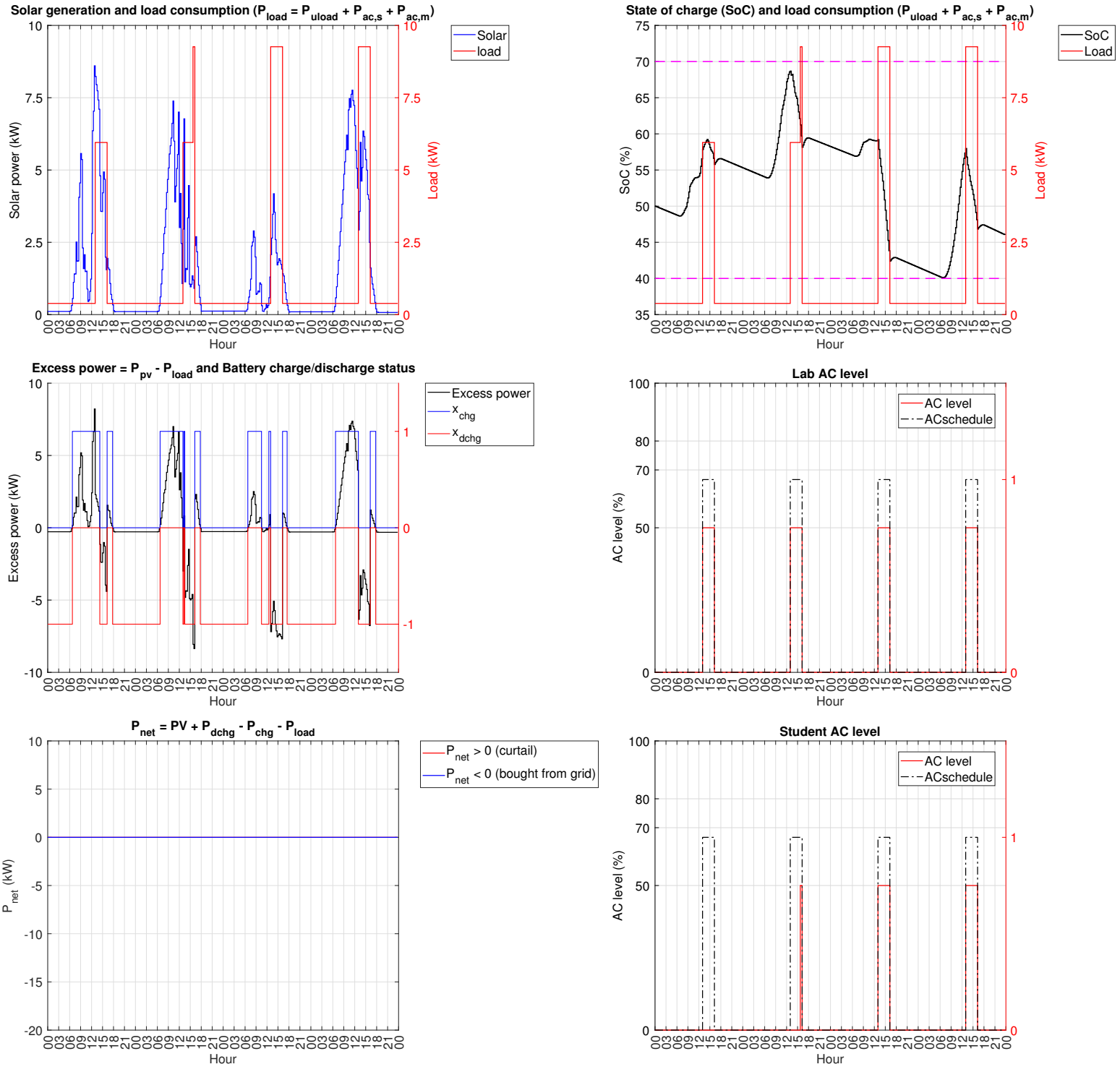

Figure 34: Encouraging the use of ACs in both the machine laboratory room and the student room under **low solar generation scenario**.

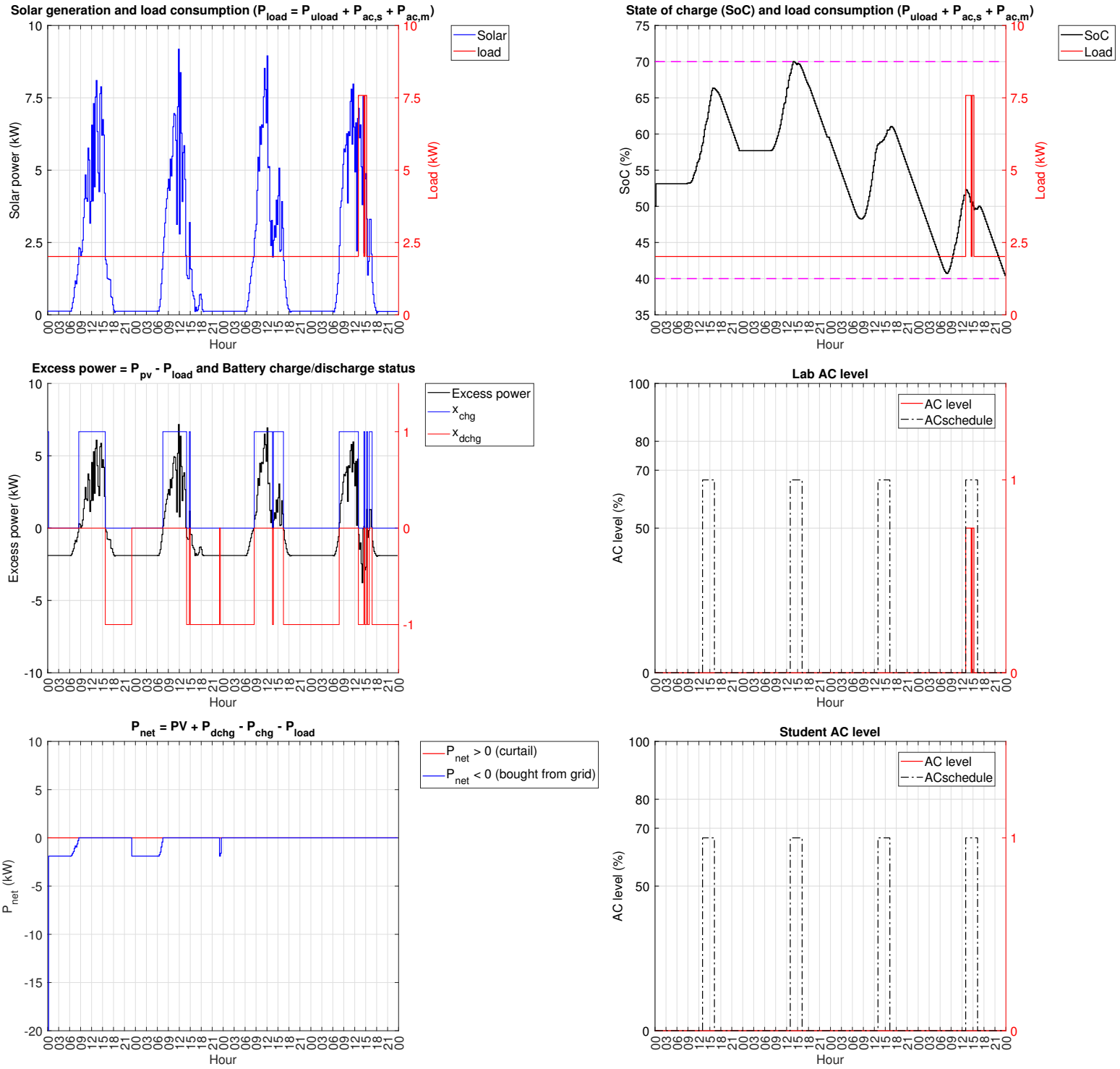

Figure 35: The infeasible case of being an islanding mode.

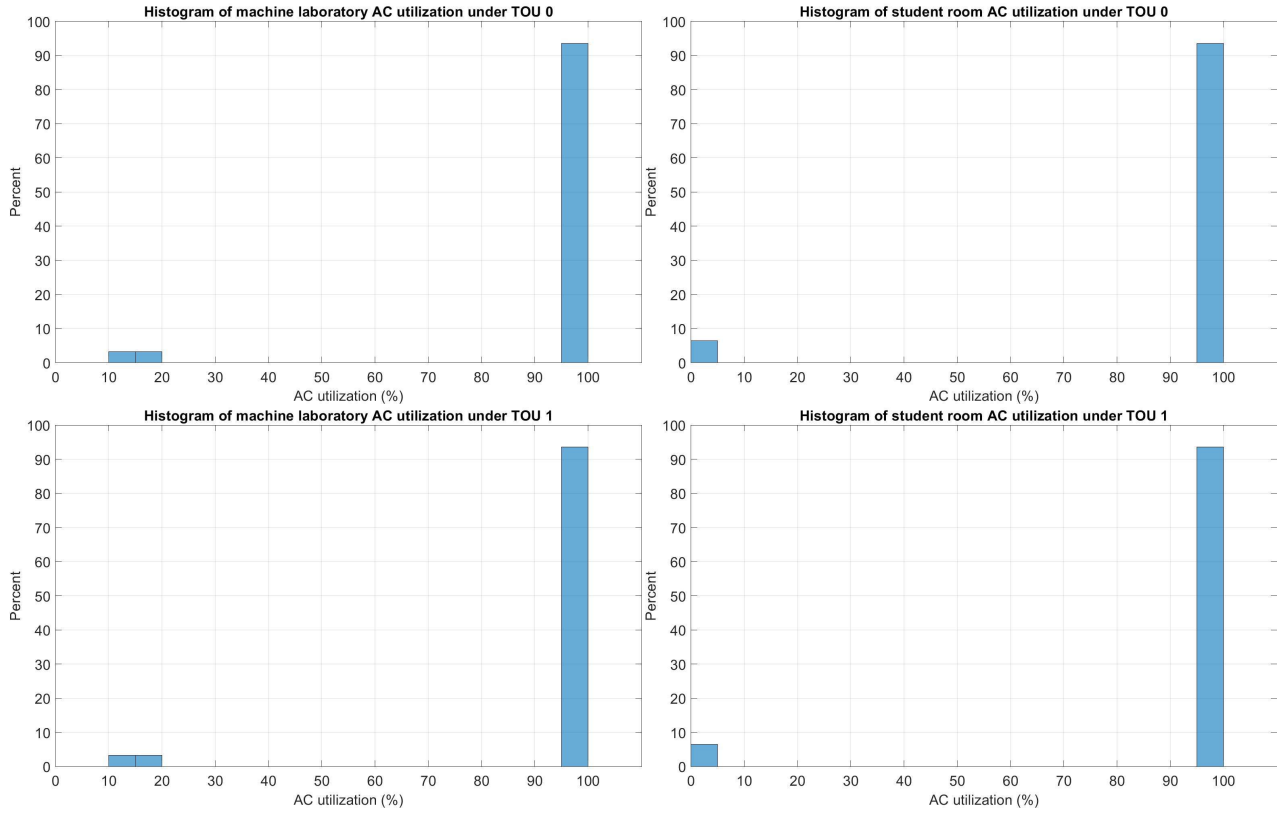

(a) High solar generation scenario.

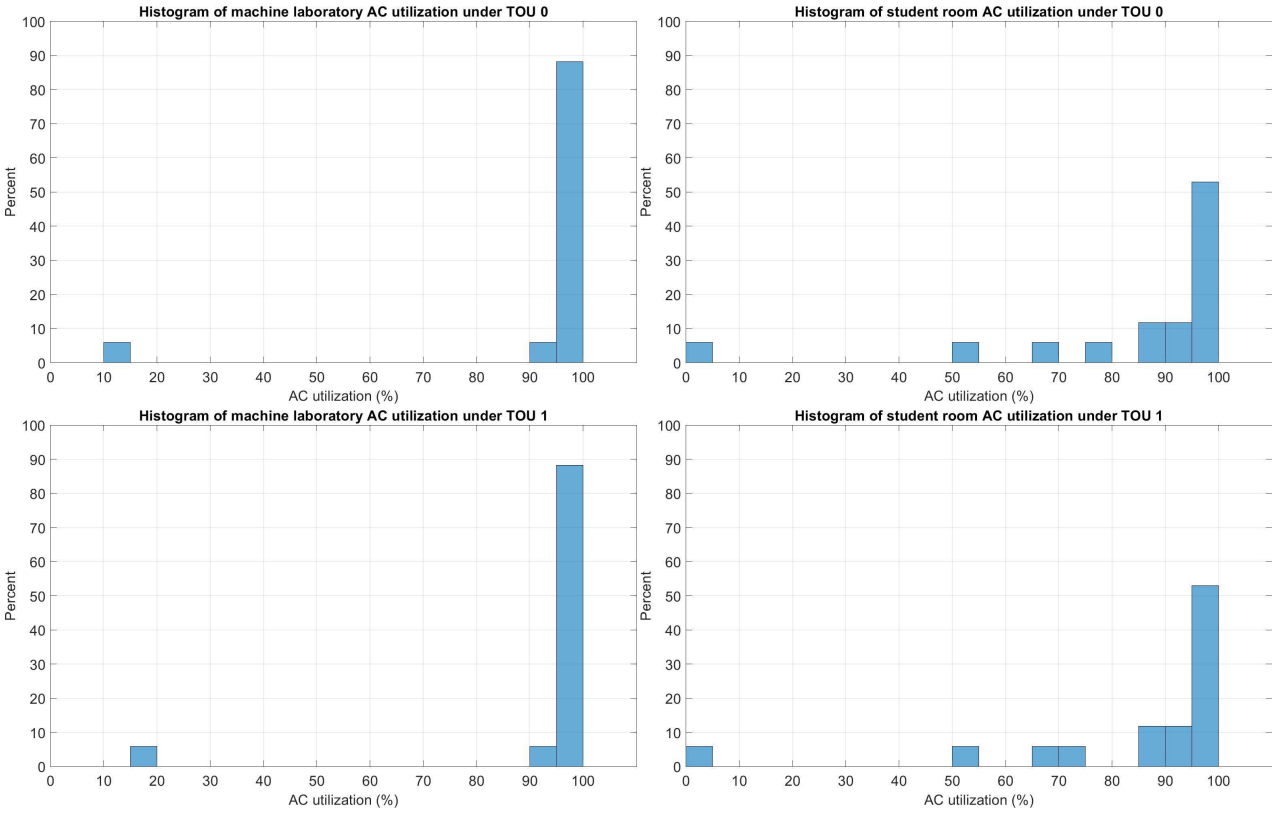

(b) Low solar generation scenario.

Figure 36: Histogram of ACs activation byOperational EMS under TOU 0 and TOU 1.

5.3 Islanding EMS: number of different scenarios for being islanding mode

Figure 37 and Figure 38 demonstrate the overall operation of Islanding EMS in high solar and low solar generation, respectively. In the high solar generation scenario, the ACs in both rooms are always utilized during the schedule, and some solar generation needs to be curtailed in order to enforce zero-export to the grid. However, in the low solar generation scenario, the student's ACs is not activated in the first two days, and the solar generation is not curtailed. Similarly, the battery charges solar energy and discharges for demands. Notably, there are three batches that could not operate in islanding mode due to abnormally high base load. This suggests that islanding mode can be achieved if the base load is small, and the users comfort is not considered.

The reason of infeasibility for being an islanding system was illustrated in Figure 35. Despite ACs in both rooms are turned off, the system consistently purchases grid electricity (P_{net} is always negative.) due to the high amount of based load consumption during daytime,. Although SoC reached its maximum on the second day, ACs activation in both rooms was not feasible. Doing so the SoC would be inadequate for power consumption by the base load later on, leading to the cause that SoC drop down below 40 %, which is infeasible. The initial charge occurred because the EMS anticipated that by the end of day 4, the battery must be discharged to supply the base load until it reached its minimum threshold. Moreover, the initial charging of the battery probably results from excessive weight w_{c} that encourage charging the battery.

In this EMS, investigating the system's infeasibility can be achieved by setting parameters within Operational EMS. For instance, the solutions for infeasible cases are similar, involving turning off all ACs in both rooms. Then, the base load becomes the sole factor that solar generation must supply. If the initial solar generation is lower than the base load, the battery must self-discharge by at most 10% to supply the base load; if insufficient, grid electricity usage becomes necessary. Therefore, grid electricity is used to charge the battery initially, ensuring later provision of the base load.

Figure 39 shows the percentage of ACs activation in both rooms in high solar and low solar scenarios, respectively. In Figure 39(a) and Figure 39(b), 100% ACs activation means the ACs can be turned on at the lowest level of power consumption, which is 50% of rated power of AC, during the schedule for four days, while 0% ACs activation means the ACs can not be turned on at all. In the high solar generation scenario, the ACs in both rooms can be turned on for four days in most cases. However, when the solar generation is low, the student's ACs is activated for four days in only half of the low solar generation cases.

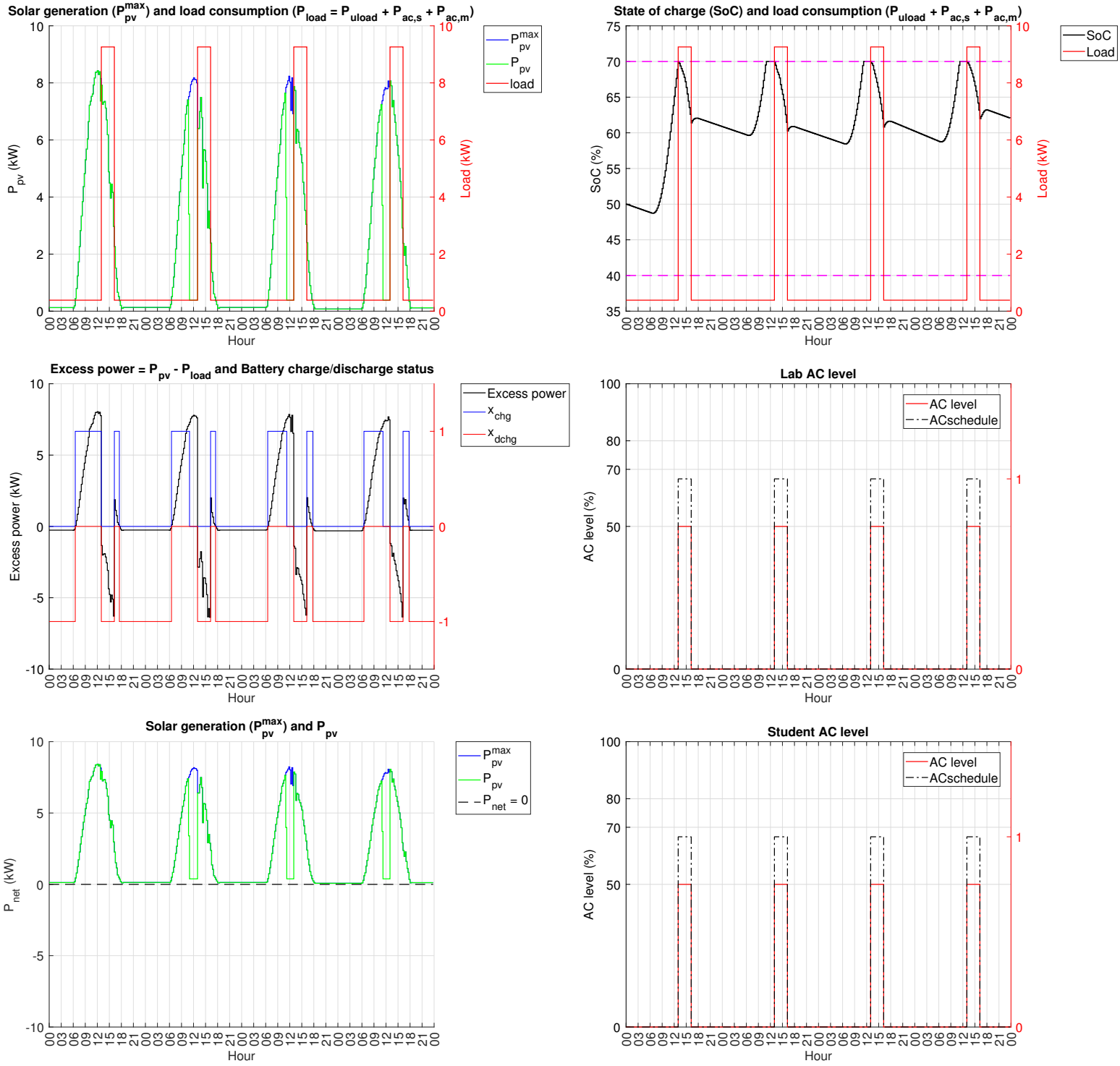

Figure 37: Overall operation of Islanding EMS under **high solar generation**.

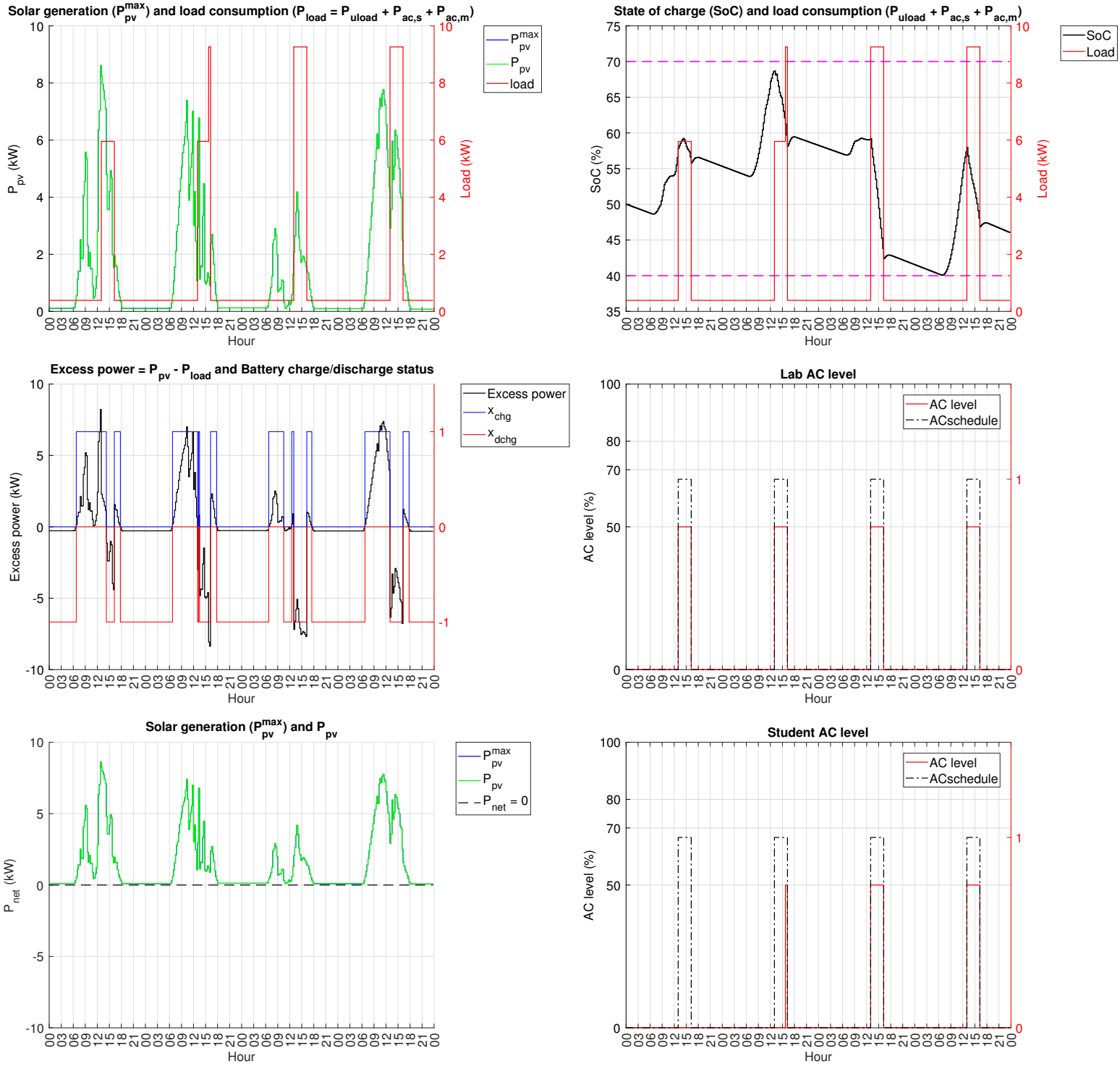

Figure 38: Overall operation of Islanding EMS under **low solar generation**.

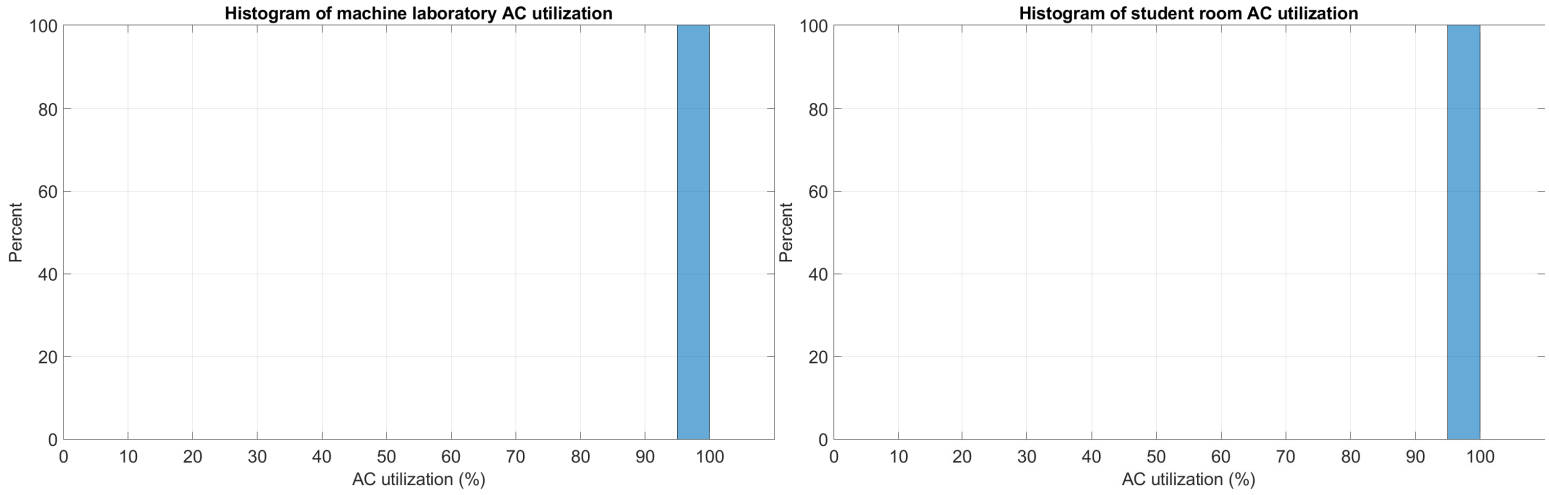

(a) High solar generation scenario.

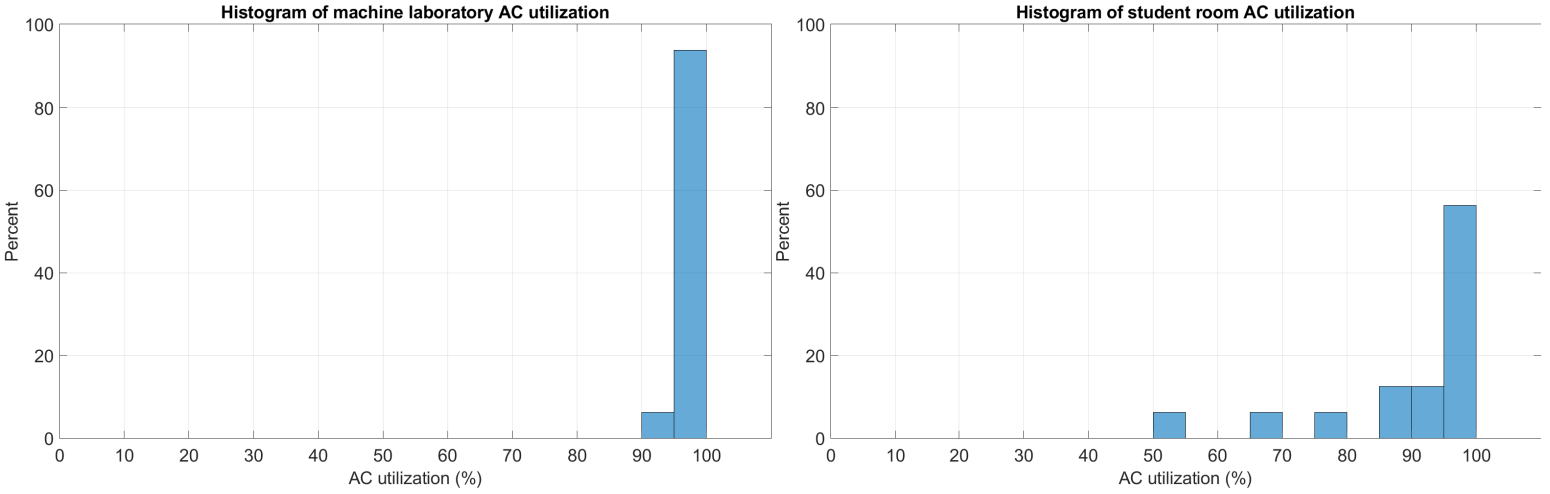

(b) Low solar generation scenario.

Figure 39: Histogram of ACs activation by Islanding EMS.

5.4 RE 100 EMS: maximize the number of RE 100 days

In this section, the results of RE 100 EMS, whose objective is to achieve RE 100 for as many days as possible, are discussed. To begin with, the double battery system is also considered in this EMS, so the functionality of both batteries is enhanced to be identical. As can be seen in Figure 40, the patterns of charging and discharging are identical, as well as the amount of power utilization from the grid at each time index. Even though the battery functionality is enhanced to be the same, the optimal value remains unchanged compared to the scenario without this objective, this will be discussed later in section 5.5.

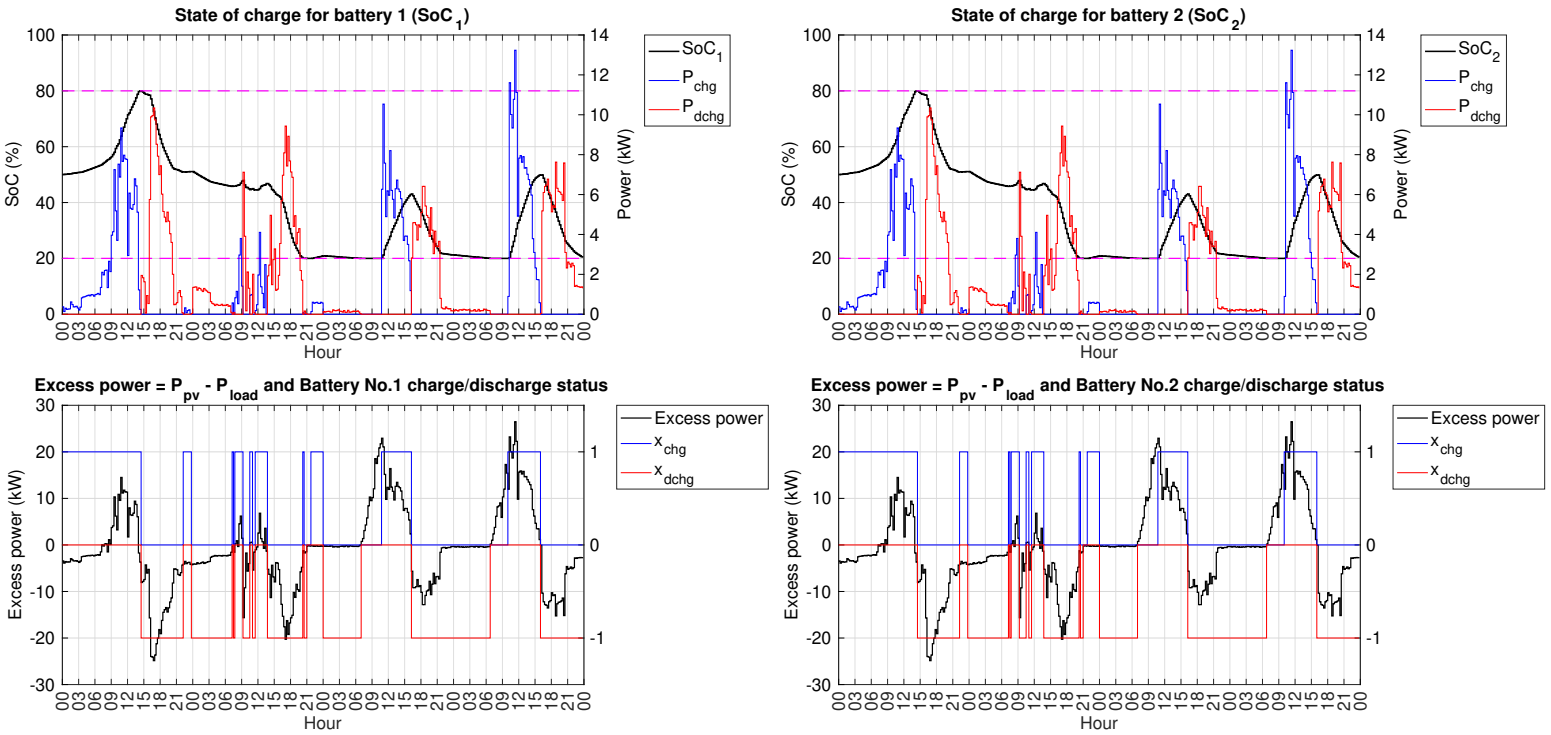

Figure 40: Batteries functionality under RE 100 EMS.

Figure 41 demonstrates the EMS operation across various scenarios, highlighting differences in achieving RE 100 based on load consumption and solar generation. The RE 100 EMS operates to minimize the upper bound of $P_{\text{net}}(t)$, of which its absolute represented by the blue lines in the second row of the figure, for each scenario throughout the day, ensuring that electricity required from the grid never exceeds its upper limit. Consequently, the different datasets reveal varying results: some cannot achieve RE 100 for all four days, some achieve it on certain days, and others can achieve RE 100 consistently. These outcomes are observed in the high load & low solar, high load & high solar, and low load & high solar datasets, respectively.

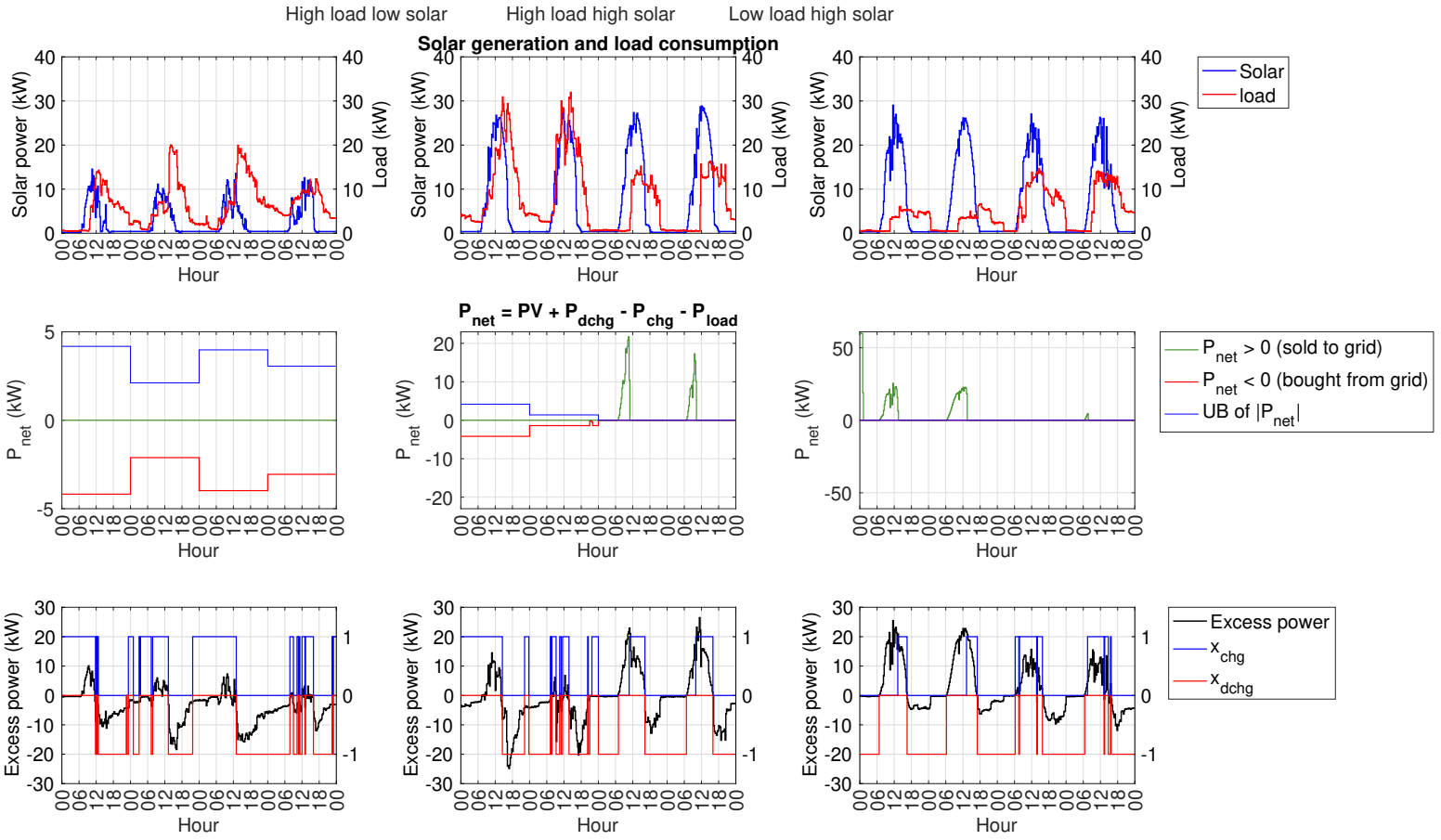

Figure 41: Overall operation of RE 100 EMS under different scenarios. $P_{\text{net}}(t)$ is broken down into $P_{\text{net}}(t) > 0$ (green), $P_{\text{net}}(t) < 0$ (red), and upper bound of absolute of $P_{\text{net}}(t)$ (blue).

5.5 Multiple batteries

In this experiment, we compared the performance of a single battery and double batteries under the objective to minimize electricity cost. We investigated three aspects: (i) optimal values for both systems, (ii) comparison of optimal values for the double battery system between with and without managing the identical SoC objective, and (iii) comparison of average SoC deviation for the double battery system between with and without managing the identical SoC objective. The single battery has the specification as show in Table 6 which is simply the summation of two batteries' specifications in maximum charge rate and maximum discharge rate.

Table 6: Specification of battery in the single battery system and double battery system.

Specification detail	Value of single battery system	Value of each battery in double battery system	unit
η_c	0.95	0.95	no unit
η_d	0.95×0.93	0.95×0.93	no unit
MAX CHARGE RATE	60	30	kW
MAX DISCHARGE RATE	60	30	kW
SoC(1)	50	50	%
SoC_{min}	20	20	%
SoC_{max}	80	80	%

In Figure 42(a), both systems give the same optimal values under TOU 0 and TOU 1, but TOU 1 yields a lower optimal value as discussed in section 5.1.1. However, the optimal solutions vary across datasets, indicating non-unique optimal solutions for the double battery system. As depicted in Figure 42(b), adding this objective ensures identical charging and discharging patterns without affecting the optimal values. When both batteries have different initial SoC, they equalize before operating identically, leading to higher expenses. In Figure 42(c) for double battery system, with this objective, the average percentage deviation is around 10^{-15}. But without this, the deviation stays below 35%. Notably, higher deviations often coincide with lower expenses, as demonstrated in Figure 42(d).

In conclusion, adding the term identical SoC in the objective function ensures the same optimal value while effectively distributing battery workload.

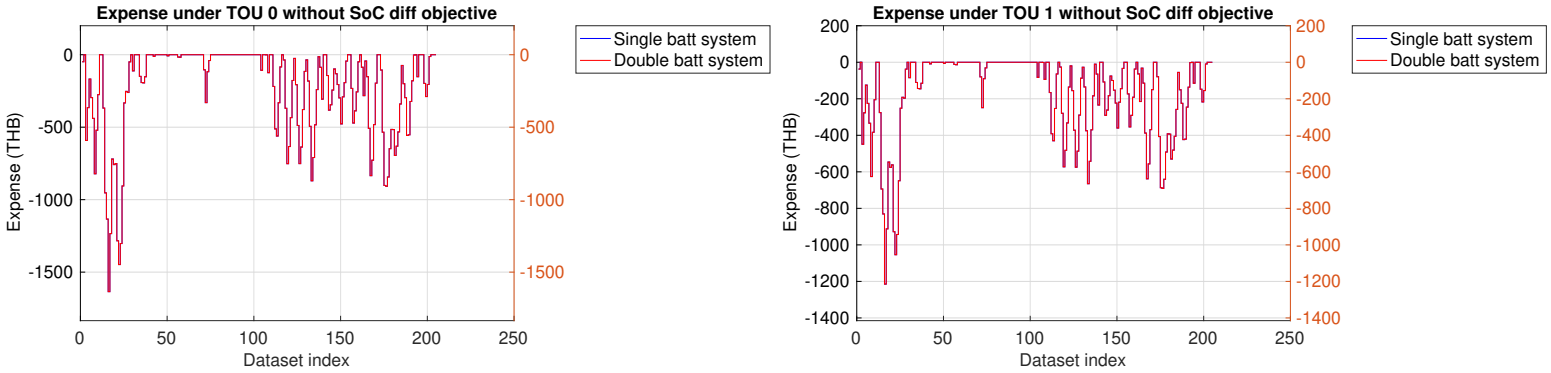

(a) Expense comparation between single and double battery system under TOU 0 and TOU 1.

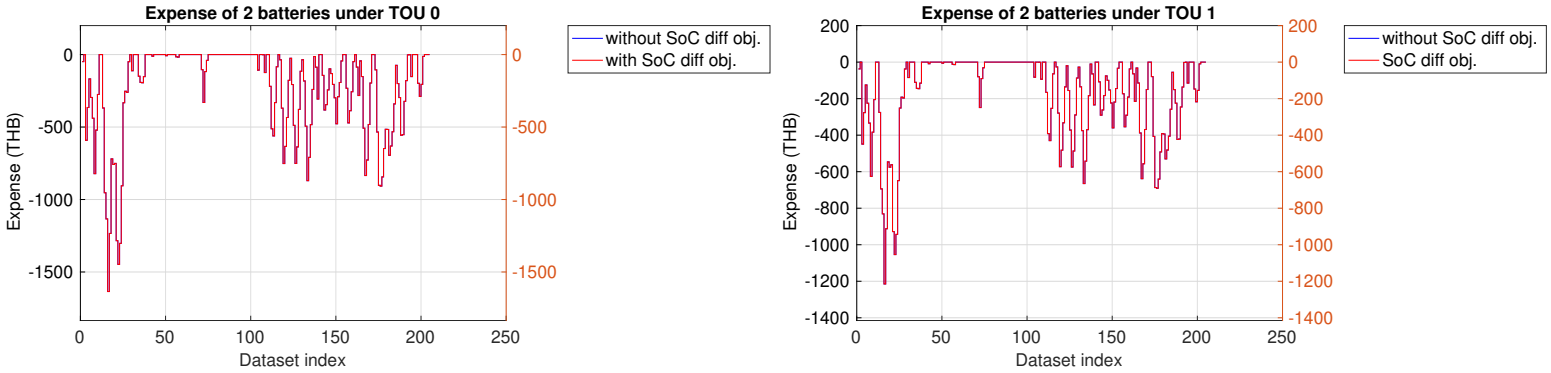

(b) Expense comparation of double battery system between with and without SoC diff obj.

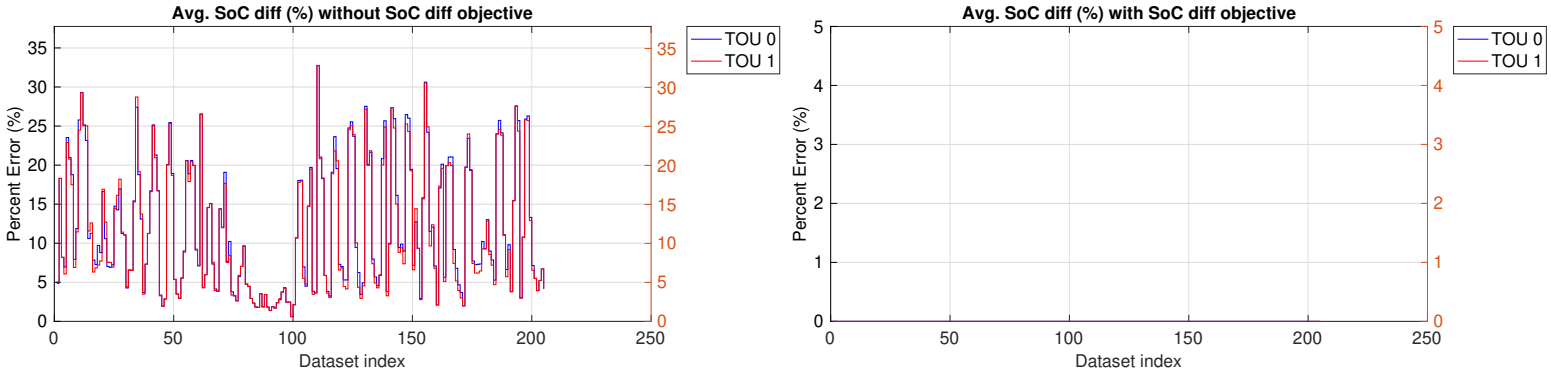

(c) Average SoC difference comparation of each dataset between with and without SoC diff obj.

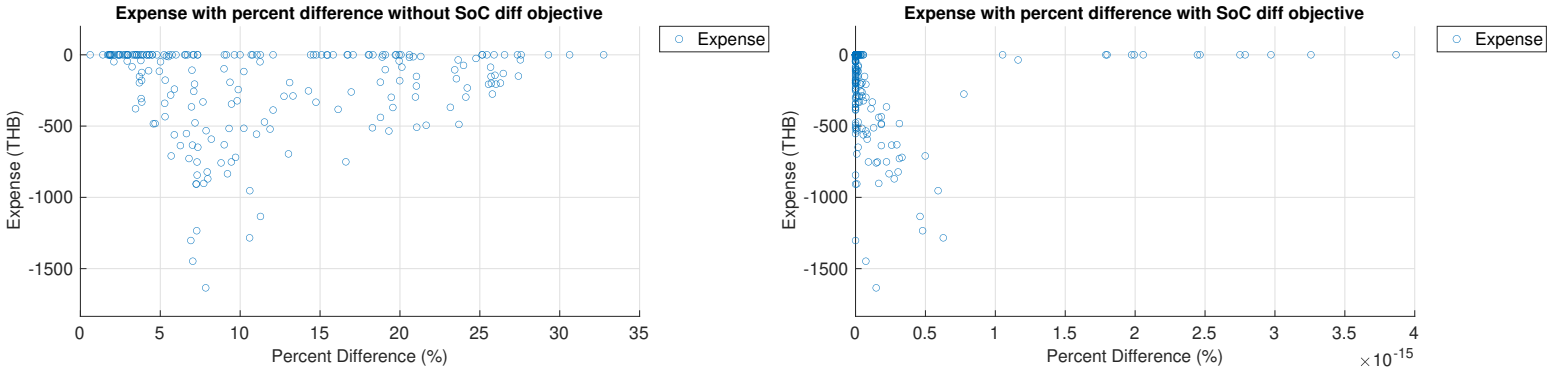

(d) Expense comparation of double battery system of each percent difference between with and without SoC diff obj.

Figure 42: Performance comparation between the system of single battery and double batteries.

5.6 RE 100 achievement

To achieve 100% renewable energy (RE 100), the major factors are the system size, which includes the battery capacity and the solar generation power. In this experiment, the actual capacities of the batteries (ranging from 125 kWh to 333 kWh each) and the solar panel installation capacity (ranging from 60 kWp to 70 kWp) were investigated under Economic EMS and RE 100 EMS. In this project, since each dataset consists of four consecutive days, the RE 100 achievement of each day in the dataset is determined by whether there is no power bought from the grid at any time index within that day; then the percentage of RE for each system size is calculated from every dataset.

Overall, the RE 100 percentage correlates with both actual battery capacity and solar panel installation capacity. The RE achievement percentages under various system sizes from different EMS are depicted in heatmaps shown in Figure 43, Figure 44, and Figure 45, with conclusions summarized in Table 7, Table 8, and Table 9 regarding the appropriate system size of each EMS.

Table 7: A battery size (kWh) when PV = 66 kW.

PV= 66 kW	TOU 0		TOU 1		RE 100 EMS
	Energy cost	Profit	Energy cost	Profit	
RE 50	< 125	329	< 125	-	125
RE 60	< 125	> 333	< 125	-	125
RE 70	196	> 333	138	-	125
RE 80	271	> 333	238	-	200
RE 90	325	> 333	333	-	333

Table 8: A battery size (kWh) when PV = 58 kW.

PV= 58 kW	TOU 0		TOU 1		RE 100 EMS
	Energy cost	Profit	Energy cost	Profit	
RE 50	< 125	> 333	<125	-	< 125
RE 60	< 136	>333	129	-	< 125
RE 70	204	>333	196	-	< 125
RE 80	313	> 333	308	-	200
RE 90	> 333	> 333	> 333	-	333

Table 9: PV installation capacity (kW) when one battery actual capacity = 125 kWh.

Batt = 125 kWh	TOU 0		TOU 1		RE 100 EMS
	Energy cost	Profit	Energy cost	Profit	
RE 50	51	-	51	-	< 50
RE 60	59	-	59	-	54
RE 70	68	-	68	-	63
RE 80	> 70	-	> 70	-	> 70
RE 90	> 70	-	> 70	-	> 70

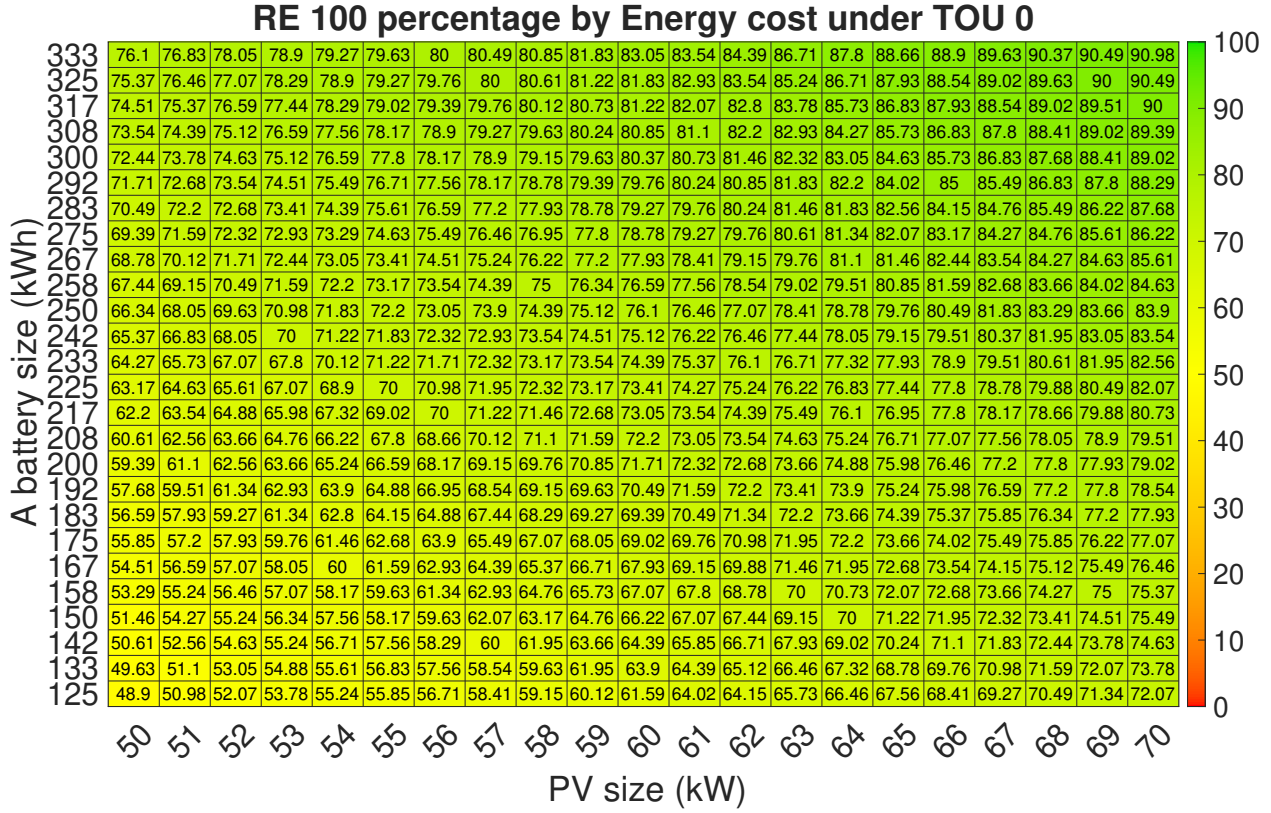

(a) under TOU 0.

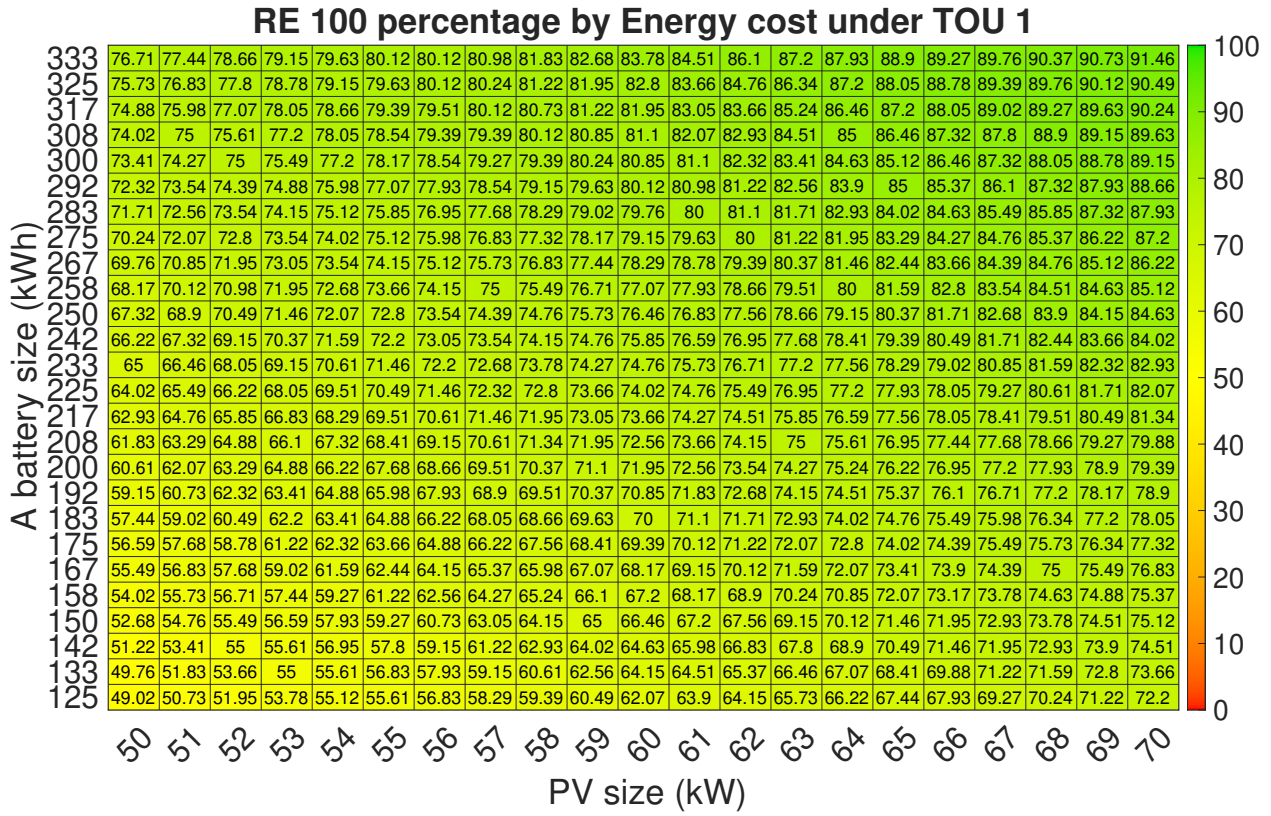

(b) under TOU 1.

Figure 43: RE percentage achievement under different system size in **Economic EMS: Energy cost**.

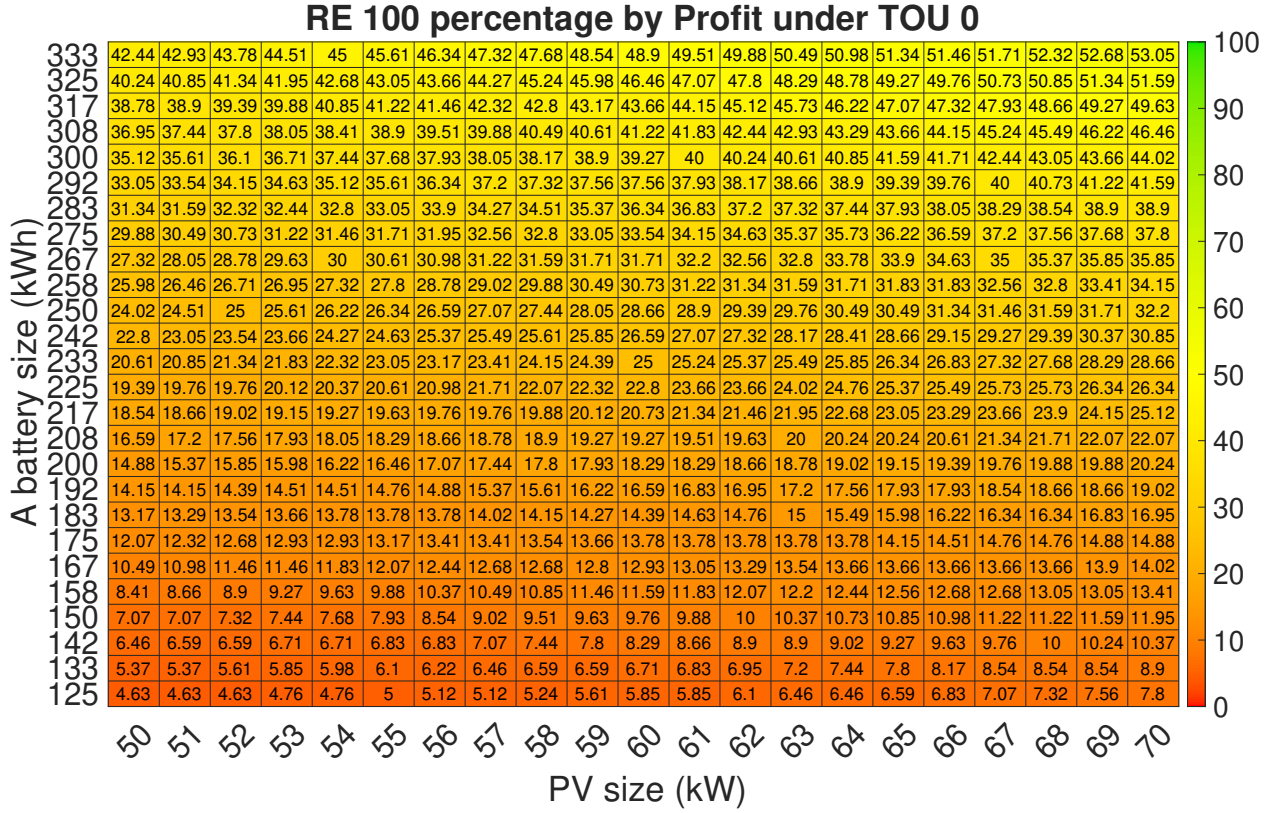

(a) under TOU 0.

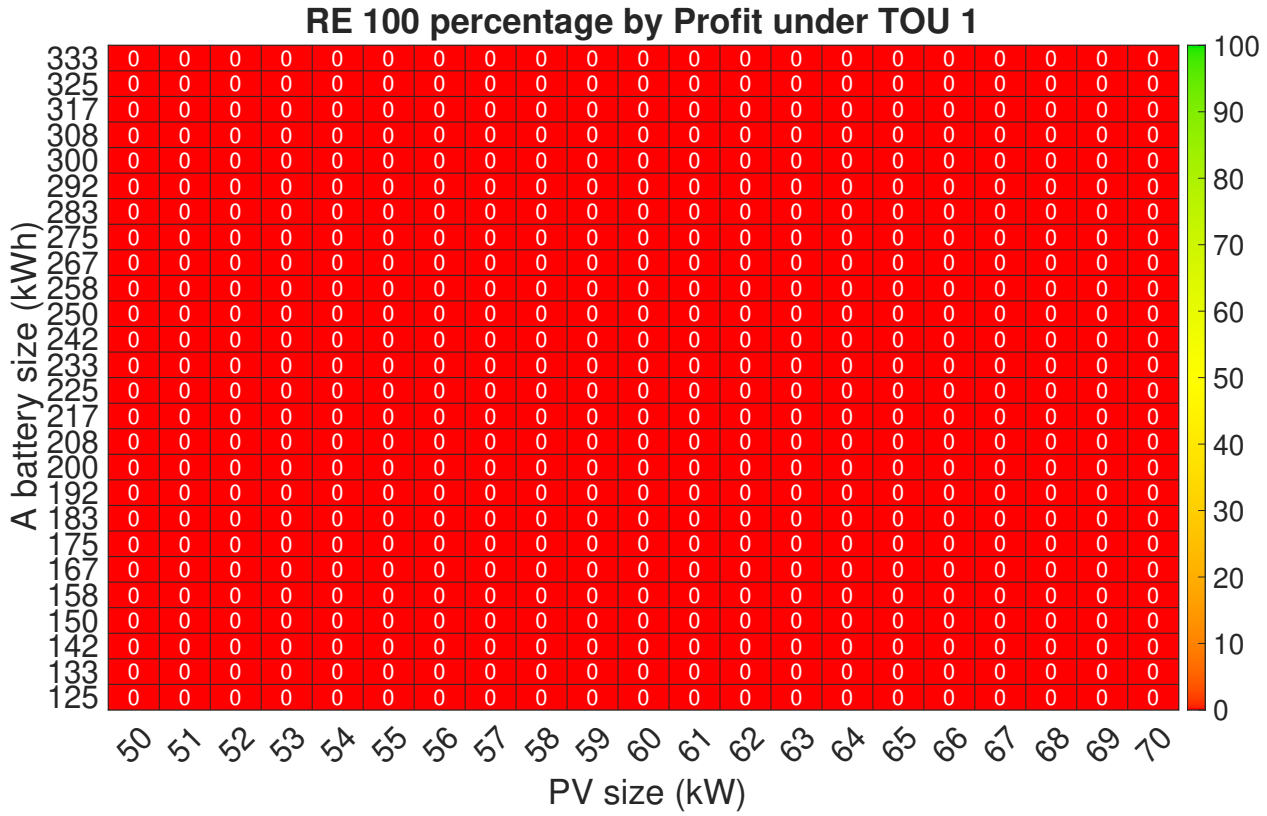

(b) under TOU 1.

Figure 44: RE percentage achievement of different system size under **Economic EMS: Profit**.

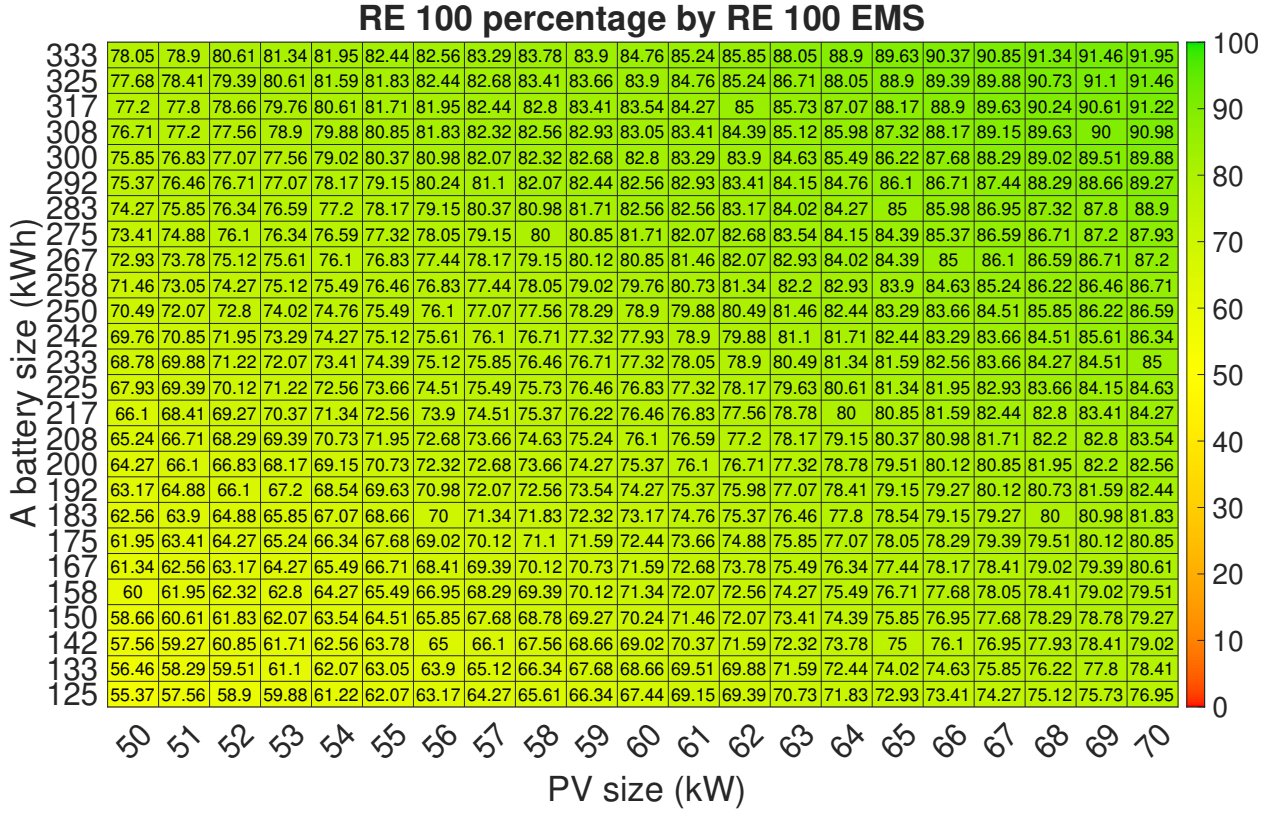

Figure 45: RE percentage achievement of different system size under **RE 100 EMS**.

5.6.1 Economic EMS: Energy cost

As shown in Figure 43, achieving a higher percentage of RE requires both a higher actual battery capacity and higher installation of solar panel capacity. The TOU pattern affects the optimal operating point, as the solution obtained from TOU 1 exhibits specific patterns of charging and discharging the battery corresponding to low and high electricity tariffs, respectively. However, the difference in the system size to achieve each level of RE under TOU 0 and TOU 1 is not significant. Moreover, in order to achieve the same percentage of RE, reducing solar panal installation capacity for 1 kWp results to the increase of the single battery actual capacity for 8-12 kWh.

5.6.2 Economic EMS: Profit

Since the objective function is to maximize profit, the optimal solution is to buy electricity from the grid when the electricity tariff is low to charge the battery. Consequently, the percentage of RE 100 under TOU 0 for the EMS 2 is lower than that of the EMS 1, as can be seen from the gradient color in Figure 44(a). Subsequently, the battery can be discharged or the electricity sold to the grid when the tariff is high. Therefore, under TOU 1, which has a specific pattern of buy rate and sell rate, every day in each dataset will yield a solution that consistently purchases grid electricity; there is no day that does not buy electricity from the grid, resulting in a zero percentage of RE from this calculation, as shown in Figure 44(b). Moreover, in order to achieve the same percentage of RE, reducing solar panal installation capacity for 1 kWp results to the increase of the single battery actual capacity for 4 kWh.

5.6.3 RE 100 EMS

Since the goal is to obtain a solution that relies on self-generation as much as possible, each system size yields a higher percentage of renewable energy than the Economic EMS. This is because the small power bought from the grid can be shifted to other days, and that day can be counted as a renewable energy day. In conclusion, in order to achieve the same RE percentage as Economic EMS, the system size becomes lower as shown in Figure 45. Moreover, in order to achieve the same percentage of RE, reducing solar panal installation capacity for 1 kWp results to the increase of the single battery actual capacity for 8-12 kWh.

5.7 Load forecasting model performance

The time series of total load forecasting value are shown in Figure 47. As shown in Figure 48, the MAPE of all predicted load experienced the same trend over each day which was the MAPE. The trend of MAPE was the MAPE start to increased at 6:00, peaked at 9:00, then decreased until 18:00. The MAPE of all predicted loads were high during the daytime, i.e. 7:00 - 15:00. This is possibly caused by different load profile in each hour of different day. For the Day-Ahead scheme, the MAPE of all predicted loads exhibits the same trend, but with a different pattern from Hour-Ahead prediction. The trend of MAPE is over 100% for almost all hours except 8:00 - 9:00 and 17:00 - 21:00. The high MAPE during 23:00 - 7:00 might caused by the lower load consumption, whereas the high MAPE during 10:00 - 16:00 possibly caused by high standard deviation in load consumption during this period as can be seen in Figure 46. In conclusion, the performance of Day-Ahead load prediction is low and the predicted load consumption is highly deviated from the actual load consumption.

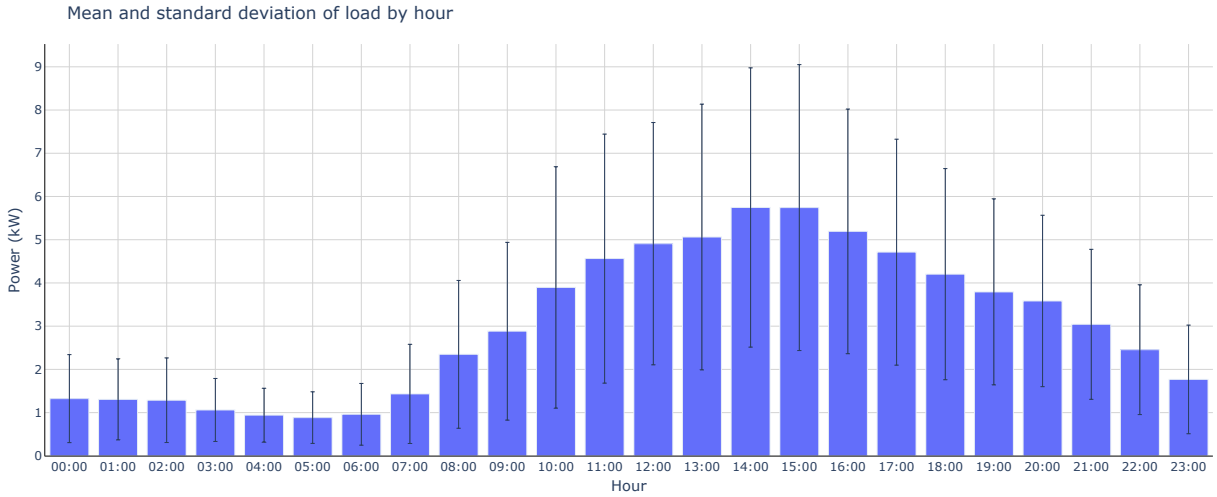

Figure 46: Mean (bar) and standard deviation (error bar) of load consumption by hour.

The seasonality and trend can be decomposed as shown in Figure 49. For the Hour-Ahead model, the trend line was approximately 3 kW and increased over time with small slope .The weekly seasonality showed a pattern of decrease to around -2 kW on Saturdays and Sundays, while fluctuating around 1 kW during weekdays. The daily seasonality increased to 3 kW then dropped to -2 kW in each day. For the Day-Ahead model, the pattern of all components is the same as in the Hour-Ahead result except for the trend line, which remains constant at 3 kW.

The performance of the total load forecasting model measured by other types of error is shown in Table 10.

Table 10: Error of predicted values of total load consumption.

Minutes-ahead	**MAE [kW]**	**RMSE [kW]**	**MAPE [%]**	**MBE [kW]**	**NMAE [%]**
5	0.4328	0.7225	17.35	-0.0440	2.09
15	0.5680	0.9382	25.74	-0.0888	2.74
30	0.7146	1.0883	37.51	-0.1518	3.45
60	0.9784	1.3852	57.89	-0.2850	4.72
Days-ahead	**MAE [kW]**	**RMSE [kW]**	**MAPE [%]**	**MBE [kW]**	**NMAE [%]**
1	1.6288	2.1036	121.14	-0.7122	10.16
2	1.7559	2.2719	129.27	-0.8556	10.95
3	1.7834	2.2984	131.66	-0.9098	11.12

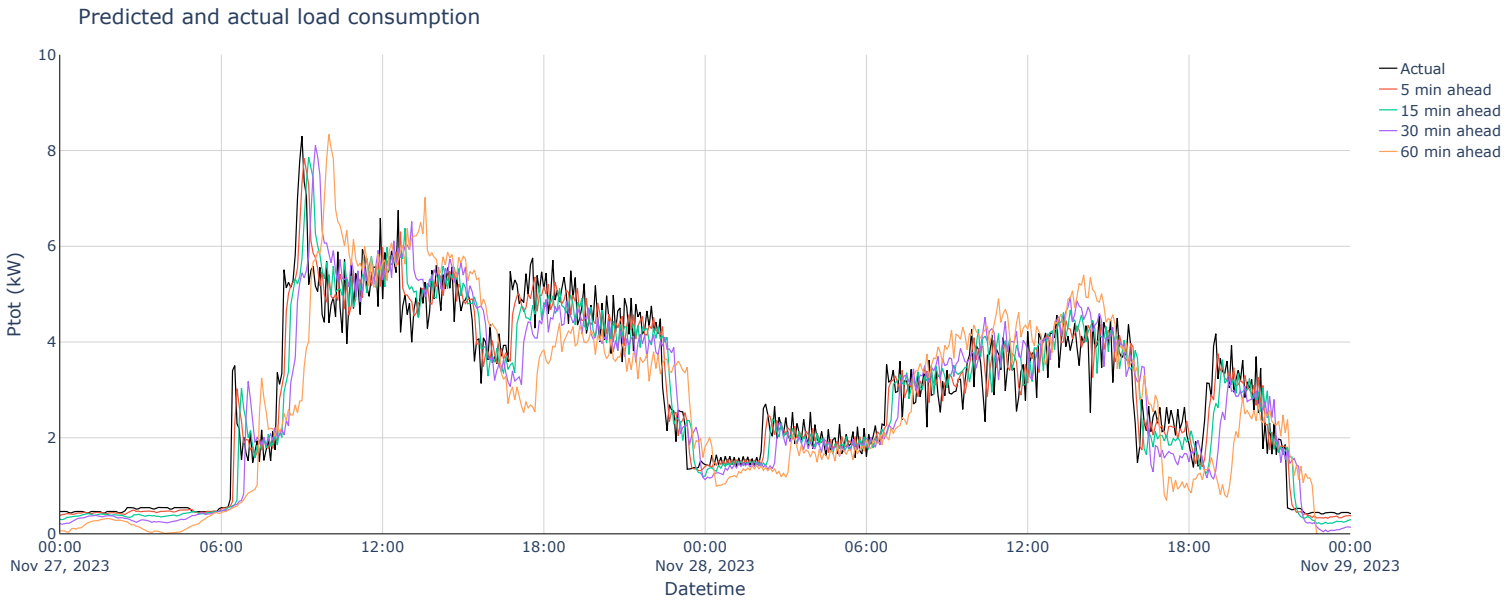

(a) **HA** scheme.

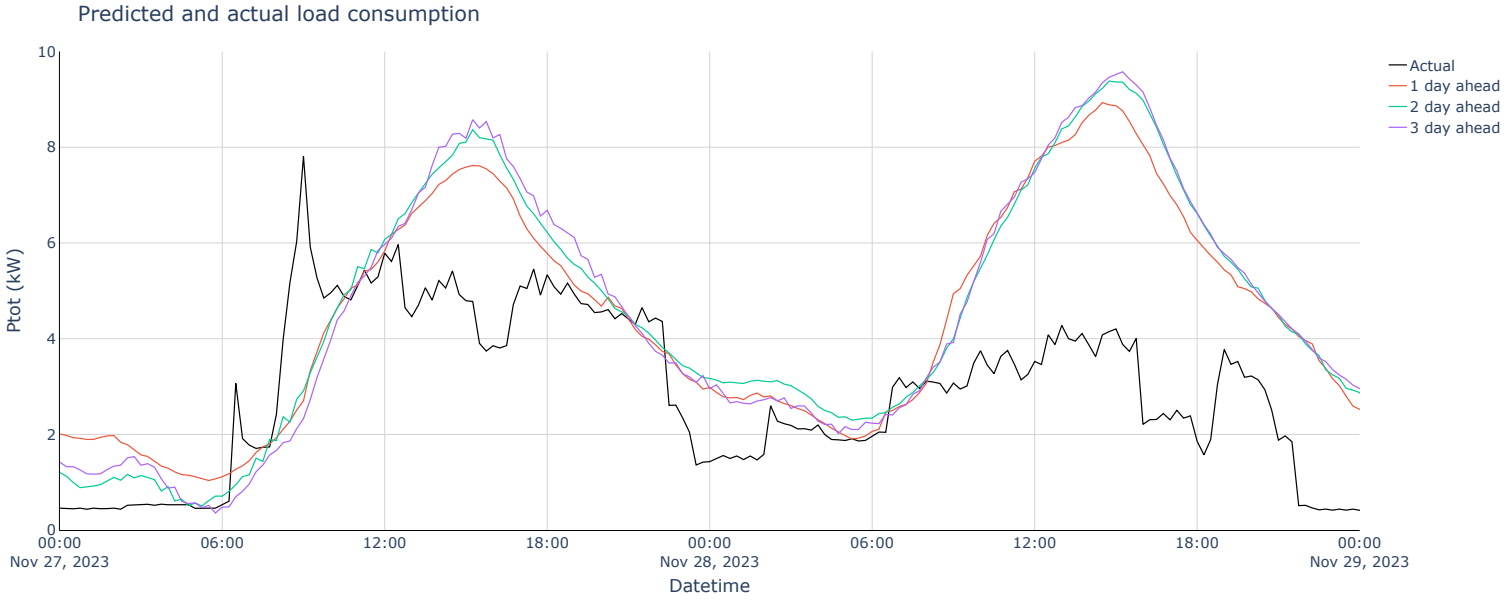

(b) **DA** scheme.

Figure 47: Time series of total load forecasting value under different scheme.

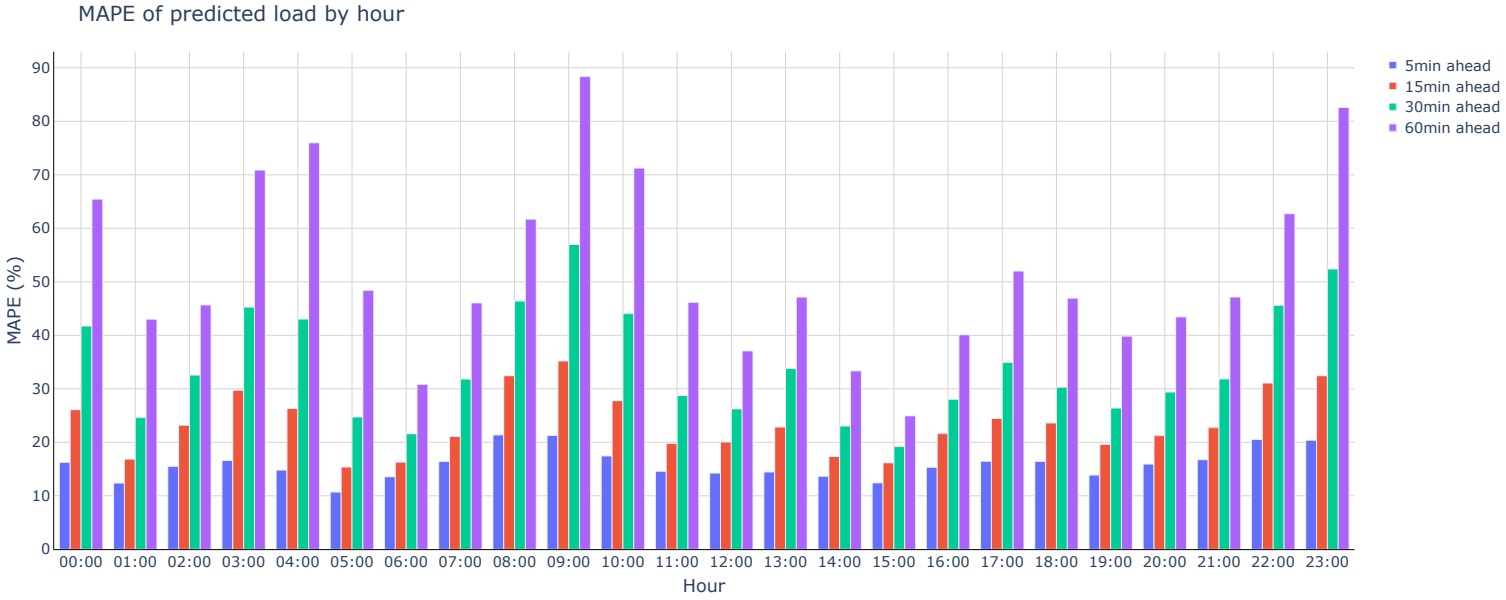

(a) **HA** scheme.

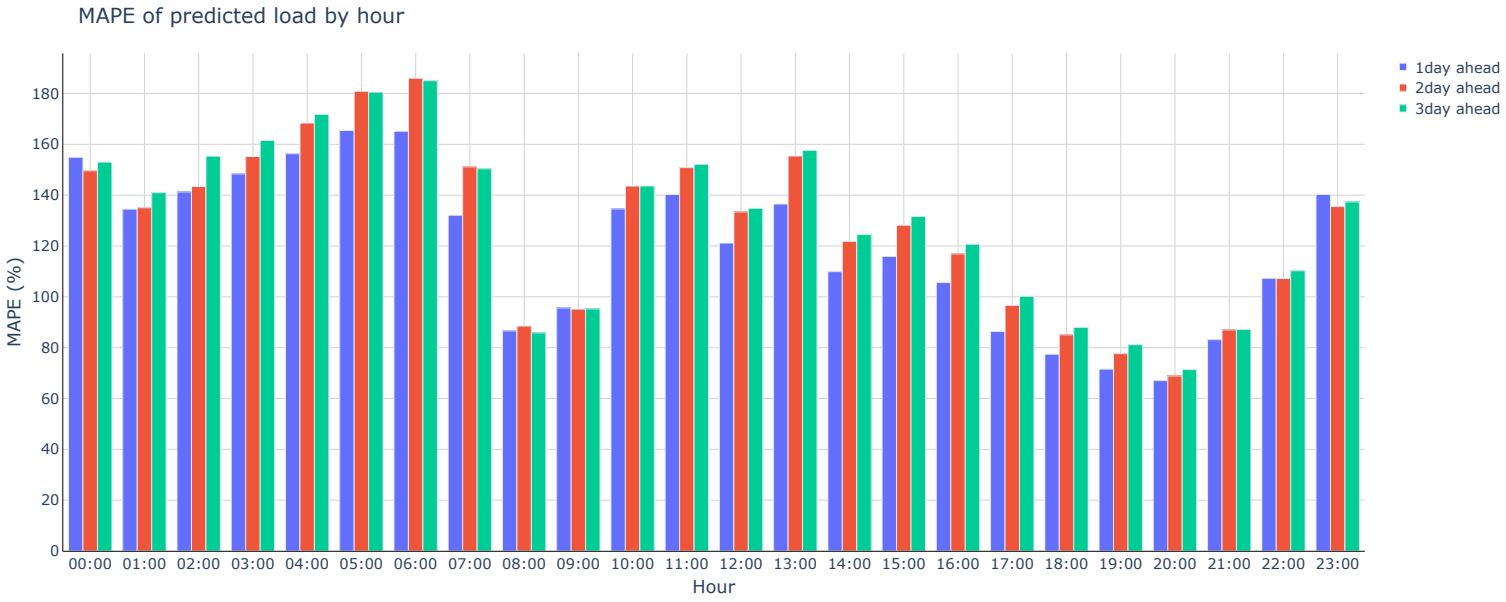

(b) **DA** scheme.

Figure 48: Hourly mean absolute percentage error (MAPE) of predicted total load consumption under different scheme.

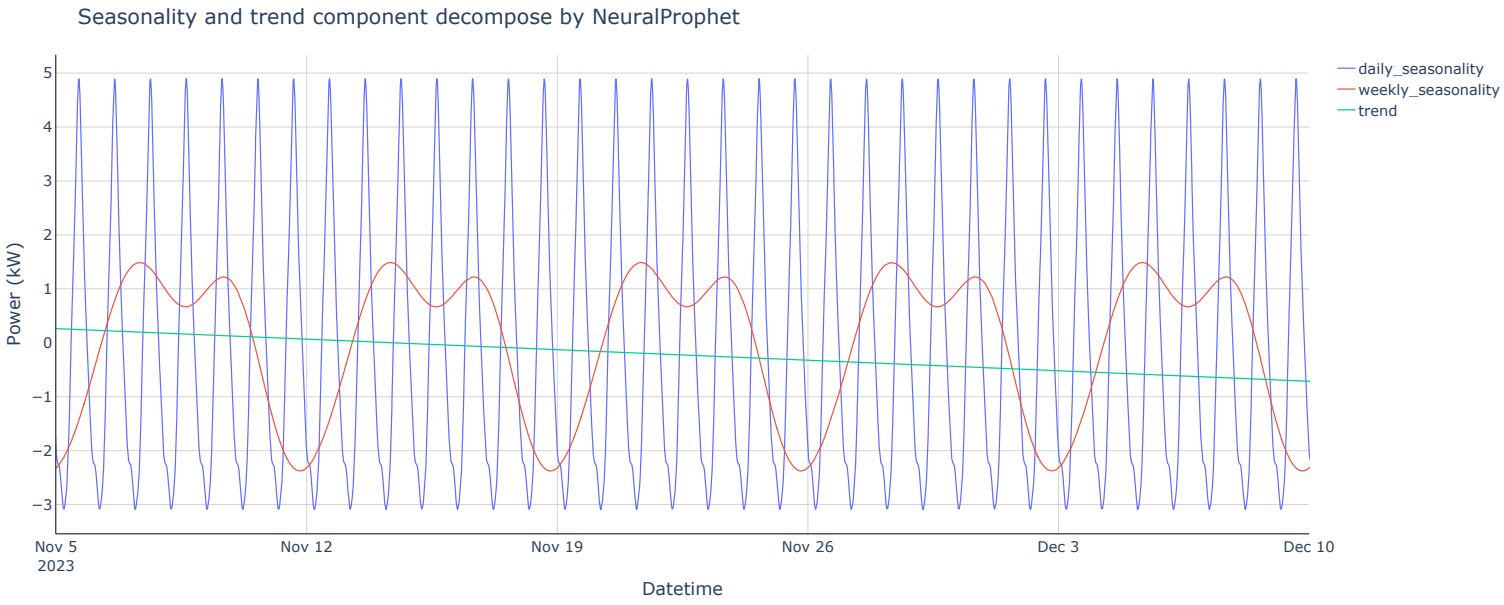

(a) **HA** scheme.

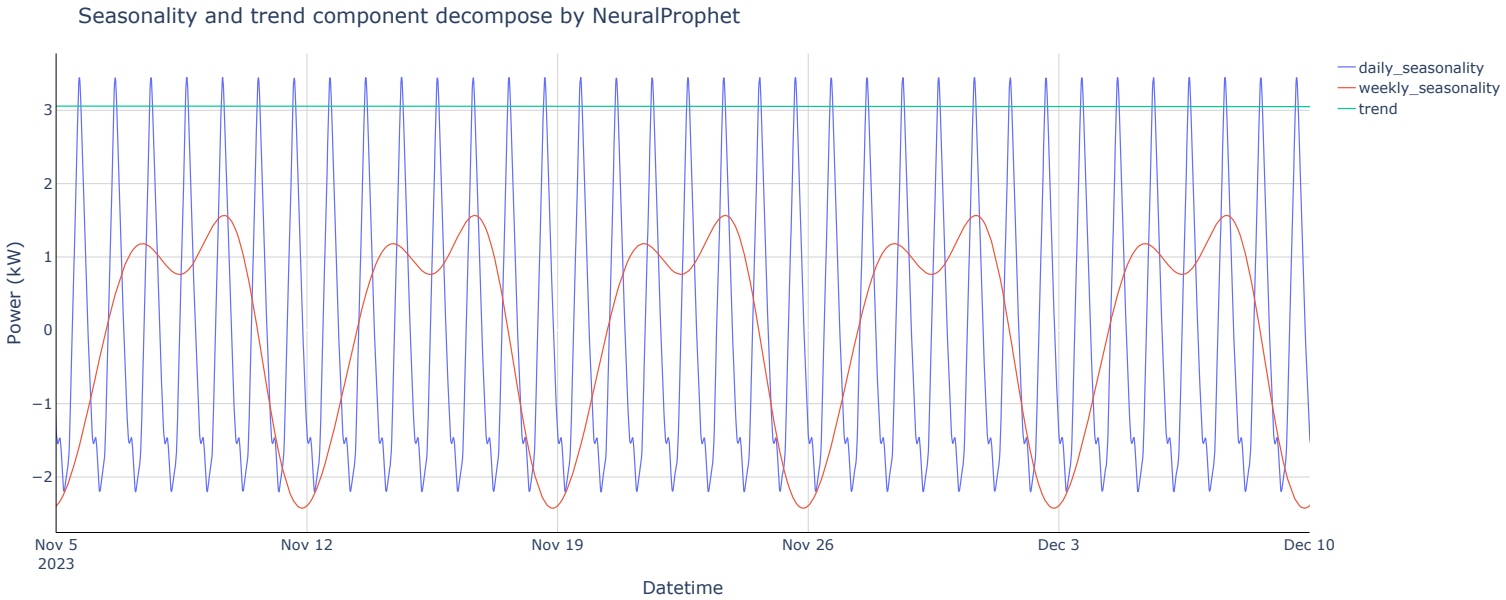

(b) **DA** scheme.

Figure 49: Seasonality and trend component from load forecasting model under different scheme.

5.8 Solar forecasting model performance

The model of irradiance-to-solar-generation power conversion can be expressed as (40). The trends, shown in Figure 50, can be split into two periods: one before August 2023 and one after August 2023. This indicates that the solar panels have degraded. The irradiance can be converted to solar generation power by,

$$P_{\text{pv}}(t) = \alpha I(t) + b, \tag{40}$$

where

- $\alpha = 0.004369$ $(\frac{\text{kW}}{\text{W/m}^2})$, $b = 0.02772$ (kW), during March to July 2023, and
- $\alpha = 0.002517$ $(\frac{\text{kW}}{\text{W/m}^2})$, $b = -0.04123$ (kW), during August 2023 to February 2024.

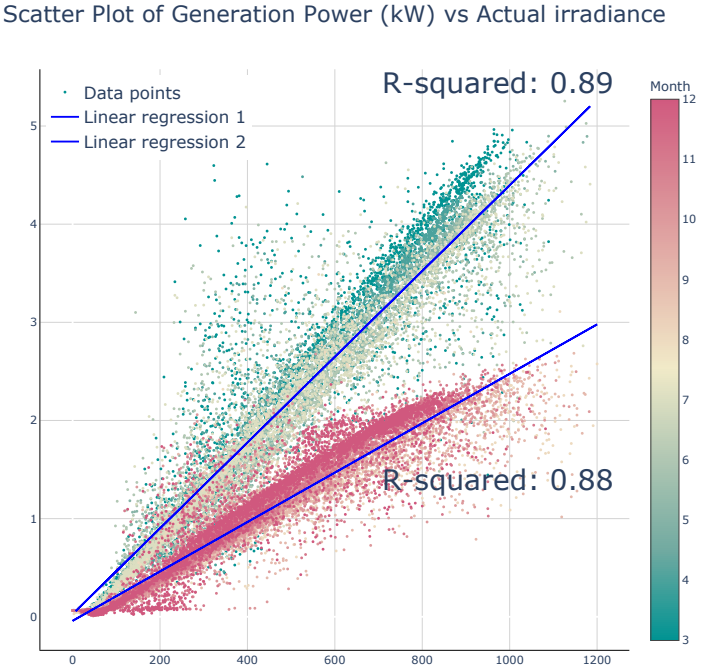

Figure 50: Irradiance to solar generation power.

In this experiment, the predicted irradiance from NCEP is selected as a future regressor discussed in section 4.2.1. In irradiance prediction, we forecast irradiance only for the period between 7:00 and 17:00, as most of the sunlight occurs during this time. Figure 51 displays the predicted and actual irradiance for both the HA and DA schemes. It is evident that while the HA model captures some fluctuations, the DA model fails to predict the fluctuations in actual irradiance.

Figure 52 illustrates the Mean Absolute Error (NMAE) of forecasted irradiance for both the HA and DA schemes. More closer prediction target for both schemes has lower error. In the HA scheme, the MAE remains under 60 W/sqm except during the 11:00 - 14:00, where it peaks at 80 W/sqm. This is possibly caused by the fluctuation of irradiance during this period. In the DA scheme, the MAE peaks at approximately 130 W/sqm during 11:00, whereas in other hours, it fluctuates around 20 - 60 W/sqm. This indicates that both models can roughly estimate the irradiance during the daytime in both schemes. The daily seasonality and trend decomposes by NeuralProphet in both scheme are shown in Figure 53, the daily seasonality from both the HA and DA models ranged from roughly -100 W/sqm to approximately 220 W/sqm and -50 W/sqm to 140 W/sqm, respectively, on each day. Additionally, the trend line from the HA model remained constant at 90 W/sqm, whereas the trend line from the DA model increased over time.

The performance of the irradiance forecasting model measured by other types of error is shown in Table 11.

Table 11: Error of predicted irradiance.

Minutes-ahead	MAE [W/sqm]	RMSE [W/sqm]	MAPE [%]	MBE [W/sqm]	NMAE [%]
5	54.40	101.67	20.95	2.93	5.03
15	71.60	115.92	31.56	6.22	6.62
30	80.54	120.88	38.42	7.73	7.45
60	88.06	124.46	44.06	7.95	8.15
Days-ahead	**MAE [W/sqm]**	**RMSE [W/sqm]**	**MAPE [%]**	**MBE [W/sqm]**	**NMAE [%]**
1	89.86	127.61	37.49	3.80	8.36
2	96.02	132.73	40.92	3.09	8.93
3	94.95	131.42	40.20	3.02	8.83

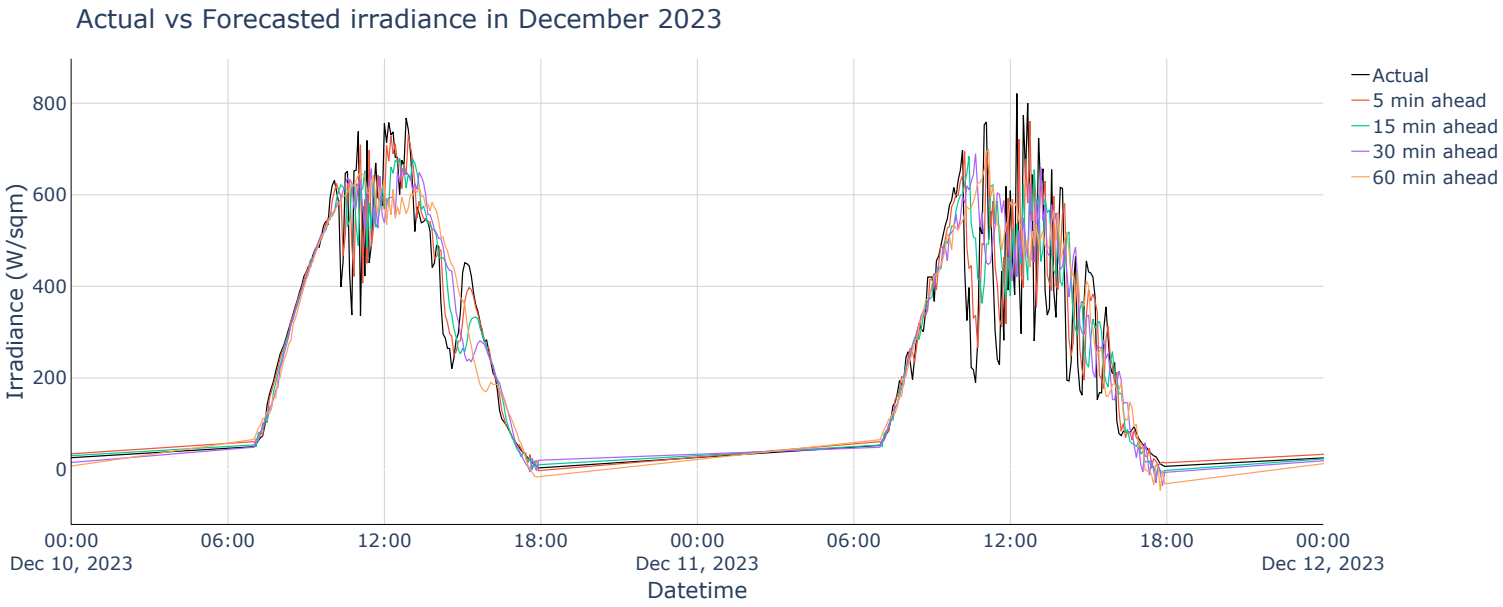

(a) **HA** scheme.

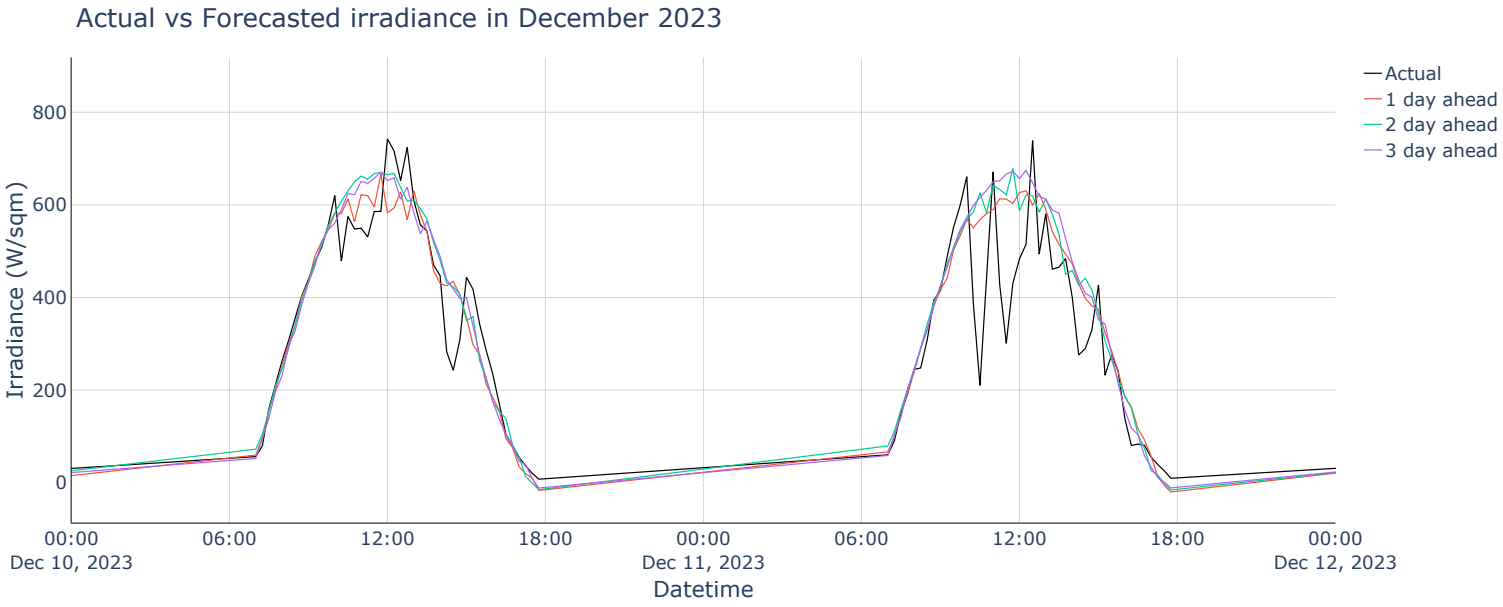

(b) **DA** scheme.

Figure 51: Time series of irradiance forecasting value under different scheme.

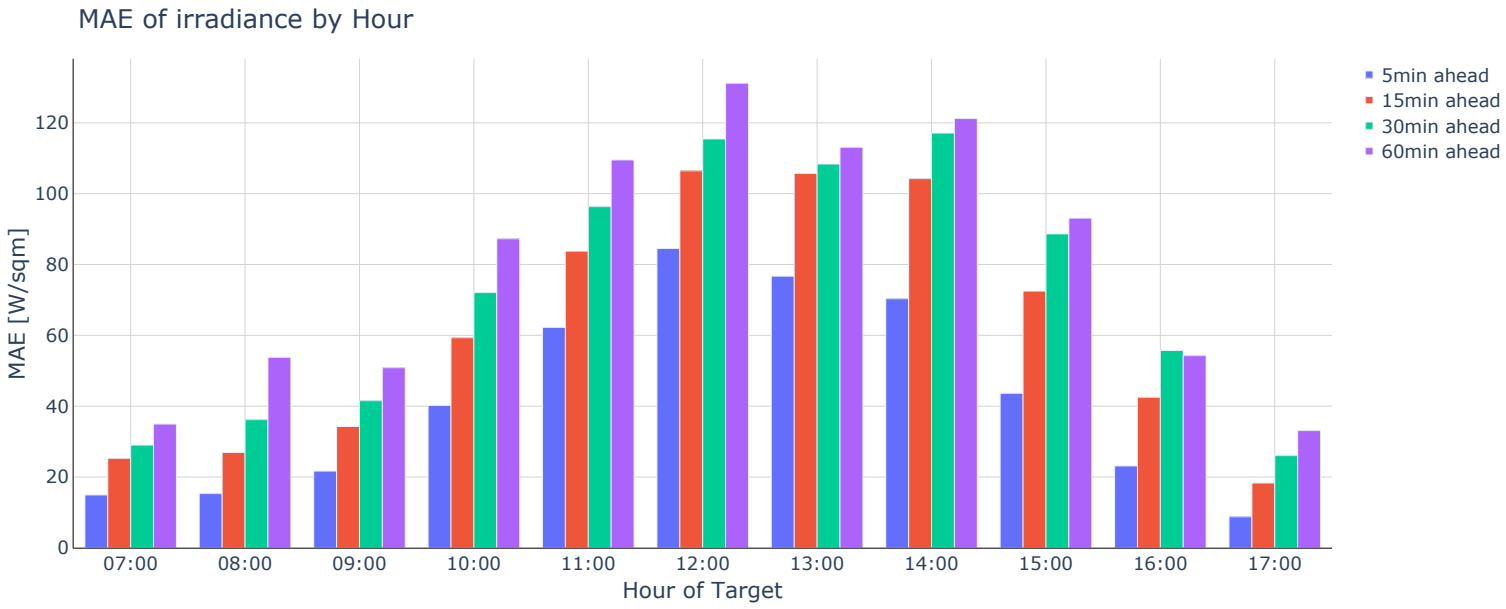

(a) **HA** scheme.

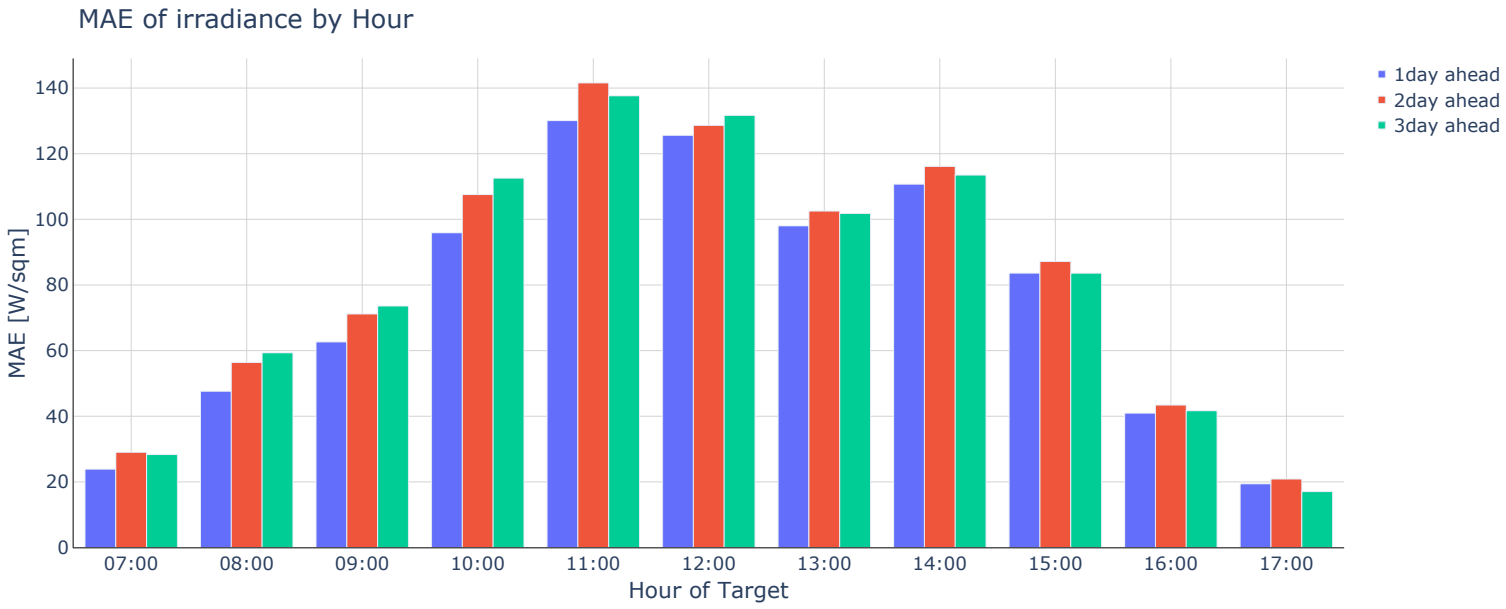

(b) **DA** scheme.

Figure 52: Hourly mean absolute error (MAE) of predicted irradiance under different scheme.

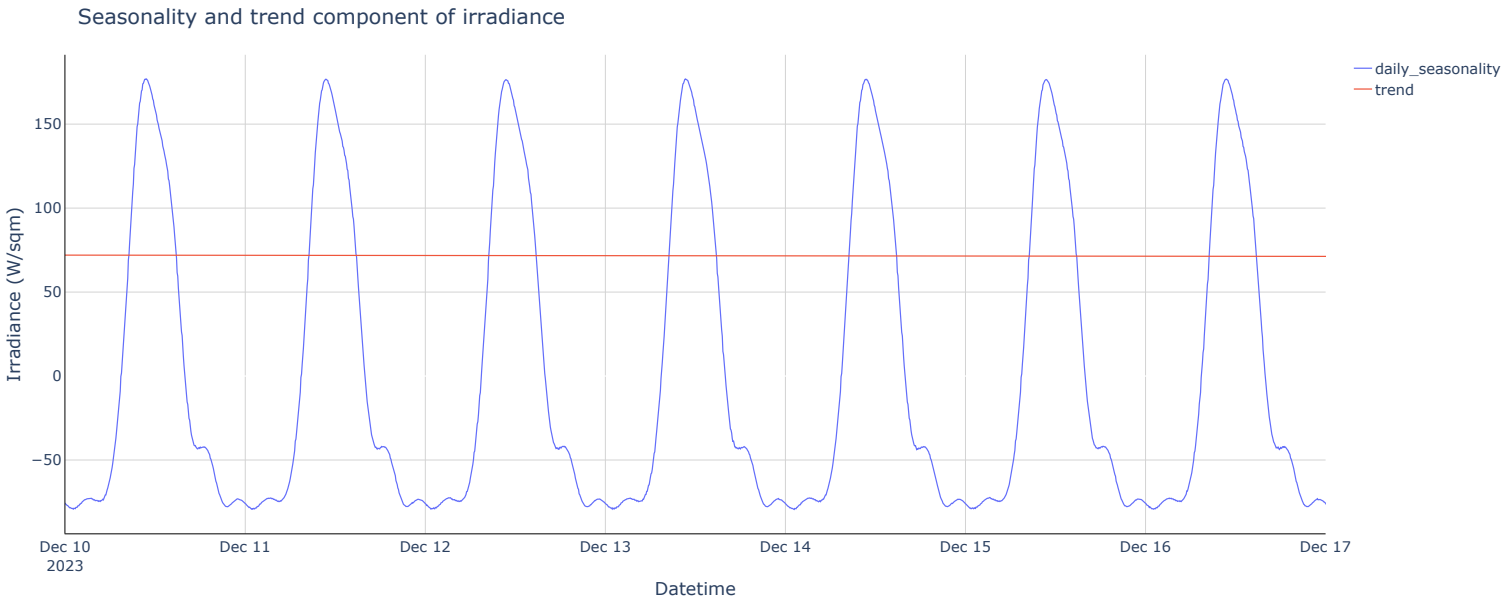

(a) **HA** scheme.

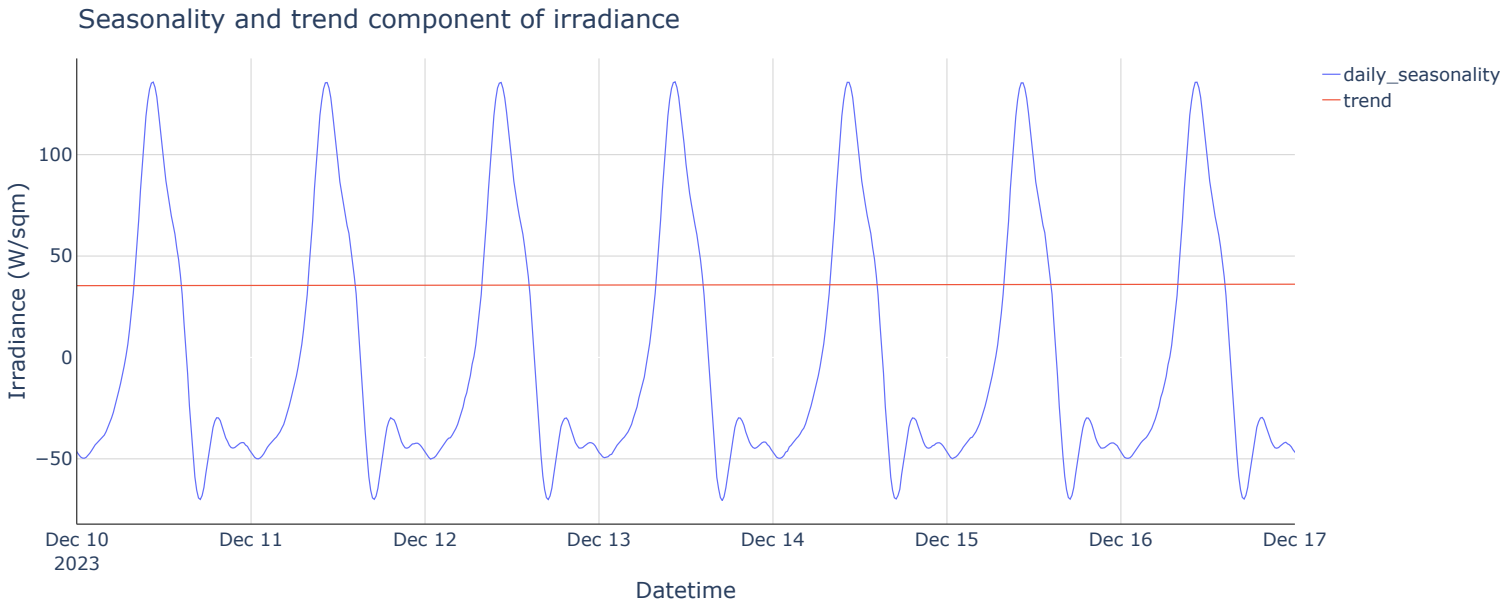

(b) **DA** scheme.

Figure 53: Seasonality and trend component from solar forecasting model under different scheme.

5.9 Rolling optimization for EMS implementation

Figure 54 shows the charging and discharging power of the batteries in the DA and HA plans during November $1^{st} - 4^{th}$, 2023. Without the DA plan, as a guideline for HA EMS, the HA EMS did not work as designed, as the batteries were first discharged until they reached 20% SoC and then remained almost idle throughout the rolling period. In the HA plan with DA tracking objective, while the batteries were charged around 00:00 of each day as determined by the DA plan, the charging power was corrected during 9:00 to 15:00 as the excess generation in HA was lower than predicted in the DA plan. This can be clearly seen during November $2^{nd} - 4^{th}$, 2023. In addition, the batteries also discharged more than calculated in the DA plan as the inadequate power was higher than the DA prediction, which can be clearly seen during 12:00 to 18:00 of the first two days. Another interesting point was the fluctuation in charging and discharging between 03:00 and 06:00 on November 3^{rd}, which might have occurred because the DA plan for the batteries was to charge during this period. However, in the HA plan, there was a small load consumption instead. This was possibly due to $w_s = 0.06$ was significantly smaller than $w_{chg} = 0.3$.

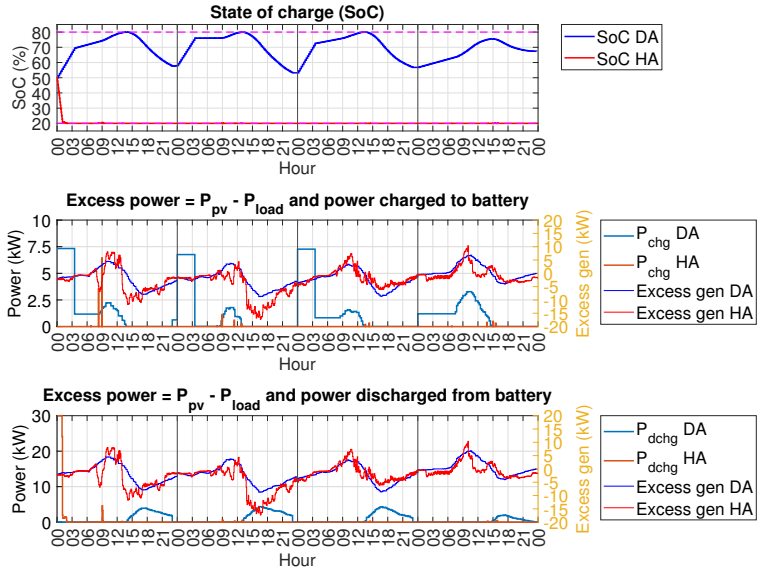

(a) Without $J_{trackDA}$.

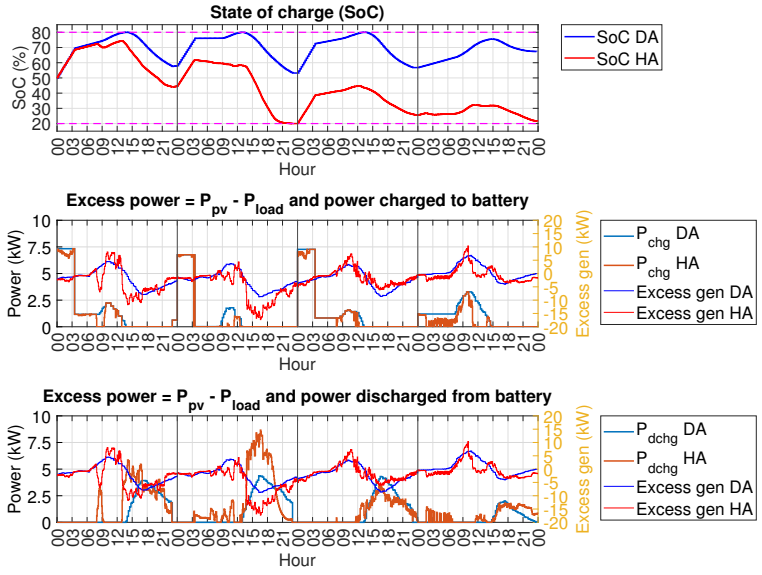

(b) With $J_{trackDA}$.

Figure 54: State of Charge with charging and discharging power in DA and HA schemes during November $1^{st} - 4^{th}$, 2023.

Figure 55 demonstrates $P_{\text{net}}(t)$ and expenses of the DA and HA plans during November $1^{\text{st}} - 4^{\text{th}}$, 2023. It was found that $P_{\text{net}}(t)$ of the HA plan mostly followed the DA plan except during 18:00 to 00:00 of November 2^{nd}, 2023, when the batteries could not discharge and needed to buy energy from the grid, causing the expense to be higher than expected in the DA plan. Furthermore, in the HA plan, the batteries discharged slightly more than the consumption as it followed the DA plan. In conclusion, the DA and HA planning procedures worked almost as intended, with the exception of slightly excessive discharging and charge/discharge fluctuations in some periods.

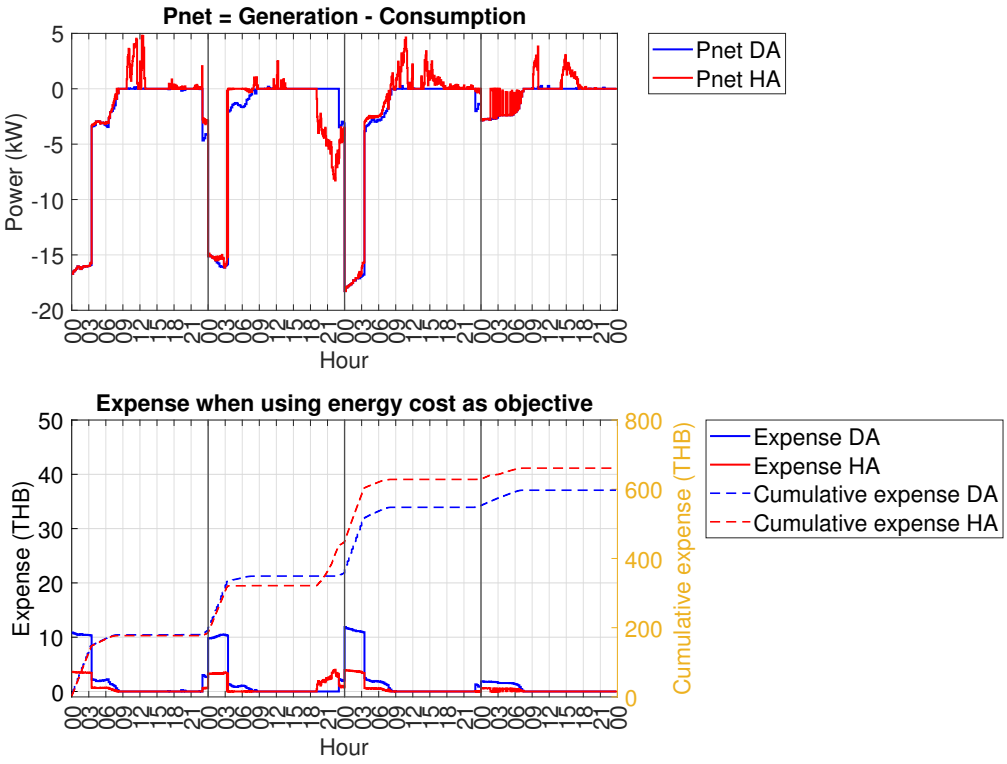

Figure 55: $P_{\text{net}}(t)$ and expenses of the DA and HA plans during November $1^{\text{st}} - 4^{\text{th}}$, 2023.

6 Open Energy Management System (OpenEMS)

Open Energy Management System (OpenEMS) is an open-source platform designed for managing energy in diverse applications. This platform serves as a robust simulation platform for energy management built by Java.

There are 3 main pillars in OpenEMS for IoT stack as can be seen in Figure 56. OpenEMS Edge is used to simulate the electric devices for individual site enabling monitor, control, and communicate with the backend. The user-friendly OpenEMS UI provides a web-based interface for local device configuration, allowing users to adjust the characteristics of the devices in details. Meanwhile, OpenEMS backend is the centralized server on clouds which can run the decentralized edge units, ensuring comprehensive oversight and management of the entire edge system. The role of the OpenEMS edge is to collect information from each device and send it to the OpenEMS backend. The information from the OpenEMS backend is then passed to the forecast module to predict solar generation and load consumption. After this, the forecasted information for load consumption and solar generation, including the state of devices, is sent to the EMS optimization module. Next, the optimal schedule for each device is passed through the OpenEMS backend to the OpenEMS edge. Finally, the OpenEMS edge converts the optimal schedule into a control signal, which is then sent to each device. The block diagram of the OpenEMS system is shown in Figure 57.

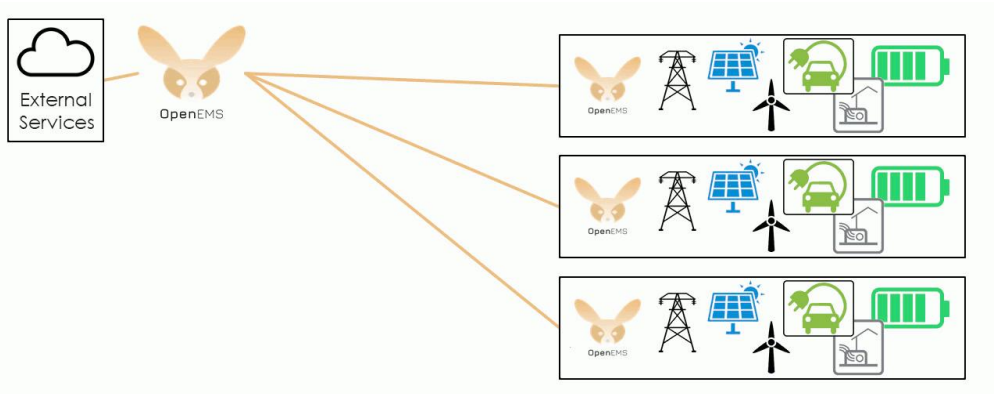

Figure 56: OpenEMS structure, Photo credit: www.openems.github.io.

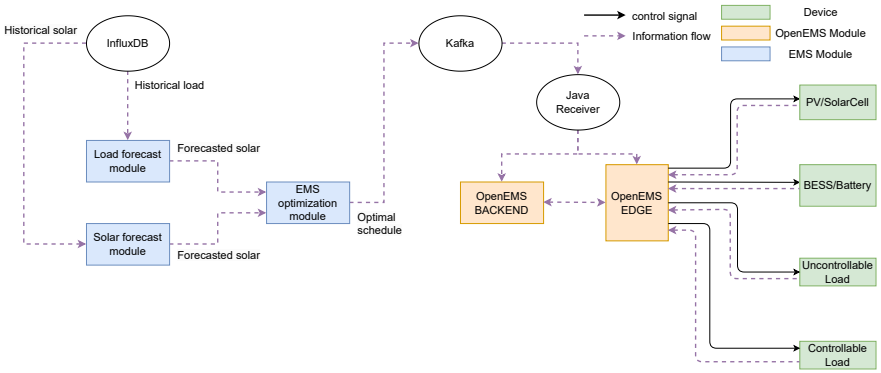

Figure 57: OpenEMS overview.

The simulation procedure proposed in EE490. After obtaining the complete optimization solutions for different mathematical formulations of optimization problems under different economic and operational objectives, the next step is the testing OpenEMS procedure. First, the load consumption data, solar generation data, and dynamical model of the battery must be prepared by the simulation before deployment in OpenEMS platform as the offline simulation. The load forecasted simulation data and the solar forecasted data are obtained from the existing machine learning model, while the dynamical

model of the battery can be obtained from the simulation by Simscape. Hence, the input for implementation in OpenEMS platform are the set of energy policies from the optimization solutions, the load and solar forecasted data, and the battery simulation. The result of running OpenEMS as the offline operation is the simulation result of how electrical components in the system function. Finally, analyze and investigate the correctness of the simulation results.

OpenEMS operation in EE499. We explored the components and modules offered by OpenEMS and were able to simulate solar panels, load, and batteries. While the load and solar cells used historical data, the battery required a controller to operate. In this project, our aim was to use Kafka as a means to send a solution to OpenEMS. However, a problem arose as it required a Java receiver, which is a module to receive solutions from Kafka and assign values to the OpenEMS platform. This module needed to be implemented in Java. The current OpenEMS operation used historical data for the simulation as shown in Figure 58(a).

In the real-time simulation experiment setting, OpenEMS enables us to incorporate historical data by importing .csv files. The simulation then parses each row of these data profiles, encompassing load generation and solar generation through the micro-grid systems. We have configured the components and hyperparameters of the micro-grid to align with those used in all EMS formulations. To streamline the experiment, we utilize pre-calculated solutions for each timestamp of both the load and solar instances to control the BESS. These solutions help reduce the computational time required during the optimization process. The setting is shown in Figure 58(b).

OpenEMS simulation result. Collaborating with Natanon, we utilized historical data from March 16-18, 2023 of the CUEE building as examples and experimented with prepared hour-ahead solutions. We added two BESS components with fixed-power controllers, allowing us to specify the charge and discharge power values for each BESS. However, we adjusted the battery capacity from 125 kWh to 25 kWh to downscale the simulation time. The control signal is then transmitted through embedded OpenEMS REST APIs, with timestamps aligned to those of the load and solar data, to OpenEMS EDGE. OpenEMS subsequently stores all data in InfluxDB, enabling us to analyze and visualize the results. The OpenEMS UI page depicted in Figure 59 displays the installed components and indicates the power that each BESS has charged or discharged by a specific value. It also presents grid power metering, equivalent to the $P_{\text{net}}(t)$ of our settings.

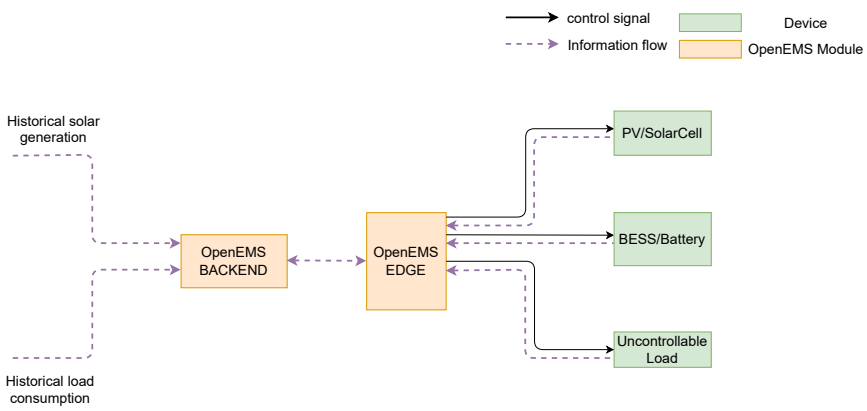

(a) Operation.

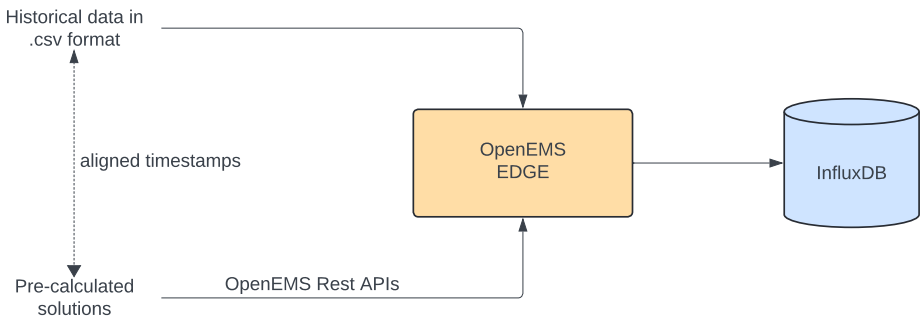

(b) Real-time simulation setting.

Figure 58: OpenEMS simulation.

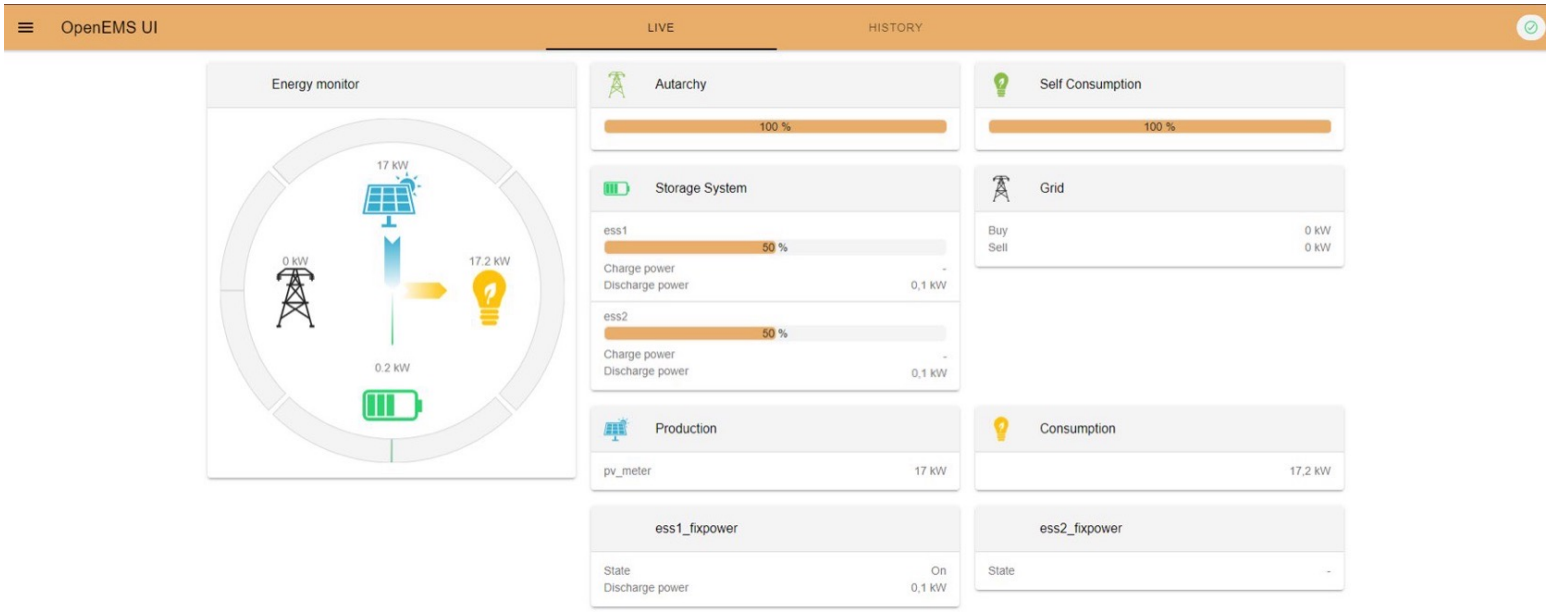

Figure 59: OpenEMS overview.

7 Conclusion

In this project, we aim to develop optimization problems based on different objectives of EMS. The battery is the main component that operates the system to behave as desired. In the Economic EMS, the total load consumption treated as uncontrollable load was considered. The decision-making process of the battery depends on load consumption, solar generation, and characteristics of electricity tariff. When there is excess generation, the battery is charged; conversely, when there is no excess generation, the battery discharges, resulting in lower electricity expenses compared to the case without EMS. Also, the characteristics of TOU, which have lower and higher price periods, explicitly affect the battery's charge and discharge, resulting in lower expenses than the flat rate TOU. Moreover, with the assumption that we can sell the electricity to the grid, the EMS can manage the system to make a profit instead of incurring expenses. In the operational EMS, the load consumption from two rooms with different priority originating from ACs, treated as controllable load, was considered. The EMS enhances the ACs in both rooms when there is enough solar generation; it can also turn off the ACs in the minor priority room to reduce electricity expenses. The islanding EMS can be achieved only when the solar generation is enough, which can be curtailed to prevent damage to electrical components. The RE 100 EMS was considered for total load consumption, the purpose of which is either to draw grid electricity for the entire day or not to draw at all. Implementation of the EMS advances the desired purpose, resulting in a higher RE percentage. However, the RE percentage to achieve depends on the system size. Increasing the solar panel installation capacity by 1 kWp can reduce a single battery capacity by at least 4 kWh. Notably, these simulations used historical data as parameters of the system for planning scheme.

For real-time EMS, the EMS is called rolling optimization, the procedure consists of two time scales for planning: DA and HA EMS. The DA EMS is executed at the end of each day to obtain a rough plan for the next day, while the HA EMS is initiated every 5 minutes to mitigate the effects of inaccurate DA plans. All EMS formulations and rolling optimization framework are tested through simulation. In the future, the OpenEMS implementation and the model predictive control will be considered as a way to achieve better understanding of real appliances control and to obtained better results.

Problem. The problems in this project lie with the OpenEMS platform, as it is implemented in the Java programming language. Additionally, there is no explicit way to control the simulated devices in real-time using an optimal schedule obtained from the Python module.

8 Acknowledgement

We extend our sincere gratitude to Assoc. Prof. Jitkomut Songsiri for her invaluable comments and insightful discussions throughout the duration of this project. Her guidance and expertise were instrumental in shaping our understanding and approach. Special thanks are also due to Assoc. Prof. Dr. Wijarn Wangdee for his helpful suggestion on actual EMS operation. We are grateful to Assoc. Prof. Surapong Suwankawin and his advisee Pimnapat Phonthani for providing the aggregation data for the EE building and assisting with problem specifications design for this project. Our thanks extend to Assist. Prof. Somboon Sangwongwanich for information regarding air conditioning system specifications in Gewertz square. We acknowledge Supatana Hengyotmak for his guidance on OpenEMS, and Natanon Tongamrak for his contributions to OpenEMS simulation and the forecasting model experiments, which significantly accelerated our progress. Finally, we express our appreciation to our fellow EE students for their encouragement and support throughout this year.

References

[1] S. Hussain, C. Z. El-Bayeh, C. Lai, and U. Eicker, "Multi-level energy management systems toward a smarter grid: A review," *IEEE Access*, vol. 9, pp. 71994–72016, 2021.

[2] M. Rastegar, M. Fotuhi-Firuzabad, and H. Zareipour, "Home energy management incorporating operational priority of appliances," *International Journal of Electrical Power & Energy Systems*, vol. 74, pp. 286–292, 2016.

[3] J. H. Yoon, R. Bladick, and A. Novoselac, "Demand response for residential buildings based on dynamic price of electricity," *Energy and Buildings*, vol. 80, pp. 531–541, 2014.

[4] D. Menniti, A. Pinnarelli, N. Sorrentino, P. Vizza, A. Burgio, G. Brusco, and M. Motta, "A real-life application of an efficient energy management method for a local energy system in presence of energy storage systems," in *2018 IEEE International Conference on Environment and Electrical Engineering and 2018 IEEE Industrial and Commercial Power Systems Europe (EEEIC / I&CPS Europe)*, pp. 1–6, 2018.

[5] M. Gholami and M. Sanjari, "Multiobjective energy management in battery-integrated home energy systems," *Renewable Energy*, vol. 177, pp. 967–975, 2021.

[6] J. M. Raya-Armenta, N. Bazmohammadi, J. G. Avina-Cervantes, D. Sáez, J. C. Vasquez, and J. M. Guerrero, "Energy management system optimization in islanded microgrids: An overview and future trends," *Renewable and Sustainable Energy Reviews*, vol. 149, p. 111327, 2021.

[7] A. E. Nezhad, A. Rahimnejad, and S. A. Gadsden, "Home energy management system for smart buildings with inverter-based air conditioning system," *International Journal of Electrical Power & Energy Systems*, vol. 133, p. 107230, 2021.

[8] M. Killian, M. Zauner, and M. Kozek, "Comprehensive smart home energy management system using mixed-integer quadratic-programming," *Applied Energy*, vol. 222, pp. 662–672, 2018.

[9] V. Dao, H. Ishii, Y. Takenobu, S. Yoshizawa, and Y. Hayashi, "Intensive quadratic programming approach for home energy management systems with power utility requirements," *International Journal of Electrical Power & Energy Systems*, vol. 115, p. 105473, 2020.

[10] Y. He, Z. Li, J. Zhang, G. Shi, and W. Cao, "Day-ahead and intraday multi-time scale microgrid scheduling based on light robustness and mpc," *International Journal of Electrical Power & Energy Systems*, vol. 144, p. 108546, 2023.

[11] F. Luo, G. Ranzi, C. Wan, Z. Xu, and Z. Dong, "A multistage home energy management system with residential photovoltaic penetration," *IEEE Transactions on Industrial Informatics*, vol. 15, no. 1, pp. 116–126, 2019.

[12] C. Orozco, A. Borghetti, B. De Schutter, F. Napolitano, G. Pulazza, and F. Tossani, "Intra-day scheduling of a local energy community coordinated with day-ahead multistage decisions," *Sustainable Energy, Grids and Networks*, vol. 29, p. 100573, 2022.

[13] J. Zhai, X. Wu, Z. Li, S. Zhu, B. Yang, and H. Liu, "Day-ahead and intra-day collaborative optimized operation among multiple energy stations," *Energies*, vol. 14, no. 4, 2021.

[14] Z. Yuan, J. Xia, and P. Li, "Two-time-scale energy management for microgrids with data-based day-ahead distributionally robust chance-constrained scheduling," *IEEE Transactions on Smart Grid*, vol. 12, no. 6, pp. 4778–4787, 2021.

[15] F. Conte, S. Massucco, G. Schiapparelli, and F. Silvestro, "Day-ahead and intra-day planning of integrated BESS-PV systems providing frequency regulation," *IEEE Transactions on Sustainable Energy*, vol. 11, no. 3, pp. 1797–1806, 2020.

[16] O. Triebe, H. Hewamalage, P. Pilyugina, N. P. Laptev, C. Bergmeir, and R. Rajagopal, "Neuralprophet: Explainable forecasting at scale," *ArXiv*, vol. abs/2111.15397, 2021.

9 Appendices

9.1 Math formulation of EMS formulations

9.1.1 Economic EMS

Let $z = \left(P_{\text{net}}(t), P^{(i)}_{\text{chg}}(t), P^{(i)}_{\text{dchg}}(t), x^{(i)}_{\text{chg}}(t), x^{(i)}_{\text{dchg}}(t), \text{SoC}_i(t)\right)$ be the optimization variable where $i = 1, 2$ for $t = 1, \ldots, T$.
The optimization formulation is

$$
\begin{aligned}
\underset{z}{\text{minimize}} \quad & J_{\text{cost}} + J_{\text{battery}} \\
\text{subject to} \quad & P_{\text{net}}(t) = P_{\text{pv}}(t) + P^{(i)}_{\text{dchg}}(t) - P_{\text{uload}}(t) - P^{(i)}_{\text{chg}}(t), \quad \text{for } t = 1, ..., T \\
& \text{SoC}_i(t+1) = \text{SoC}_i(t) + \frac{100}{\text{BattCapacity}} \left(\eta_c P^{(i)}_{\text{chg}}(t) \Delta t - \frac{P^{(i)}_{\text{dchg}}(t) \Delta t}{\eta_d} \right), \quad \text{for } t = 1, ..., T \\
& \text{SoC}_{\text{min}} \leq \text{SoC}_i(t) \leq \text{SoC}_{\text{max}}, \quad \text{for } t = 1, ..., T \\
& P^{(i)}_{\text{chg}}(t) \leq x^{(i)}_{\text{chg}}(t) \cdot \text{MAX CHARGE RATE}, \quad \text{for } t = 1, ..., T \\
& P^{(i)}_{\text{dchg}}(t) \leq x^{(i)}_{\text{dchg}}(t) \cdot \text{MAX DISCHARGE RATE}, \quad \text{for } t = 1, ..., T \\
& 0 \leq x^{(i)}_{\text{chg}}(t) + x^{(i)}_{\text{dchg}}(t) \leq 1, \quad \text{for } t = 1, ..., T
\end{aligned}
\tag{41}
$$

where $x^{(i)}_{\text{chg}}(t), x^{(i)}_{\text{dchg}}(t) \in \{0, 1\}$, and

- if the option is Energy unit, $J_{\text{cost}} = \sum_{t=1}^{T} \max(0, -P_{\text{net}}(t)) \Delta t$,
- if the option is Energy cost, $J_{\text{cost}} = \sum_{t=1}^{T} b(t) \max(0, -P_{\text{net}}(t)) \Delta t$,
- if the option is Profit, $J_{\text{cost}} = \sum_{t=1}^{T} \left[b(t) \max(0, -P_{\text{net}}(t)) - s(t) \max(0, P_{\text{net}}(t)) \right] \Delta t$.

and

$$
\begin{aligned}
J_{\text{battery}} =& w_{\text{m}} |\text{SoC}_1(t) - \text{SoC}_2(t)| + w_{\text{c}} \left(\text{SoC}_{\text{max}} - \text{SoC}_1(t) \right) / \left(\text{SoC}_{\text{max}} - \text{SoC}_{\text{min}} \right) \\
& + w_{\text{s}} \sum_{i=1}^{2} \sum_{t=1}^{T-1} \left| x^{(i)}_{\text{chg}}(t) - x^{(i)}_{\text{chg}}(t+1) \right| + \left| x^{(i)}_{\text{dchg}}(t) - x^{(i)}_{\text{dchg}}(t+1) \right|.
\end{aligned}
\tag{42}
$$

9.1.2 Operational EMS

Let $z = \left(P_{\text{net}}(t), P^{(i)}_{\text{chg}}(t), P^{(i)}_{\text{dchg}}(t), x^{(i)}_{\text{chg}}(t), x^{(i)}_{\text{dchg}}(t), \text{SoC}_i(t), P_{\text{ac,m}}(t), P_{\text{ac,s}}(t), x^{(j)}_{\text{ac,m}}(t), x^{(j)}_{\text{ac,s}}(t)\right)$ be the optimization variable where $i = 1, 2$ for $t = 1, \ldots, T$.
The optimization problem is,

$$
\begin{aligned}
\underset{z}{\text{minimize}} \quad & J_{\text{cost}} + J_{\text{battery}} - \sum_{t \in O} [w_{\text{ac,m}} \sum_{j=1}^{4} x^{(j)}_{\text{ac,m}}(t) + w_{\text{ac,s}} \sum_{j=1}^{4} x^{(j)}_{\text{ac,s}}(t)] \\
\text{subject to} \quad & P_{\text{net}}(t) = P_{\text{pv}}(t) + P^{(i)}_{\text{dchg}}(t) - P_{\text{uload}}(t) - P^{(i)}_{\text{chg}}(t) - P_{\text{ac,m}}(t) - P_{\text{ac,s}}(t), \quad \text{for } t = 1, ..., T \\
& P_{\text{ac,m}}(t) = (x^{(1)}_{\text{ac,m}}(t) + 0.5x^{(2)}_{\text{ac,m}}(t) + 0.7x^{(3)}_{\text{ac,m}}(t) + 0.8x^{(4)}_{\text{ac,m}}(t))P_{\text{ac,m,rated}}, \quad \text{for } t = 1, ..., T \\
& P_{\text{ac,s}}(t) = (x^{(1)}_{\text{ac,s}}(t) + 0.5x^{(2)}_{\text{ac,s}}(t) + 0.7x^{(3)}_{\text{ac,m}}(t) + 0.8x^{(4)}_{\text{ac,s}}(t))P_{\text{ac,s,rated}}, \quad \text{for } t = 1, ..., T \\
& 0 \leq \sum_{j=1}^{4} x^{(j)}_{\text{ac,m}}(t) \leq 1, \quad \text{for } t = 1, ..., T \\
& 0 \leq \sum_{j=1}^{4} x^{(j)}_{\text{ac,s}}(t) \leq 1, \quad \text{for } t = 1, ..., T \\
& \text{SoC}_i(t+1) = \text{SoC}_i(t) + \frac{100}{\text{BattCapacity}} \left(\eta_c P^{(i)}_{\text{chg}}(t)\Delta t - \frac{P^{(i)}_{\text{dchg}}(t)\Delta t}{\eta_d} \right), \quad \text{for } t = 1, ..., T \\
& \text{SoC}_{\text{min}} \leq \text{SoC}_i(t) \leq \text{SoC}_{\text{max}}, \quad \text{for } t = 1, ..., T \\
& P^{(i)}_{\text{chg}}(t) \leq x^{(i)}_{\text{chg}}(t) \cdot \text{MAX CHARGE RATE}, \quad \text{for } t = 1, ..., T \\
& P^{(i)}_{\text{dchg}}(t) \leq x^{(i)}_{\text{dchg}}(t) \cdot \text{MAX DISCHARGE RATE}, \quad \text{for } t = 1, ..., T \\
& 0 \leq x^{(i)}_{\text{chg}}(t) + x^{(i)}_{\text{dchg}}(t) \leq 1, \quad \text{for } t = 1, ..., T
\end{aligned}
\tag{43}
$$

where $x^{(j)}_{\text{ac,m}}(t), x^{(j)}_{\text{ac,s}}(t) \in \{0, 1\}$, for $i = 1, 2, 3, 4$ and $x^{(i)}_{\text{chg}}(t), x^{(i)}_{\text{dchg}}(t) \in \{0, 1\}$.

9.1.3 Islanding EMS

Let $z = \left(P_{\text{net}}(t), P_{\text{pv}}(t), P^{(i)}_{\text{chg}}(t), P^{(i)}_{\text{dchg}}(t), x^{(i)}_{\text{chg}}(t), x^{(i)}_{\text{dchg}}(t), \text{SoC}_i(t), P_{\text{ac,m}}(t), P_{\text{ac,s}}(t), x^{(j)}_{\text{ac,m}}(t), x^{(j)}_{\text{ac,s}}(t)\right)$ be the optimization variable where $i = 1, 2$ for $t = 1, \ldots, T$.
The optimization problem is,

$$
\begin{aligned}
\underset{z}{\text{minimize}} \quad & -\sum_{t\in O}[w_{\text{ac,m}} \sum_{j=1}^{4} x^{(j)}_{\text{ac,m}}(t) + w_{\text{ac,s}} \sum_{j=1}^{4} x^{(j)}_{\text{ac,s}}(t)] \\
\text{subject to} \quad & P_{\text{net}}(t) = P_{\text{pv}}(t) + P^{(i)}_{\text{dchg}}(t) - P_{\text{uload}}(t) - P^{(i)}_{\text{chg}}(t) - P_{\text{ac,m}}(t) - P_{\text{ac,s}}(t) = 0, \quad \text{for } t = 1, ..., T \\
& P_{\text{pv}}(t) \le P^{\text{max}}_{\text{pv}}(t), \quad \text{for } t = 1, ..., T \\
& P_{\text{ac,m}}(t) = (x^{(1)}_{\text{ac,m}}(t) + 0.5x^{(2)}_{\text{ac,m}}(t) + 0.7x^{(3)}_{\text{ac,m}}(t) + 0.8x^{(4)}_{\text{ac,m}}(t))P_{\text{ac,m,rated}}, \quad \text{for } t = 1, ..., T \\
& P_{\text{ac,s}}(t) = (x^{(1)}_{\text{ac,s}}(t) + 0.5x^{(2)}_{\text{ac,s}}(t) + 0.7x^{(3)}_{\text{ac,m}}(t) + 0.8x^{(4)}_{\text{ac,s}}(t))P_{\text{ac,s,rated}}, \quad \text{for } t = 1, ..., T \\
& 0 \le \sum_{j=1}^{4} x^{(j)}_{\text{ac,m}}(t) \le 1, \quad \text{for } t = 1, ..., T \\
& 0 \le \sum_{j=1}^{4} x^{(j)}_{\text{ac,s}}(t) \le 1, \quad \text{for } t = 1, ..., T \\
& \text{SoC}_i(t+1) = \text{SoC}_i(t) + \frac{100}{\text{BattCapacity}}\left(\eta_c P^{(i)}_{\text{chg}}(t)\Delta t - \frac{P^{(i)}_{\text{dchg}}(t)\Delta t}{\eta_d}\right), \quad \text{for } t = 1, ..., T \\
& \text{SoC}_{\text{min}} \le \text{SoC}_i(t) \le \text{SoC}_{\text{max}}, \quad \text{for } t = 1, ..., T \\
& P^{(i)}_{\text{chg}}(t) \le x^{(i)}_{\text{chg}}(t) \cdot \text{MAX CHARGE RATE}, \quad \text{for } t = 1, ..., T \\
& P^{(i)}_{\text{dchg}}(t) \le x^{(i)}_{\text{dchg}}(t) \cdot \text{MAX DISCHARGE RATE}, \quad \text{for } t = 1, ..., T \\
& 0 \le x^{(i)}_{\text{chg}}(t) + x^{(i)}_{\text{dchg}}(t) \le 1, \quad \text{for } t = 1, ..., T
\end{aligned}
\tag{44}
$$

where $x^{(j)}_{\text{ac,m}}(t), x^{(j)}_{\text{ac,s}}(t) \in \{0, 1\}$, for $i = 1, 2, 3, 4$ and $x^{(i)}_{\text{chg}}(t), x^{(i)}_{\text{dchg}}(t) \in \{0, 1\}$.

9.1.4 RE 100 EMS

Let $z = \left(P_{\text{net}}(t), P^{(i)}_{\text{chg}}(t), P^{(i)}_{\text{dchg}}(t), x^{(i)}_{\text{chg}}(t), x^{(i)}_{\text{dchg}}(t), \text{SoC}_i(t)\right)$ be the optimization variable where $i = 1, 2$ for $t = 1, \ldots, T$.
The optimization problem is,

$$
\begin{aligned}
\underset{z}{\text{minimize}} \quad & \sum_{d=1}^{D} \|P^{-}_{\text{net},d}\|_\infty + J_{\text{battery}} \\
\text{subject to} \quad & P_{\text{net}}(t) = P_{\text{pv}}(t) + P^{(i)}_{\text{dchg}}(t) - P_{\text{uload}}(t) - P^{(i)}_{\text{chg}}(t), \quad \text{for } t = 1, ..., T \\
& \text{SoC}_i(t+1) = \text{SoC}_i(t) + \frac{100}{\text{BattCapacity}}\left(\eta_c P^{(i)}_{\text{chg}}(t)\Delta t - \frac{P^{(i)}_{\text{dchg}}(t)\Delta t}{\eta_d}\right), \quad \text{for } t = 1, ..., T \\
& \text{SoC}_{\text{min}} \le \text{SoC}_i(t) \le \text{SoC}_{\text{max}}, \quad \text{for } t = 1, ..., T \\
& P^{(i)}_{\text{chg}}(t) \le x^{(i)}_{\text{chg}}(t) \cdot \text{MAX CHARGE RATE}, \quad \text{for } t = 1, ..., T \\
& P^{(i)}_{\text{dchg}}(t) \le x^{(i)}_{\text{dchg}}(t) \cdot \text{MAX DISCHARGE RATE}, \quad \text{for } t = 1, ..., T \\
& 0 \le x^{(i)}_{\text{chg}}(t) + x^{(i)}_{\text{dchg}}(t) \le 1, \quad \text{for } t = 1, ..., T,
\end{aligned}
\tag{45}
$$

where $x^{(i)}_{\text{chg}}(t), x^{(i)}_{\text{dchg}}(t) \in \{0, 1\}$

9.2 Expenses saved by Economic EMS: Energy cost option

The histogram depicting expenses saved by Economic EMS: Energy cost option under various scenarios illustrates how the EMS impacts the reduction of electricity expenses.

- **High solar & low load scenario**: saved up to 850 THB for TOU 0 and 1150 for TOU 1.
- **Low solar & low load scenario**: saved up to 850 THB for TOU 0 and 950 for TOU 1.
- **Low solar & high load scenario**: saved up to 850 THB for TOU 0 and 950 for TOU 1.

In conclusion, the EMS can reduce the electricity expenses in every dataset and can be saved better in TOU 1.

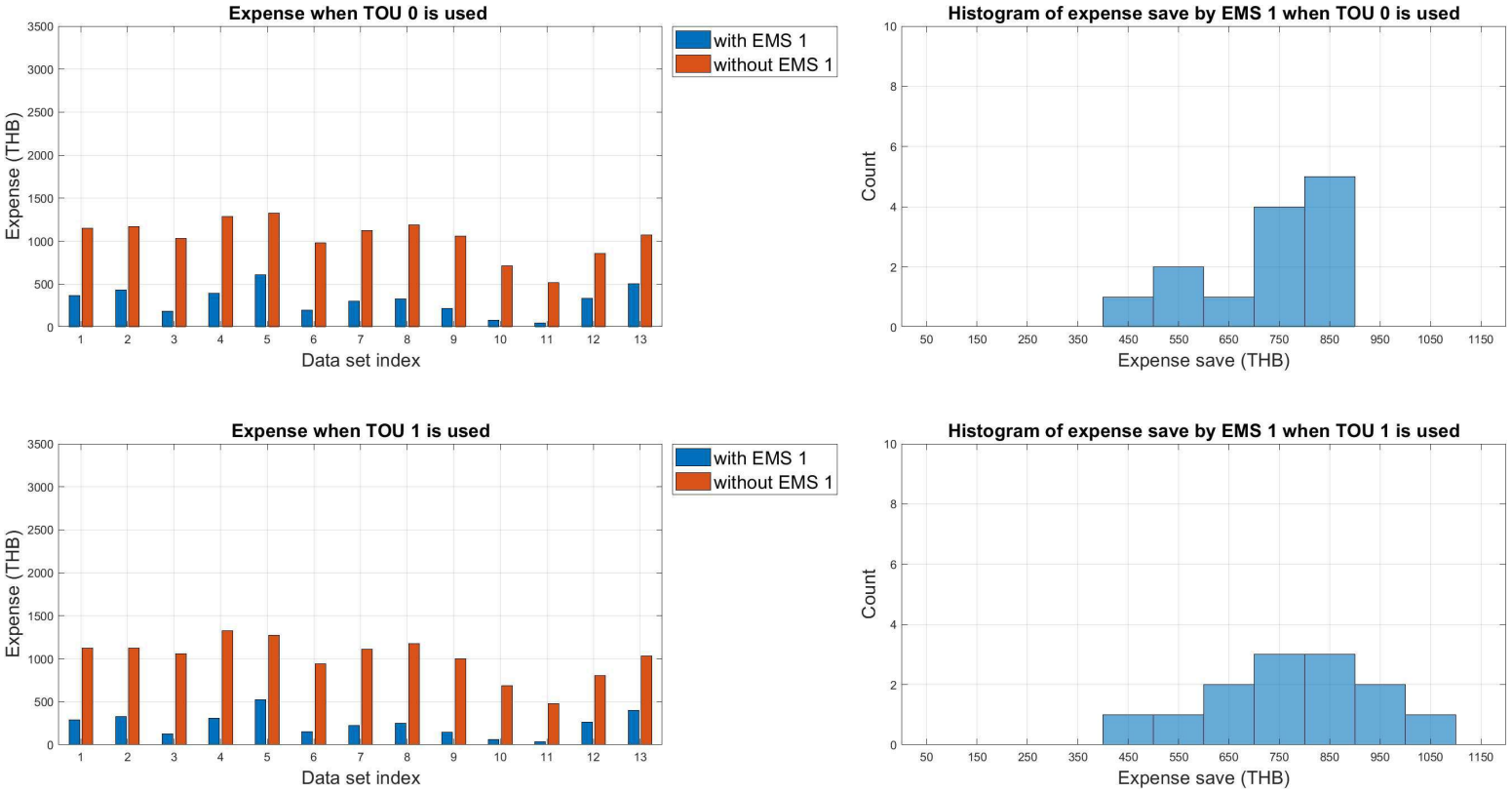

Figure 60: Histogram of expenses saved by Energy cost option in the scenario of **high solar & low load** under TOU 0 and TOU 1.

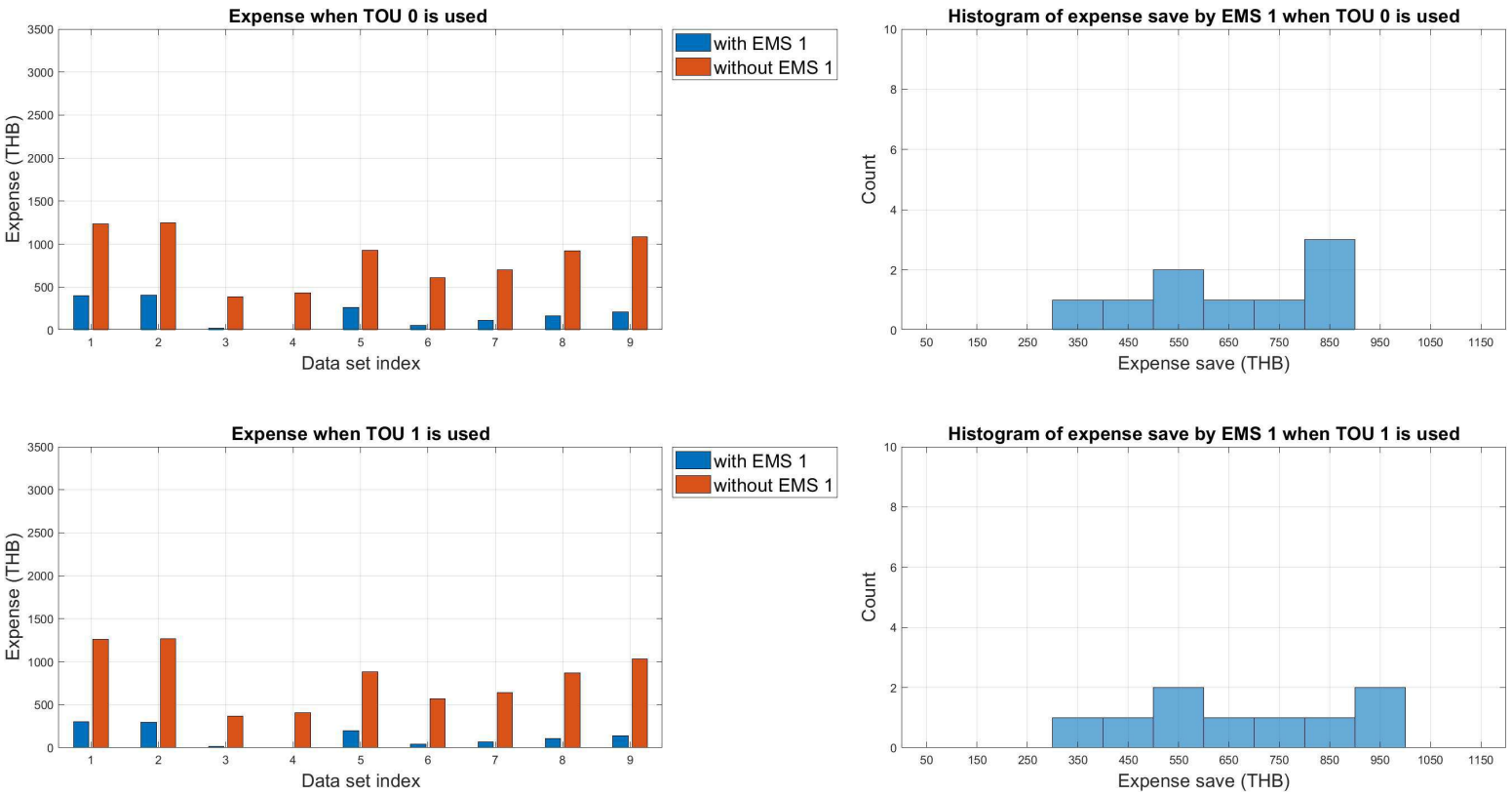

Figure 61: Histogram of expenses saved by Energy cost option in the scenario of **low solar & low load** under TOU 0 and TOU 1.

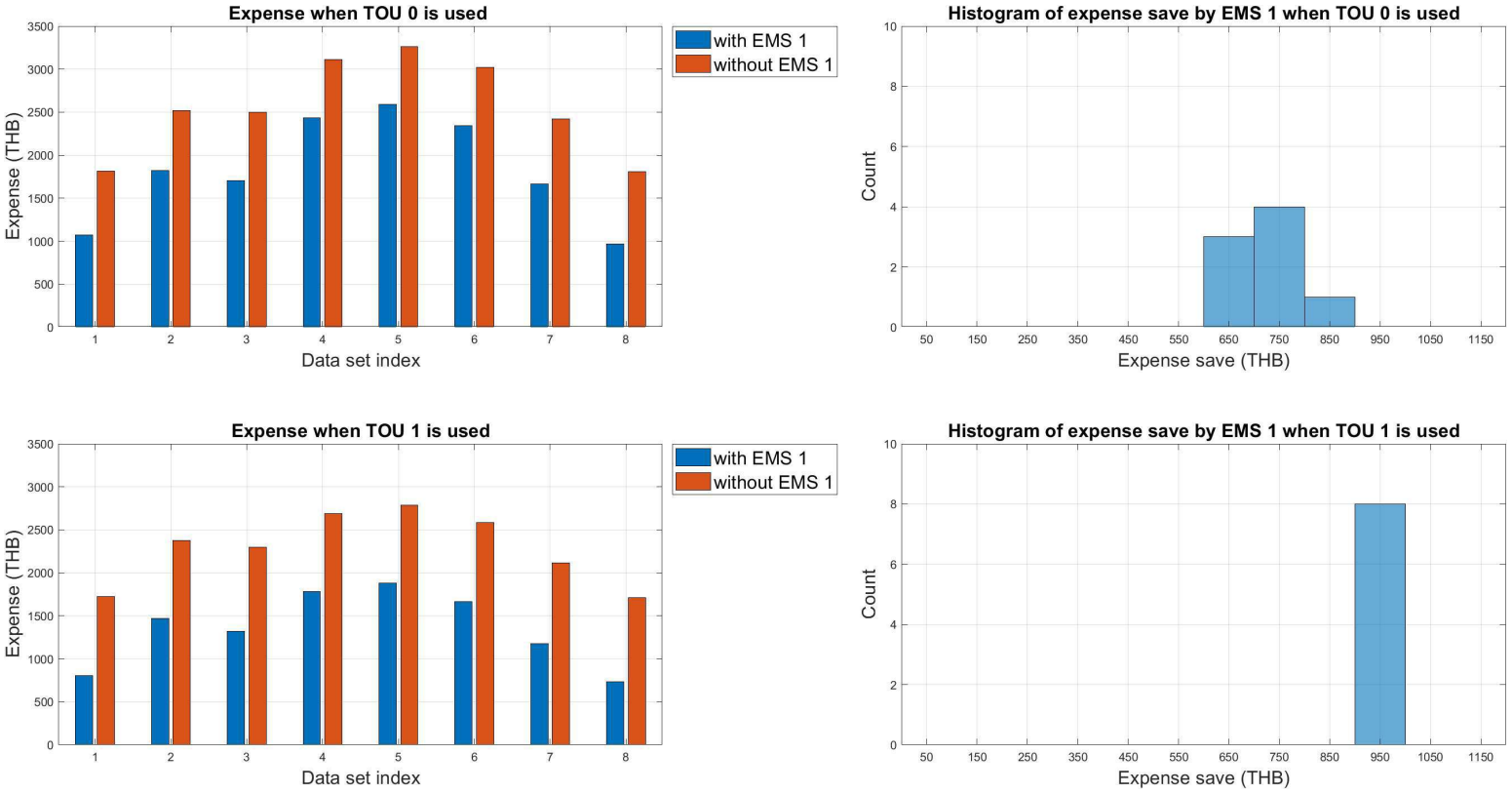

Figure 62: Histogram of expenses saved byEnergy cost option in the scenario of **low solar & high load** under TOU 0 and TOU 1.

9.3 Expenses saved by Economic EMS: Profit option

The histogram depicting expenses saved by Economic EMS: Profit option under various scenarios illustrates how the EMS impacts the reduction of electricity expenses.

- **High solar & low load scenario**: saved up to 525 THB for TOU 0 and 675 for TOU 1.
- **Low solar & low load scenario**: saved up to 575 THB for TOU 0 and 675 for TOU 1.
- **Low solar & high load scenario**: saved up to 575 THB for TOU 0 and 775 for TOU 1.

In conclusion, the EMS can reduce the electricity expenses in every dataset and can be saved better in TOU 1.

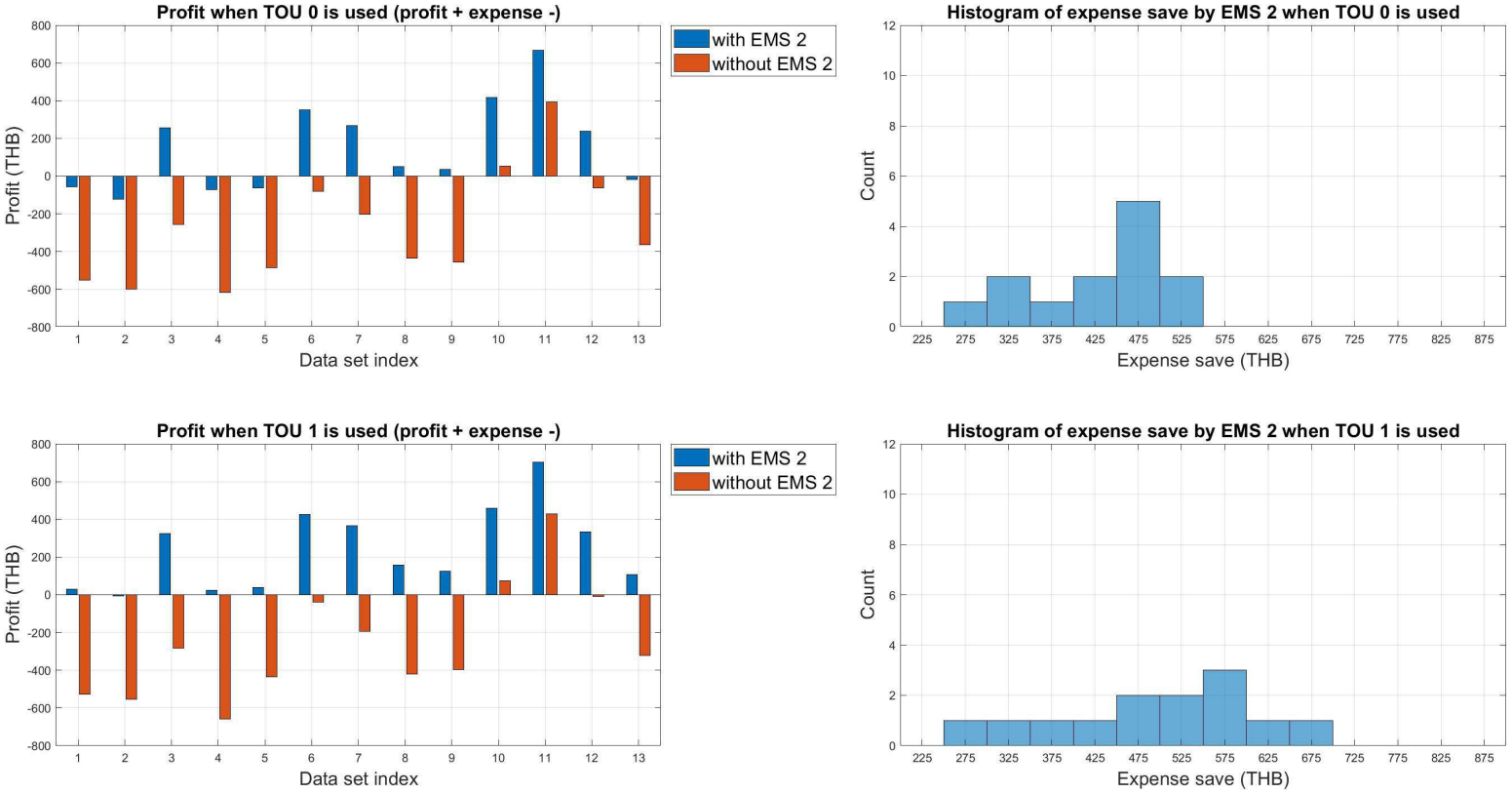

Figure 63: Histogram of expenses saved by Profit option in the scenario of **high solar & low load** under TOU 0 and TOU 1.

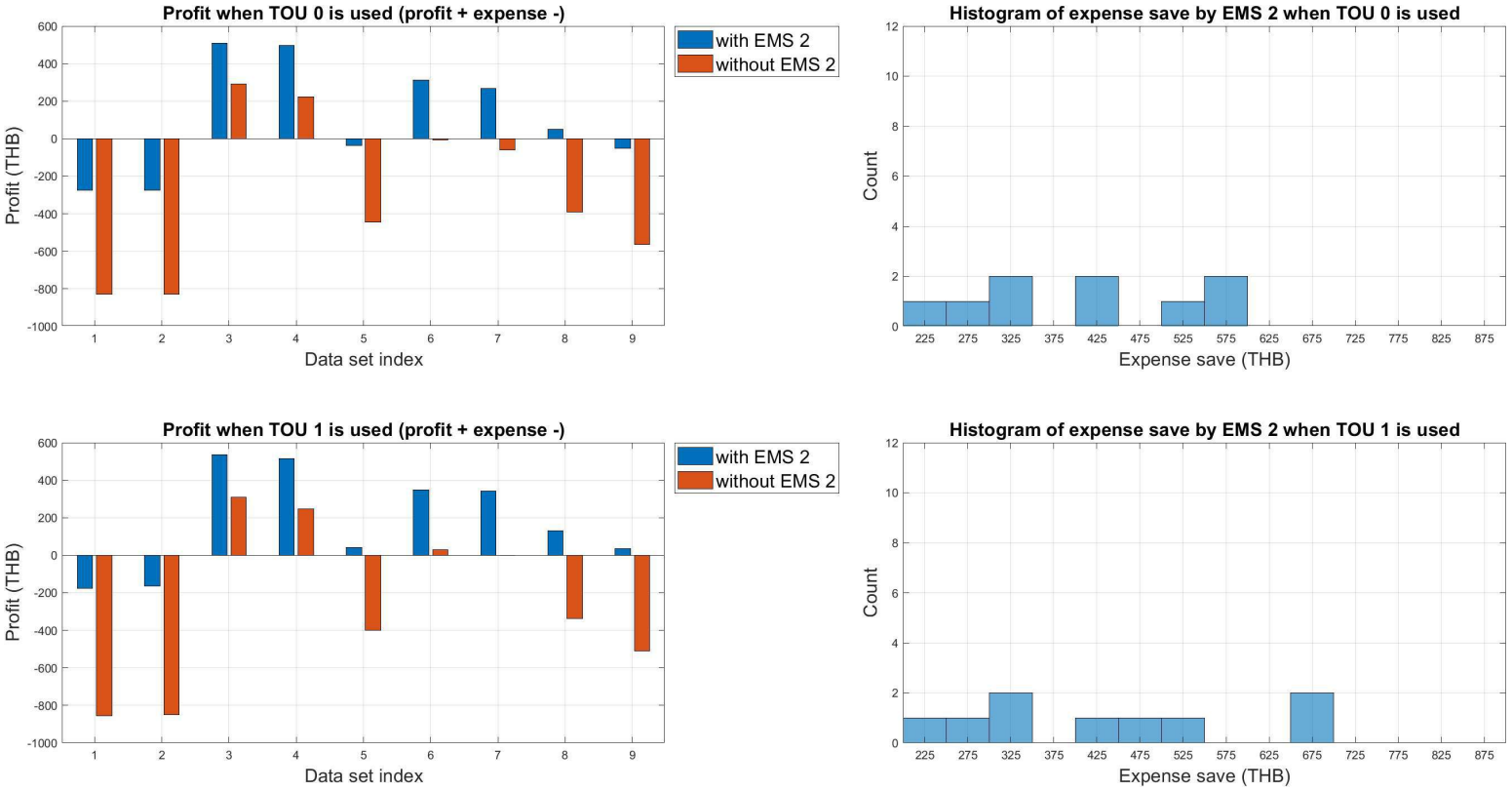

Figure 64: Histogram of expenses saved by Profit option in the scenario of **low solar & low load** under TOU 0 and TOU 1.

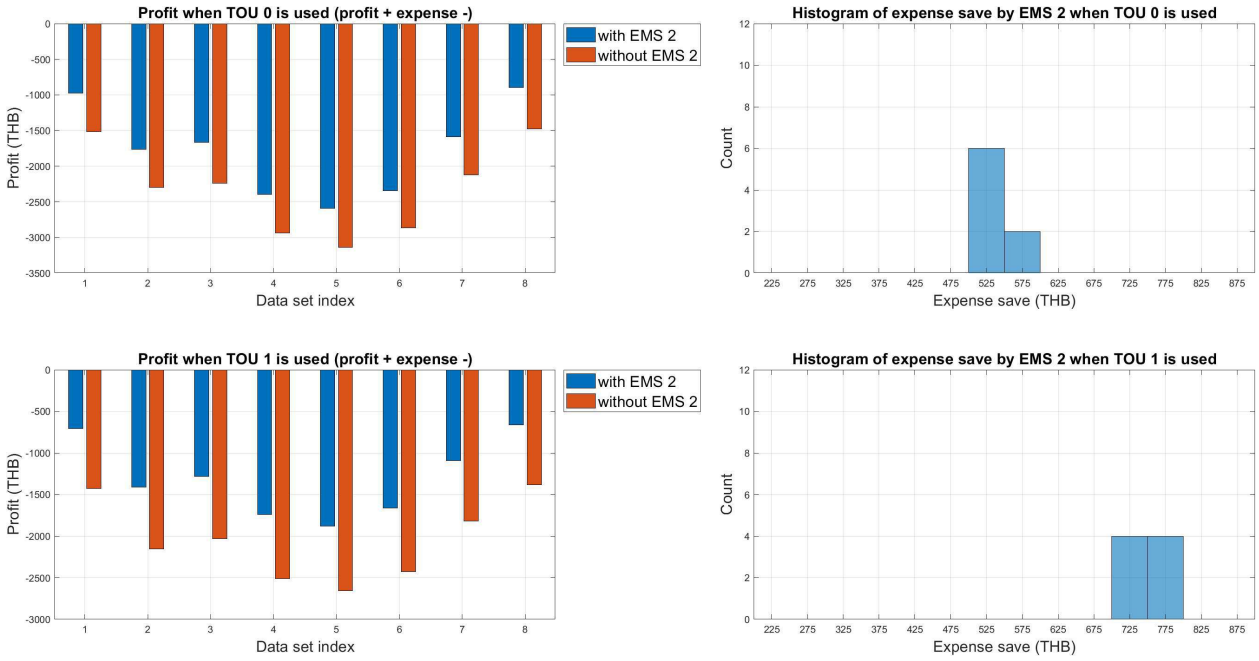

Figure 65: Histogram of expenses saved by Profit option in the scenario of **low solar & high load** under TOU 0 and TOU 1.